NTNU
Det skapende universitet

Verifikasjon og korrelering av utmattingsberegninger ved bruk av testkonstruksjon og ristebord

Andreas Michael Daving

Produktutvikling og produksjon
Innlevert: juni 2015
Hovedveileder: Bjørn Haugen, IPM
Medveileder: Ketil Pettersen, Kongsberg Automotive

Norges teknisk-naturvitenskapelige universitet
Institutt for produktutvikling og materialer

NTNU – Trondheim
Norwegian University of
Science and Technology

Product Development and Production

Department of Engineering Design and Materials

Verification and Correlation of Fatigue Calculations for a Test Structure and Shaker Table

Author:
Andreas Michael Daving

Supervisors:
Bjørn Haugen
Ketil Pettersen

June 10, 2015

Abstract

Background

This thesis is a result of a master's degree in Mechanical Engineering at The Norwegian University of Science and Technology, Department of Engineering Design and Materials.

Objective

The main objective of the thesis is to, in cooperation with Kongsberg Automotive (KA), establish a methodology for physical vibration testing using a shaker table. A concept shall be designed and manufactured. Physical vibration testing are to be correlated with analyses using finite element methods. Relevant methods are linear dynamic calculations in both time domain and frequency domain.

Results

The thesis describes the linear dynamics for performing random vibration analysis and fatigue calculation methods for dynamic systems subjected to a random load.

Four analyses are performed on different test objects, showing expected trends for the specific methods regarding estimated fatigue life.

Notes

As a consequence of unforeseen events, the physical testing at KA's lab was not completed according to the initial plan. The thesis objective is therefore aimed towards the theory and methods of fatigue life calculation due to random vibration loading in the FEA environment.

Thesis Supervisors

Bjørn Haugen	Associate Professor Department of Engineering Design and Materials, NTNU
Ketil Pettersen	Structural Analyst Kongsberg Automotive

Sammendrag

Bakgrunn

Denne rapporten er et resultat av en maskiningeniør mastergrad utført ved Norges Teknisk-Naturvitenskapelige Universitet, Institutt for Produktutvikling og Materialer.

Mål

Hovedmålet med masteroppgaven er å etablere en metode for fysisk vibrasjonstesting ved bruk av et ristebord i samarbeid med Kongsberg Automotive (KA). Et konsept skal designes og produseres, og fysisk vibrasjonstesting skal korreleres med analyser ved bruk av elementmetoden. Relevante metoder innenfor temaet er lineærdynamikk i både tids- og frekvensplanet.

Resultat

Masteroppgaven tar for seg vibrasjonsanalyse ved bruk av lineærdynamikk og metoder for å beregne utmatting for et dynamisk system påvørt en varierende last.

Fire analyser er utført på ulike test objekter av ulik geometri for å vise forventede trender for de spesifikke beregningsmetodene iht å estimere levetid.

Notis

Som en konsekvens av uforutsette hendelser ble ikke fysisk vibrasjonstesting utført ved KAs lab. Masteroppgaven er dermed rettet mot teorien og metodene bak analysene og levetidsberegningene som er gjennomført.

Veiledere

Bjørn Haugen	Førsteamanuensis
	Institutt for Produktutvikling og Materialer, NTNU
Ketil Pettersen	Strukturell Analytiker
	Kongsberg Automotive

Acknowledgement

This thesis concludes my master's degree in Mechanical Engineering at The Norwegian University of Science and Technology, Department of Engineering Design and Materials.

I will sincerely gratitude my external supervisor Ketil Pettersen, Structural Analyst at Kongsberg Automotive, for giving me the opportunity to write a master thesis in cooperation with Kongsberg Automotive. Also for guiding me through problems related to the work of this thesis and giving me valuable inputs and feedback throughout the process.

At the same time I will give a special thanks to my supervisor at NTNU, Bjørn Haugen, Associate Professor at Department of Engineering Design and Materials, for helping me make this thesis possible as well as providing valuable input and feedback when needed.

Finally I would like to thanks my fellow students at the office for great support and a fantastic last year at Department of Engineering Design and Materials, NTNU.

Andreas Michael Daving
Trondheim, 10. June 2015

Contents

Abstract i

Sammendrag ii

Acknowledgement iii

List of Figures viii

List of Tables x

Abbrevations xii

1 Introduction 1
- 1.1 Background . . . 1
- 1.2 Thesis Outline . . . 1
- 1.3 Software Used . . . 2

2 Linear Dynamics 3
- 2.1 Introduction . . . 3
  - 2.1.1 Single Degree of Freedom System . . . 4
  - 2.1.2 Multi Degree of Freedom System . . . 7
  - 2.1.3 Damping . . . 8
- 2.2 Linear Dynamics in FEA . . . 9
  - 2.2.1 Eigenvalue Extraction . . . 9
  - 2.2.2 Transient Modal Dynamics . . . 10
  - 2.2.3 Response Spectrum . . . 10
  - 2.2.4 Steady-State Dynamics . . . 11
  - 2.2.5 Random Response . . . 12

3 Stochastic Process 13
- 3.1 Random Vibration . . . 13
  - 3.1.1 Time and Frequency Domain . . . 17
- 3.2 Converting a Time History . . . 18
  - 3.2.1 Fourier Analysis . . . 18

3.2.2 Creating an input PSD 20
3.3 Vibration Fatigue Calculation 22
3.3.1 The Transfer Function 22
3.3.2 The PSD Moments 22
3.3.3 Probability Density Function 24
3.3.4 Expected Fatigue Damage 24
3.3.5 Narrow-Band Method 24
3.3.6 Steinberg Solution 25
3.3.7 The Dirlik Method 25
3.4 Accelerated Vibration Testing 26
3.4.1 Miner-Palmgren Hypothesis 26
3.4.2 Biot's Shock Response Spectrum 27
3.4.3 Miles' Extreme Response Spectrum 28
3.4.4 Lalanne's Fatigue Damage Spectrum 29
3.4.5 Halfpenny's Synthesized PSD 30

4 Vibration Testing **32**
4.1 Vibration Testing Procedure 32
4.1.1 Fixture Requirements 32
4.1.2 Placement of Sensors 33

5 Designing The Problem **35**
5.1 Test Object Design 35
5.2 Fixture Design 36

6 Linear Dynamic FE Analysis **39**
6.1 Pre-Processing Input Data 39
6.1.1 Units 39
6.1.2 Mesh 40
6.1.3 Boundary Conditions 41
6.1.4 Constraints 42
6.1.5 Load Case 44
6.2 Performing Modal Analysis in Abaqus/CAE 45
6.2.1 Eigenvalue Extraction 45
6.2.2 Steady-State Dynamics 45
The step editor 46
Specifying the input load 46
Defining output requests 47
6.2.3 Random Response 47
The step editor 48
Specifying the input load 48
Defining output requests 48
6.3 Post-Processing Output Data 49
6.3.1 Eigenvalue Extraction 49

6.3.2 Steady-State Dynamics . . . 49
6.3.3 Random Response . . . 49

7 FEA Results **50**
7.1 Eigenvalue Extraction Data . . . 51
7.2 Modal Analysis Results . . . 52
7.2.1 RMS Plots . . . 52
7.2.2 Transfer Functions . . . 53
7.2.3 Response PSDs . . . 55
7.3 Fatigue Life Calculation . . . 57
7.3.1 Hand Calculation in Frequency Domain . . . 58
Simplified PSD Approach . . . 58
Direct RMS Approach . . . 60
7.3.2 Computer Based Calculations . . . 61
7.3.3 High Amplitude Cycle Hypothesis . . . 61
7.4 Summary of Fatigue Life Results . . . 63

8 Discussion **65**
8.1 Boundary Conditions and Interactions . . . 65
8.2 Response and Fatigue Life . . . 65
8.3 Fixture Design . . . 66

9 Conclusion **68**

10 Further Work **69**

Bibliography **70**

A Figures and Tables **72**
A.1 Linear Dynamic FE Analysis . . . 72

B Linear Dynamic FEA Results **73**
B.1 Model TP04 . . . 74
B.1.1 Eigenvalue Extraction Data . . . 74
B.1.2 Modal Analysis Results . . . 75
RMS Plots . . . 75
Transfer Functions . . . 76
Response PSDs . . . 77
B.1.3 Fatigue Life Calculation . . . 79
Hand Calculation in Frequency Domain - Simplified PSD Approach 79
Hand Calculation in Frequency Domain - Direct RMS Approach . 79
Computer Based Calculations . . . 80
B.1.4 High Amplitude Cycle Hypothesis . . . 80
B.2 Model TP06 . . . 81
B.2.1 Eigenvalue Extraction Data . . . 81

B.2.2 Modal Analysis Results 82
RMS Plots 82
Transfer Functions 83
Response PSDs 84
B.2.3 Fatigue Life Calculation 86
Hand Calculation in Frequency Domain - Simplified PSD Approach 86
Hand Calculation in Frequency Domain - Direct RMS Approach . 86
Computer Based Calculations 87
B.2.4 High Amplitude Cycle Hypothesis 87
B.3 Model TP06C 88
B.3.1 Eigenvalue Extraction Data 88
B.3.2 Modal Analysis Results 89
RMS Plots 89
Transfer Functions 90
Response PSDs 91
B.3.3 Fatigue Life Calculation 93
Hand Calculation in Frequency Domain - Simplified PSD Approach 93
Hand Calculation in Frequency Domain - Direct RMS Approach . 93
Computer Based Calculations 94
B.3.4 High Amplitude Cycle Hypothesis 94

C Mechanical Drawings **95**

D Assignment Description **102**

List of Figures

2.1 FRF plot . . . 6
2.2 Effect of damping on the response . . . 8

3.1 Typical random vibration signal . . . 14
3.2 Random vibration signal expressed in σ-limits . . . 15
3.3 Histogram showing amplitude distribution . . . 16
3.4 Example square signal . . . 18
3.5 The concept of Fourier analysis . . . 19
3.6 FFT amplitude plot . . . 19
3.7 Created PSD from random vibration signal . . . 21
3.8 Calculating moments from response PSD . . . 23

4.1 Illustration of single-axis shaker table . . . 33

5.1 CAD rendering of test design . . . 36
5.2 Analysis including two point masses . . . 37
5.3 Analysis including single point mass . . . 38

6.1 Mesh convergence plot . . . 40
6.2 Mesh density and mode shape . . . 41
6.3 Fixed boundary condition region . . . 42
6.4 Slave surfaces . . . 43
6.5 Master surfaces . . . 43
6.6 Input PSD plot . . . 44
6.7 Steady-state dynamics procedure . . . 45
6.8 Random response procedure . . . 47

7.1 CAD model showing fixture and TP04C . . . 50
7.2 RS11 color plot . . . 52
7.3 RMS of stress at critical integration point . . . 52
7.4 Acceleration transfer function (G/G) (log-log) . . . 53
7.5 Tip acceleration amplification (log-log) . . . 54
7.6 Displacement transfer function (mm/G) (log-log) . . . 54
7.7 Max principal stress (MPa/G) (log-log) . . . 55

7.8 Vertical tip acceleration response, RR vs SSD (log-log) 56
7.9 Vertical tip displacement response, RR vs SSD (log-log) 56
7.10 Maximum stress response RR vs SSD (log-log) 57
7.11 Simplified stress response PSD 59
7.12 Fatigue life for different calculation methods 63
7.13 Fatigue life for $\pm 1\sigma$ to $\pm 3\sigma$ limits 64

8.1 Fixture acceleration response in longitudinal x-axis (log-log) 66

B.1 CAD model showing fixture and TP04 74
B.2 RS11 color plot 75
B.3 RMS of stress at critical integration point 75
B.4 Acceleration transfer function (G/G) (log-log) 76
B.5 Displacement transfer function (mm/G) (log-log) 76
B.6 Max principal stress (MPa/G) (log-log) 77
B.7 Vertical tip acceleration response, RR vs SSD (log-log) 77
B.8 Vertical tip displacement response, RR vs SSD (log-log) 78
B.9 Maximum stress response RR vs SSD (log-log) 78
B.10 CAD model showing fixture and TP06 81
B.11 RS11 color plot 82
B.12 RMS of stress at critical integration point 82
B.13 Acceleration transfer function (G/G) (log-log) 83
B.14 Displacement transfer function (mm/G) (log-log) 83
B.15 Max principal stress (MPa/G) (log-log) 84
B.16 Vertical tip acceleration response, RR vs SSD (log-log) 84
B.17 Vertical tip displacement response, RR vs SSD (log-log) 85
B.18 Maximum stress response RR vs SSD (log-log) 85
B.19 CAD model showing fixture and TP06C 88
B.20 RS11 color plot 89
B.21 RMS of stress at critical integration point 89
B.22 Acceleration transfer function (G/G) (log-log) 90
B.23 Displacement transfer function (mm/G) (log-log) 90
B.24 Max principal stress (MPa/G) (log-log) 91
B.25 Vertical tip acceleration response, RR vs SSD (log-log) 91
B.26 Vertical tip displacement response, RR vs SSD (log-log) 92
B.27 Maximum stress response RR vs SSD (log-log) 92

List of Tables

3.1 Statistical parameters for the random vibration signal 15
3.2 Statistical probability for normal distribution 16
3.3 GRMS value check 21

5.1 Test object specifications 36
5.2 Material properties of 6082-T6 36
5.3 Fixture eigenfrequencies 37
5.4 Fixture eigenfrequencies with two point masses 37
5.5 Fixture eigenfrequencies with single point mass 38

6.1 Units used in analysis 39
6.2 Mesh types suitable for analysis 41
6.3 Input PSD definition 44
6.4 Input variables for SSD analysis 46
6.5 Input variables for random response analysis 48

7.1 Eigenvalue output 51
7.2 Modal participation factors 51
7.3 Effective modal mass (Mg) 51
7.4 PSD moments and RMS values 57
7.5 Stress amplitudes from stress response PSD 58
7.6 Sine wave stress ranges (magnitudes) 59
7.7 Cycles to failure for corresponding stress ranges 60
7.8 Cycles to failure for corresponding stress range 60
7.9 Fatigue life obtained from computer based methods 61
7.10 RMS and σ relationship 62
7.11 Max principal stress response PSD moments 62
7.12 Estimated damage using Dirlik method 62
7.13 Total estimated damage from statistical probabilities 63
7.14 Total fatigue life for corresponding limits 63
7.15 Total fatigue life for corresponding limits 64

A.1 Mesh convergence table 72

B.1 Eigenvalue output 74
B.2 Modal participation factors 74
B.3 Effective modal mass (Mg) 74
B.4 PSD moments and RMS values 79
B.5 Stress amplitudes from stress response PSD 79
B.6 Cycles to failure for corresponding stress ranges 79
B.7 Cycles to failure for corresponding stress range 79
B.8 Fatigue life obtained from computer based methods 80
B.9 Total fatigue life for corresponding limits 80
B.10 Eigenvalue output 81
B.11 Modal participation factors 81
B.12 Effective modal mass 81
B.13 PSD moments and RMS values 86
B.14 Stress amplitudes from stress response PSD 86
B.15 Cycles to failure for corresponding stress ranges 86
B.16 Cycles to failure for corresponding stress range 86
B.17 Fatigue life obtained from computer based methods 87
B.18 Total fatigue life for corresponding limits 87
B.19 Eigenvalue output 88
B.20 Modal participation factors 88
B.21 Effective modal mass (Mg) 88
B.22 PSD moments and RMS values 93
B.23 Stress amplitudes from stress response PSD 93
B.24 Cycles to failure for corresponding stress ranges 93
B.25 Cycles to failure for corresponding stress range 93
B.26 Fatigue life obtained from computer based methods 94
B.27 Total fatigue life for corresponding limits 94

Abbrevations

CAD	**C**omputer **A**ided **D**esign
CAE	**C**omputer **A**ided **E**ngineering
ERS	**E**xtreme **R**esponse **S**pectrum
FDS	**F**atigue **D**amage **S**pectrum
FEA	**F**inite **E**lement **A**nalysis
FEM	**F**inite **E**lement **M**ethod
FRF	**F**requency **R**esponse **F**unction
MDOF	**M**ulti **D**egree **O**f **F**reedom
PDF	**P**robability **D**ensity **F**unction
PSD	**P**ower **S**pectral **D**ensity
RMS	**R**oot **M**ean **S**quare
SDOF	**S**ingle **D**egree **O**f **F**reedom
SRS	**S**hock **R**esponse **S**pectrum

1. Introduction

1.1 Background

Any system, structure or component will at some point be subjected to some form of load. In the design process it is absolutely critical to identify possible scenarios the product can or will experience. From analyses, prototyping and testing a statement of how capable the product is to withstand different loads can be obtained.

Whether the product is a suspension component of a automotive vehicle or the internal structure of a airplane wing there are probably many hours, days or even years of development before the product is commercially released. The consequences of a airplane wing to structurally fail in operation are of immense proportions. The reason of failure can be traced to faults in the manufacturing process, sudden impacts of high magnitude, or frequent loads of relatively small but varying magnitude. The last allegation is often referred to as vibrations.

Expected fatigue life of a structure is obtained by processing random time histories, defining random variables using statistical approaches, and performing linear dynamic fatigue life analyses in the FE environment.

This thesis describes and investigates the methods of fatigue life estimation for a structure subjected to a random vibration load.

1.2 Thesis Outline

The thesis begins with giving an introduction to relevant theory of linear dynamics, followed by a description of available procedures for solving linear dynamic problems in the finite element environment. Methods of characterizing a random dynamic event and a description of statistical variables are presented in chapter 3. Random dynamic events in both time and frequency domain are described together with methods for creating analysis input data and fatigue calculation methods.

General procedures for physical vibration testing, fixture requirements and placement of sensors are presented chapter 4.

Chapters 5 and 6 describes the modeled problem case and the analysis setup used for analyses presented in the thesis. Results from one of the four performed analyses and fatigue calculations are thoroughly presented in chapter 7.

Finally the conclusion and suggestions of further work are presented in chapters 9 and 10.

Large figures, results from the remaining analyses, mechanical drawings and assignment description are listed in the appendix.

1.3 Software Used

- Abaqus/CAE, general-purpose finite element program used for analysis of static and dynamic problems. Dassault Systèmes.
- Solidworks, solid modeling CAD and CAE software program. Dassault Systèmes.
- Microsoft Excel, spreadsheet application used for processing output data and creating response plots.

2. Linear Dynamics

2.1 Introduction

A problem is considered dynamic when the inertial forces that results from structural accelerations are both significant and are varying rapidly in time. The inertial forces are proportional to the structure's mass and acceleration.

The general dynamic problem can be described as

$$P - I = M\ddot{u} \tag{2.1}$$

Where P is the external forces, I is the internal forces and $M\ddot{u}$ is the inertial forces. The expression is know as the *equation of motion*, or *dynamic equation of equilibrium*, and applies to the behaviour of all mechanical systems containing all non-linearities.

A derivative of this expression is the *equation of static equilibrium* by setting the acceleration, $\ddot{u}$, equal to 0.

$$P - I = M\ddot{u} = 0 \tag{2.2}$$

When assumed that the resulting motion of imbalance between internal and external forces is small compared with the internal elastic forces, the response can be considered *quasi-static*. This applies for systems where the external load vary slowly with time and the inertial forces are small or zero.

$$P - I = M\ddot{u} \approx 0 \tag{2.3}$$

In linear dynamics, the internal forces are linearly dependent on the nodal displacements, accelerations and velocities. When including damping in the system, the dynamic equation of equilibrium can be rewritten as

$$I = C\dot{u} + Ku \tag{2.4}$$

By inserting equation (2.4) in the dynamic equation of equilibrium, (2.1), the complete equation of motion is written as

$$M\ddot{u} + C\dot{u} + Ku = P \tag{2.5}$$

$M\ddot{u}$ can now be described as the internal resistance, derived from $F{=}ma$. $C\dot{u}$ is the damping resistance, derived from $F{=}Cv$. Ku is the spring resistance, derived from $F{=}Kx$. This equation is often applied in matrix form, specially for multi degree of freedom (MDOF) systems, and referred to as the *matrix equation of motion* for linear dynamics.

$$\mathbf{M\ddot{u} + C\dot{u} + Ku = P} \tag{2.6}$$

Now **M** is the system mass matrix, **C** is the damping matrix, **K** is the stiffness matrix, **u** is the vector of nodal unknowns (displacement, acceleration, velocity). For a linear dynamic problem both mass, damping and stiffness is considered constant. They are not considered constant if the problem is non-linear. This makes the linear dynamic problem more efficient to solve, but could give inaccurate results in certain cases where external forces or resultant displacements are significantly large.

2.1.1 Single Degree of Freedom System

If considering an undamped single degree of freedom (SDOF) system by setting $C\dot{u} = 0$ in equation (2.5) gives

$$M\ddot{u}(t) + Ku(t) = P(t) \tag{2.7}$$

Assuming the solution on following form

$$u(t) = Asin(\omega t) \tag{2.8}$$

$$\ddot{u}(t) = -\omega^2 Asin(\omega t) \tag{2.9}$$

The natural frequency of the system is found by inserting equations of displacement (2.8) and acceleration (2.9) in the equation of motion and setting *P(t)=0*.

$$-M\omega^2 Asin(\omega t) + KAsin(\omega t) = P(t) = 0 \tag{2.10}$$

Cleaning up and sorting equation (2.10) gives

$$(-M\omega^2 + K)Asin(\omega t) = 0 \tag{2.11}$$

This means that either $Asin(\omega t) = 0$ or $-M\omega^2 + K = 0$. And by solving with regard of ω the well known equation for the natural frequency of a undamped SDOF system is found, as shown in equation (2.12).

$$\omega_n = \sqrt{\frac{K}{M}}, \quad \text{frequency in rad/s} \tag{2.12}$$

$$f_n = \frac{1}{2\pi}\sqrt{\frac{K}{M}}, \quad \text{frequency in Hz} \tag{2.13}$$

$$T_n = 2\pi\sqrt{\frac{K}{M}}, \quad \text{natural period in seconds} \tag{2.14}$$

The natural period, T_n, is useful for low frequencies. Often used in context of wave motion on offshore structures.

If still considering the undamped SDOF system, but now with an applied sinusoidal force represented by equation (2.15)

$$P(t) = Fsin(wt) \tag{2.15}$$

Inserted in equation (2.11) gives

$$(-M\omega^2 + K)Asin(\omega t) = P(t) = Fsin(wt) \tag{2.16}$$

Dividing by $sin(\omega t)$ on both sides

$$(-M\omega^2 + K)A = F \tag{2.17}$$

If solving with regard of A yields the *frequency response function* (FRF) shown in equation (2.18).

$$A(\omega) = \frac{1}{(-M\omega^2 + K)} \cdot F \tag{2.18}$$

Figure 2.1 shows the plotted FRF. The peak amplitude, located at the natural frequency, f_n, tends towards infinity because of zero damping in the system.

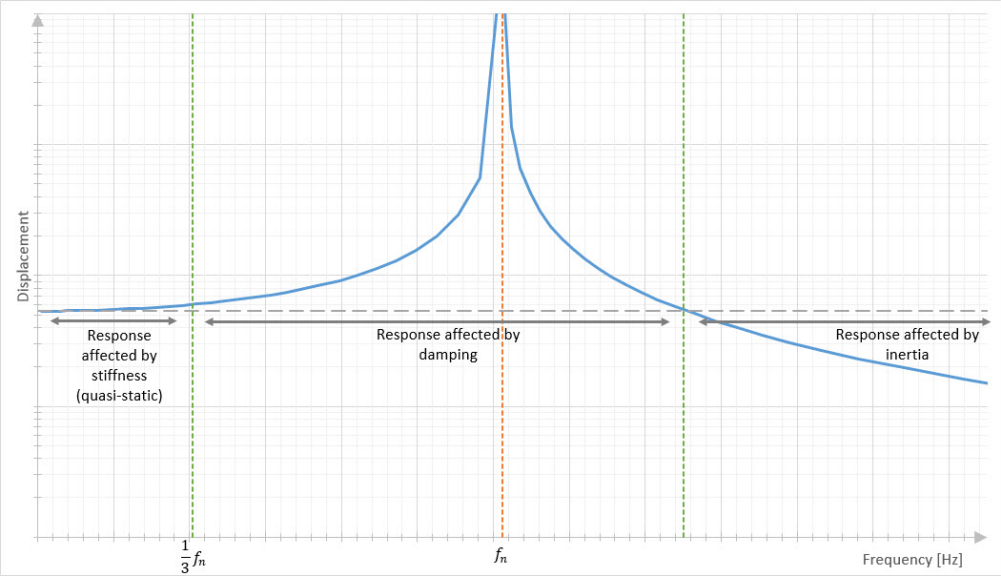

Figure 2.1: FRF plot

The FRF plot is divided in three sections. Where the response in the first section, $f = 0$ to $f = \frac{1}{3}f_n$, is affected by the structural stiffness of the system. Rule of thumb in engineering processes is often to consider this as the static or quasi-static region, where such assumptions are acceptable. The second section the response is affected by the damping in the system, hence if decreasing damping the peak tends towards infinity. In the third section the response is affected by the systems inertia.

2.1.2 Multi Degree of Freedom System

From equation (2.6), a freely vibrating undamped MDOF system can be described as

$$\mathbf{M\ddot{r}} + \mathbf{Kr} = \mathbf{0} \tag{2.19}$$

By assuming the solution on following form

$$\mathbf{r} = \mathbf{r_e} sin\omega t \tag{2.20}$$

$$\ddot{\mathbf{r}} = -\omega^2 \mathbf{r_e} sin\omega t \tag{2.21}$$

And by inserting (2.20) and (2.21) in (2.19) gives

$$(\mathbf{K} - \omega^2 \mathbf{M})\mathbf{r_e} sin\omega t = 0, \quad where \quad \omega \neq 0 \quad and \quad \mathbf{r_e} \neq 0 \tag{2.22}$$

$\omega = 0$ and $\mathbf{r_e} = 0$ are obvious solutions, but not of interest. This because $\omega = 0$ gives a eigenfrequency of 0 and $\mathbf{r_e} = 0$ means that the system is not i motion. In order to fulfill these criteria, the coefficient matrix must be singular, hence the determinant must be zero

$$|\mathbf{K} - \omega^2 \mathbf{M}| = 0 \tag{2.23}$$

Equation (2.23) is only valid for certain values for ω. These are representing the systems eigenfrequencies. The number of possible eigenfrequencies depends on the number of degrees of freedom in the system, i.e. a system with 20 degrees of freedom will have 20 eigenfrequencies.

For each ω a corresponding nodal displacement vector can be found from equation (2.22). The exact value can not be calculated, but the relation between the vector components can be found. These vectors are referred to as eigenvectors, which is used to characterize the mode shapes of the system by plotting the relative displacement for each node.

2.1.3 Damping

When introducing damping to the system, the peak amplitude of motion around the resonance frequencies will be limited. The significant effect on peak response by damping is shown in figure 2.2. The maximum dynamic response amplitude can be estimated by multiplying the static response with the dynamic amplification factor, Q.

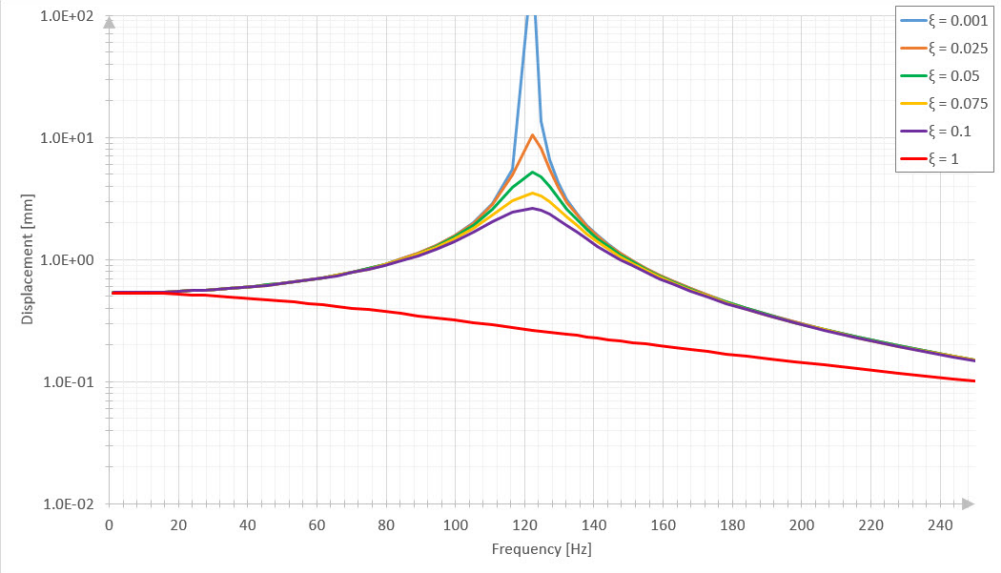

Figure 2.2: Effect of damping on the response

$$Q = \frac{1}{2\xi} \tag{2.24}$$

ξ is known as the *critical damping fraction*, which is the ratio of critical damping in percentage. The reason for using ξ is that for many systems the damping value will change depending on geometry, stiffness, inertia etc. But the critical damping fraction will stay relatively constant, at least it is assumed constant for most linear dynamic systems. The effect of damping on the system's response is evident, and as ξ approaches 1 the system is considered critically damped.

The expression origins from equations (2.25) and (2.26) and is governed by mass, M, and stiffness, K.

$$C_{crit} = 2\sqrt{MK} \tag{2.25}$$

$$\xi = \frac{C}{C_{crit}} = \frac{C}{2\sqrt{MK}} \tag{2.26}$$

The natural frequency of a system will also be reduced when introducing damping according to equation (2.27).

$$f_d = f_n\sqrt{1-\xi^2} \tag{2.27}$$

2.2 Linear Dynamics in FEA

A linear dynamic analysis is based on the idea of linear perturbation analyses. This means that the linear response is in general based on the analysis of small perturbations about a preloaded state [1].

If the linear response assumptions are applicable, the dynamic response can be approximated by a linear combination of the response of a subset of the system's normal modes. Where the normal modes are the mode shapes associated with the system's eigenfrequencies.

The procedures are described according to the procedures available in Abaqus/CAE which uses the Abaqus/Standard solver [2] [3]. The procedures and theory of linear dynamics are in most cases directly applicable for other FEA software such as MSC/Nastran, Ansys and LS-Dyna.

2.2.1 Eigenvalue Extraction

This is the initial step for all mode-based linear perturbation type of analyses. The purpose is to extract the eigenfrequencies and mode shapes that shows the harmonic oscillation of the structure. There are no external load applied, and the result shows how the structure will behave if set to vibrate freely in the designated frequency range. A eigenvalue extraction step is, depending on the complexity of the model, cheap regarding CPU time.

Both real and complex eigenvalues can be extracted. The difference relies on whether damping is inactive or active in the step. For real eigenvalues, damping is not active and the mass and stiffness matrix is symmetric. Complex eigenvalue extraction is only possible to perform after a real eigenvalue extraction step. For complex eigenvalues, viscous damping and antisymmetric matrices can be solved and is often used in dynamic

stability analysis. The eigenvalue extraction procedure can be assumed undamped for systems with no, or very little external and/or material damping.

Abaqus/Standard provides three eigensolvers. Automatic multi-level substructuring (AMS) eigensolver, a reduction method suited for large systems where a large set of eigenvalues are desired. Subspace iteration and Lanczos eigensolvers are both iterative methods suited for systems where a smaller set of eigenvalues are needed.

Both Lanczos and Subspace iteration eigensolvers outputs, in addition to eigenvalues, the modal participation factors and effective modal mass. The modal participation factor indicates the level of motion represented in the eigenvector of a specific mode. Effective modal mass is a variable of indicating the mass in motion related to a specific mode. By summing the effective modal mass in one direction over the total number of modes gives the system's total mass minus mass at kinematically restrained degrees of freedom. Both variables are presented by values in the global coordinate system.

AMS eigensolver only outputs the generalized mass in addition to eigenvalues.

2.2.2 Transient Modal Dynamics

Transient modal dynamics is a mode-based linear perturbation transient procedure. The procedure calculates the response for a system subjected to linear vibrations expressed in form of a time history. It is not required to include damping in order to obtain bounded solutions, unless the excitation is a single harmonic corresponding to a natural frequency of the system.

Time domain transient solutions are obtained with a time integration numerical algorithm where the integration time is user-specified and an amplitude curve describes the excitation time history.

If there are non-linearities in the system that are important to consider, a direct integration method can be used by employing modal subspace projection. This method gives accurate results, but is not very computational efficient. For either method it is very important to ensure that enough eigenmodes are included in the modal analysis to ensure an accurate representation of the system's response.

2.2.3 Response Spectrum

Response spectrum is a mode-based linear perturbation procedure which estimates the peak linear response of a structure subjected to a base excitation in the frequency domain. The response is defined as a function of the natural frequencies with a response spectrum.

The mode shapes are considered to behave as simple oscillators, each responding at its natural frequency. The peak response of each mode is computed, based on the user defined response spectrum. By combining the peak response of each mode makes it possible to estimate the system's peak response. The combination procedures are often predetermined and designed to be conservative.

This method is therefore often used when a conservative, worst-case-scenario estimate of the peak response is desired for design purposes.

2.2.4 Steady-State Dynamics

In a steady-state dynamics (SSD) analysis the applied load and structural response vary harmonically with time, and the solution is performed in the frequency domain. SSD analysis is only valid for linear systems since the response behaviour over each harmonic cycle in time is linear. The SSD analysis calculates the solution for the response over a range of excitation frequencies, often referred to as a sine-sweep.

Either structural or external damping must be included to ensure a bonded solution when an excitation frequency coincides with a natural frequency of the system, otherwise the peak amplitude will tend towards infinity. The analysis can bias the excitation frequencies toward the values that generate a response peak.

There are three SSD procedures available in Abaqus/Standard, all linear perturbation procedures used to find the linearized response to a system subjected to a harmonic base excitation.

- **Direct-solution** calculates the response from the physical DOFs of the model directly. It is the most computationally expensive procedure. If frequency-dependent or viscoelastic effects are included, the solution is by far the most accurate.
- **Subspace-based** based on the projection of the SSD equations on a subspace of selected modes of the undamped system. The procedure presents a compromise by providing a computationally effective solution where frequency-dependent or viscoelastic effects can be included, but not giving as accurate results as the direct-solution procedure.
- **Mode-based** calculates the response based on the eigenfrequencies and modes. It is significantly cheaper than both previous procedures, but is less accurate. Although the mode-based SSD analysis gives representable results if frequency-dependent or viscoelastic effects can be assumed negligible.

2.2.5 Random Response

Random response is also a mode-based linear perturbation procedure in the frequency domain. But unlike the mode-based SSD analysis, random response is based on prediction of the system response when subjected to a random base excitation. The base excitation is defined by a power spectral density (PSD) function [4]. The procedure calculates, based on the extracted eigenfrequencies and modes, PSD functions of response variables and their corresponding root mean square (RMS) values.

Random response analysis is a useful method for identifying critical regions in context of random vibration fatigue analysis. A RMS plot of stress for the last increment will indicate stress concentration regions in the structure. Random response analysis is often performed in order to get an overview of critical regions to be further investigated in a SSD analysis.

3. Stochastic Process

Dynamic systems can either be characterized as *deterministic* or *stochastic*. Where a deterministic system will always give the same output from a given initial state or starting condition, provided that no random variables are influencing the future states of the system.

Vibrations can in certain circumstances be deterministic. For instance if the system is subjected to a harmonic vibration load where both frequency and amplitude is constant, or not varying rapidly with time. Such harmonic vibrations are often described by a sine wave function, and referred to as *narrow band* because it is consisting of one predominant excitation frequency.

Vibrations in nature are behaving randomly. In order to replicate a lifelike scenario this random behaviour must be taken into account. These type of vibrations are stochastic and referred to as *random vibrations*. Stochastic systems are unpredictable in that manner that the future states of the system can not be precisely calculated. Therefore it is necessary to introduce statistical data and methods in order to assume and possibly predict the future states.

This chapter addresses the difference between the time and frequency domain, methods of processing measured data from random events, and using these data as an input for a linear dynamic analysis.

3.1 Random Vibration

Random vibration can generally be characterised as motion that varies randomly with time where the amplitude can not be expressed in terms of a deterministic mathematical function. Unlike narrow band, random vibration is composed of a continuous spectrum of frequencies. Random vibration is white noise which is a stationary process where mean magnitude, RMS magnitude and probability distribution of signal magnitude are variables independent of time.

> The most obvious characteristic of random vibration is that it is non-periodic. A knowledge of the past history of random motion is adequate to predict the probability of occurrence of various acceleration and displacement magnitudes, but it is not sufficient to predict the precise magnitude at a specific instant.
>
> *D. Steinberg, "Vibration Analysis for Electronic Equipment", Wiley-Interscience, New York, 1988*

Figure 3.1 below shows a generated random acceleration signal with a zero mean and units of G and seconds. The signal is not taken from physical measurements, but generated specifically for this example.

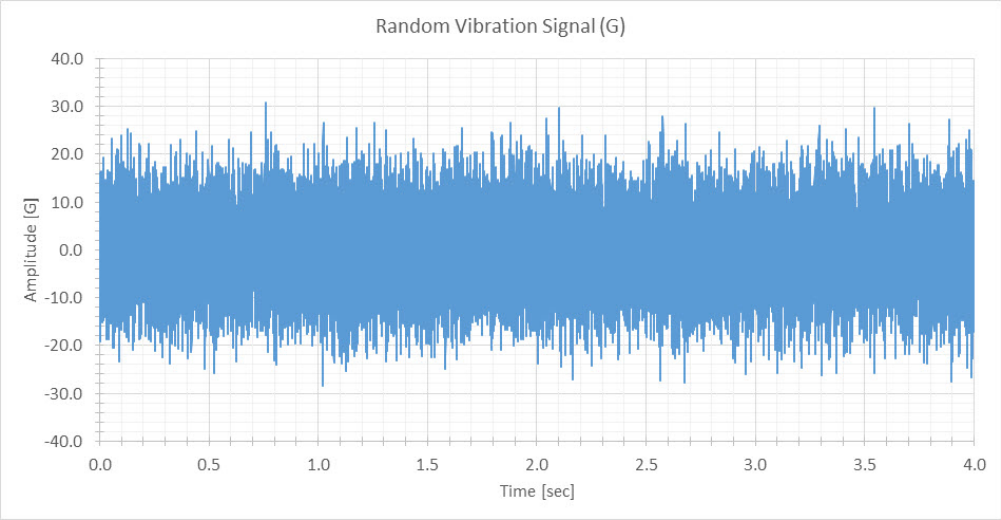

Figure 3.1: Typical random vibration signal

The root mean squared (RMS) is a statistical value used to describe a random signal. The RMS value of the signal is equal to the standard deviation value if the mean is zero, i.e the signal fluctuates about the zero axis. The standard deviation is represented by sigma, σ. Typical kurtosis value for a random vibration time history is 3, where a pure sinusoidal time history has a kurtosis value of 1.5 [5]

Parameter	Value
Sample duration	4.0 sec
Number of samples	8000
Mean	0
RMS	7.53 GRMS
Standard deviation	7.53
Kurtosis	2.98
Maximum	30.91 G
Minimum	-28.43 G

Table 3.1: Statistical parameters for the random vibration signal

The relationship between peak amplitude, RMS and sigma is given in equation (3.1). The term GRMS is an abbreviation for root mean square acceleration when amplitude is in units of G.

$$\frac{\text{Peak (G)}}{\text{GRMS}} = \text{Peak value in terms of } \sigma \tag{3.1}$$

The peak value for the random signal is therefore

$$\frac{30.91 \text{ Peak (G)}}{7.53 \text{ GRMS}} = 4.11\sigma$$

By dividing the entire random signal by the GRMS, the amplitude can be plotted in terms of σ, figure 3.2.

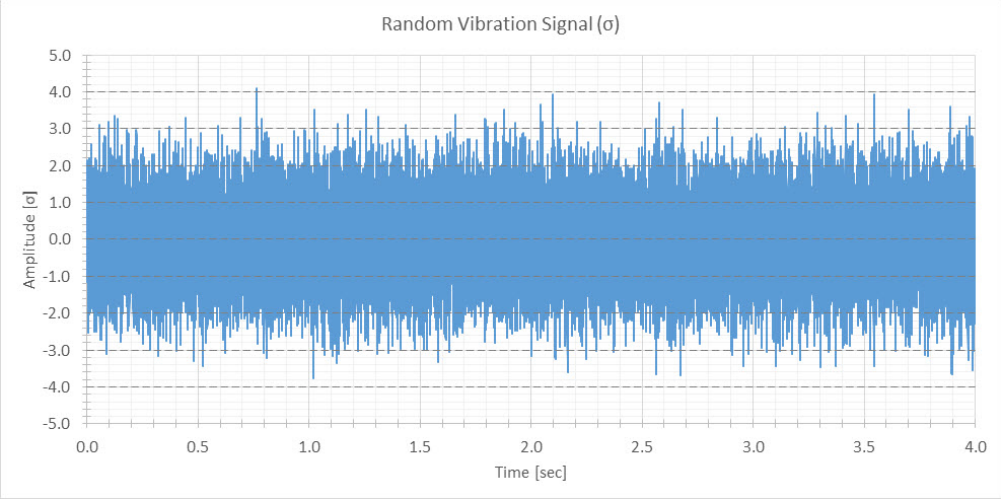

Figure 3.2: Random vibration signal expressed in σ-limits

As stated earlier, the amplitude at a given time in the random vibration time history cannot be calculated. But the probability that the amplitude is within or outside certain limits can be statistically expressed. These probability values are given in table 3.2. According to the theory of statistical probability the amplitude should be within $\pm 1\sigma$ limits 68.26% of the time, within $\pm 2\sigma$ limits 95.45% of the time, and within $\pm 3\sigma$ limits 99.73% of the time.

Statistical Probabilities for a Normal Distribution with Zero Mean		
Probability inside $\pm 1\sigma$ limits	=	68.27%
Probability outside $\pm 1\sigma$ limits	=	31.73%
Probability inside $\pm 2\sigma$ limits	=	95.45%
Probability outside $\pm 2\sigma$ limits	=	4.55%
Probability inside $\pm 3\sigma$ limits	=	99.73%
Probability outside $\pm 3\sigma$ limits	=	0.27%
Probability inside $\pm [1\sigma$ to $2\sigma]$ limits	=	27.18%
Probability inside $\pm [2\sigma$ to $3\sigma]$ limits	=	4.28%

Table 3.2: Statistical probability for normal distribution

The histogram of a random vibration time history, shown in figure 3.3, has a bell-shaped curve and is an approximate example of a Gaussian or normal distribution following the statistical properties applied in table 3.2.

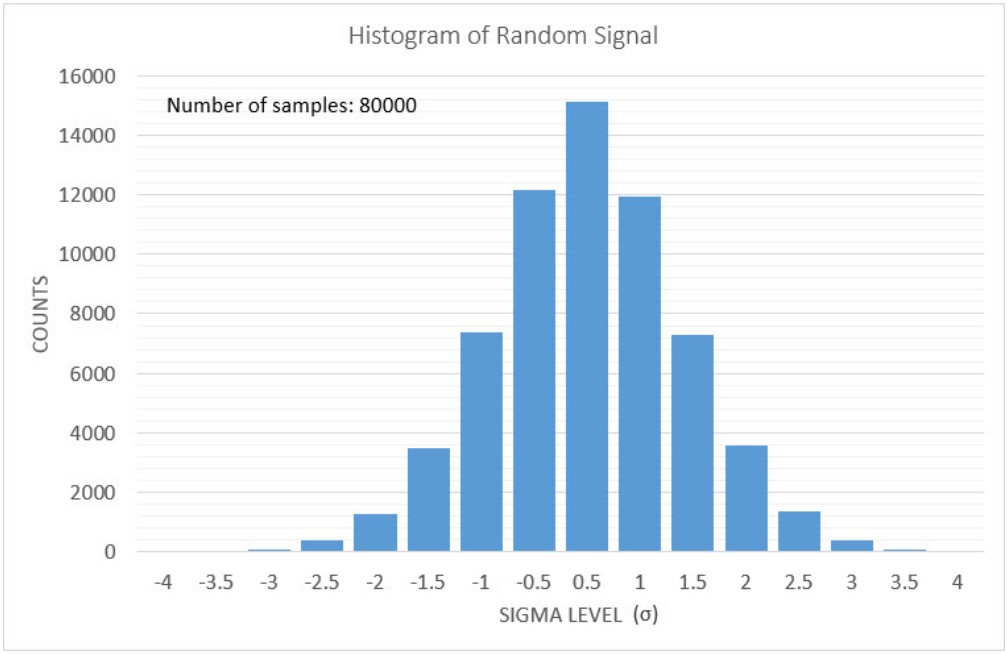

Figure 3.3: Histogram showing amplitude distribution

The histogram gives an indication of what amplitudes that is present in the signal. Typical assumption is that random vibrations has a peak value of 3σ for common design purposes. Where amplitudes inside $\pm$ 3σ limits can be described as probable loads, and amplitudes outside $\pm$ 3σ limits might be considered as the hundred-year-wave and unlikely to occur during the service time of the structure or component.

3.1.1 Time and Frequency Domain

Measured response is generally expressed with a time history signal. If this signal is made of constant amplitude cycles (narrow band) fatigue life can be estimated by referring to a S-N diagram and using the Palmgren-Miner linear damage theory to calculate the relative damage index [6].

Physical vibration measurements are rarely in compliance with this ideal amplitude cycle signal, but are characterized by random amplitudes and frequencies in a given time period. A method for counting fatigue cycles from a random time history is the Rainflow cycle counting method [7]. Rainflow counting combined with Miner's rule makes it possible to assess the fatigue life of a system subjected to complex loading. These calculations are performed in the time domain since both inputs and outputs are specified in a time span, or derivatives of, with specified length.

The frequency domain provides an alternative representation of a time history where the amplitude is given by a function of frequency. Information about a random dynamic event, such as random vibrations, are easier to read in a frequency plot. By utilizing the *fast fourier transformation* (FFT) a time history is converted to the frequency domain. Random vibration fatigue analysis in the frequency domain is performed by either a random response or SSD analysis procedure followed by a so called PSD analysis [8] [9].

3.2 Converting a Time History

3.2.1 Fourier Analysis

Fourier suggested that any signal wave that repeats its self can be decomposed into several sine waves of different amplitude and frequency [10]. Thus by adding the series of sine waves together it is possible to recreate the original signal. For demonstration a square wave signal is considered as shown in figure 3.4.

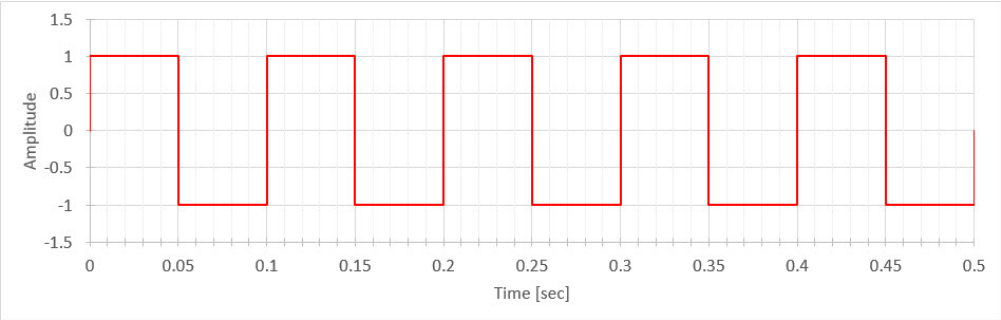

Figure 3.4: Example square signal

By assuming this signal is composed of a series of sine waves on following form

$$\left(\frac{1}{n+1}\right) A sin\left[(n+1)\theta\right] \quad \text{where } A = \frac{4}{\pi} \text{ and } n = 0,\ 2,\ 4,\ 6... \tag{3.2}$$

Figure 3.5 shows the example when adding the corresponding sine waves together. The red curve shows the replicated signal, and already with only four sine waves the characteristics of the square signal is evident. By adding the infinite number of sine waves together, the square signal will be fully recreated.

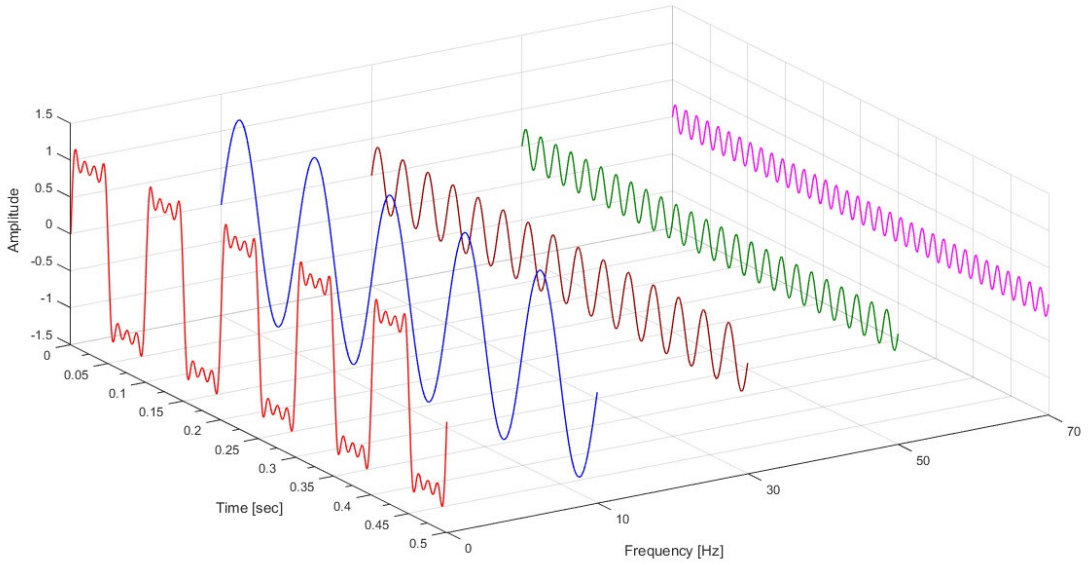

Figure 3.5: The concept of Fourier analysis

From this example the FFT amplitude is easily obtained by plotting the frequency and amplitude of each sine wave, as shown in figure 3.6.

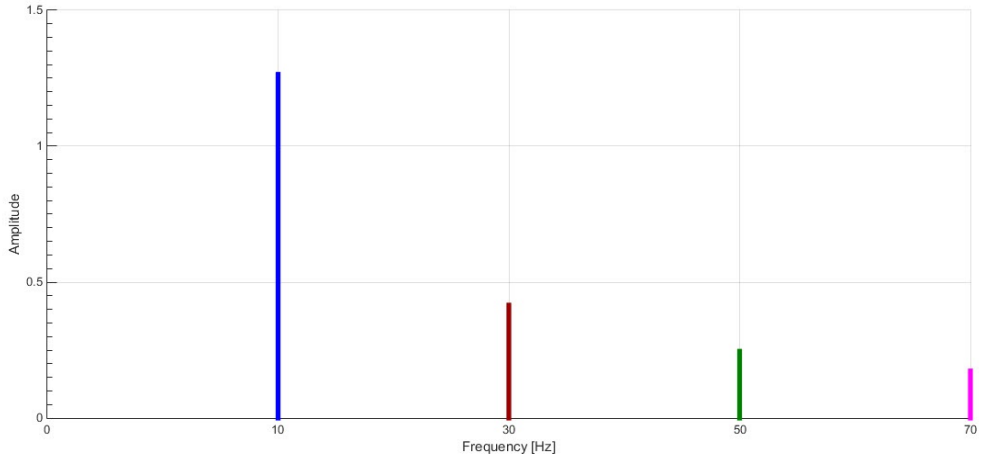

Figure 3.6: FFT amplitude plot

The example shows the FFT transform graphically. The fourier analysis outputs actually a series of complex values on $a + bi$ form, where the FFT magnitude is $\sqrt{a^2 + b^2}$. The FFT amplitude is then found through equation (3.3).

$$FFT_{amplitude} = FFT_{magnitude} \cdot \frac{2}{N} \tag{3.3}$$

Where N is the number of samples in the time history.

3.2.2 Creating an input PSD

From equation (3.4) the FFT amplitude is converted to PSD amplitude. And by plotting the PSD amplitude over the frequency range, the input PSD is created.

$$PSD_{amplitude} = \left(FFT_{amplitude}\right)^2 \cdot \frac{1}{2df} \tag{3.4}$$

$$df = \frac{S}{N} \tag{3.5}$$

N is the number of samples and S is the sampling rate. The sampling rate is defined from the *Nyquist Frequency* shown in equation (3.6) which states that the maximum frequency of the PSD function can not exceed half the sampling rate frequency.

$$S = 2 \cdot PSD_{max} \tag{3.6}$$

The PSD function will always have units of squared over hertz, which comes from equation (3.4), where the FFT amplitude is squared and divided on df [11].

For a second demonstration lets consider the random signal from section 3.1 (figure 3.1). In this case, the signal have units of G and will give a PSD function with units of G^2/Hz. It is shown to be a very much random signal because of its kurtosis and standard deviation value.

This could for instance represent the vertical vibrations measured in a car traveling on a uneven and bumpy road. If an engineer is set to perform analysis on a car component, this signal can be used in order to represent the vibrations the component must withstand. In order to perform an efficient analysis in the frequency domain this signal must be converted into a PSD representing input acceleration load over frequency.

By performing a FFT transformation and using equations (3.3) to (3.6), the input PSD is created. The same PSD can be converted back to a time history by simply using the inverse FFT. Although the regenerated time history will not be exactly the same as the original signal, it should be statistically equivalent. The PSD created from the random

time history is shown in figure 3.7, where the blue line represents the directly plotted PSD curve and the orange line represents the modified PSD which is averaged and "cleaned up" in order to make it tidier and easier to process in the analysis.

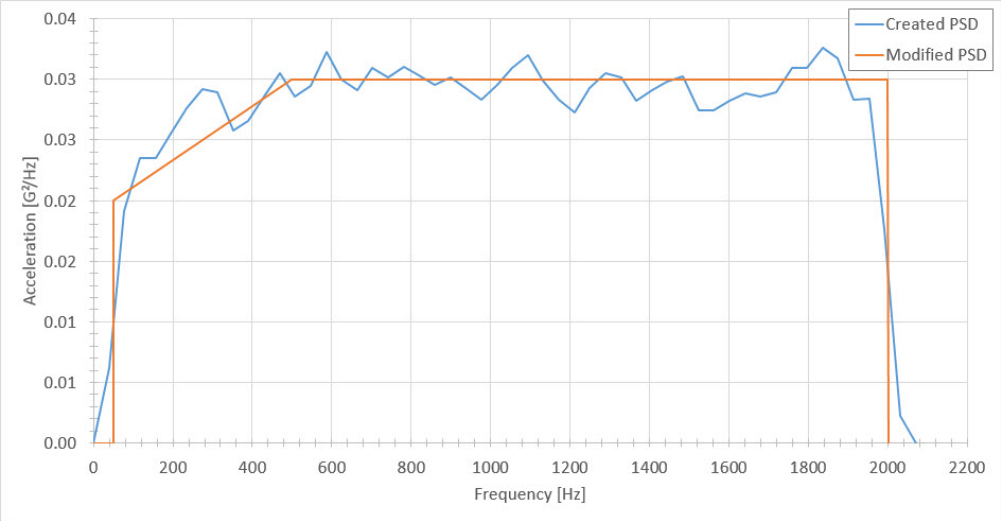

Figure 3.7: Created PSD from random vibration signal

The created PSD can be controlled by checking the GRMS values of the time history versus the GRMS value of the created PSD. These should ideally be identical, but this is not always possible and is dependent on the signal resolution and number of data points. The calculated GRMS for the random time history and both PSDs is shown in table 3.3.

Plot	**GRMS-value**
Random Signal (fig. 3.1)	7.53
Created PSD (fig. 3.7)	7.50
Modified PSD (fig. 3.7)	7.50

Table 3.3: GRMS value check

Table 3.3 shows very good correlation between the GRMS for the original random time history and the modified PSD. This modified PSD will be used as input load for the linear dynamic analyses performed and described in section 6.2.

3.3 Vibration Fatigue Calculation

3.3.1 The Transfer Function

SSD analysis gives outputs in form of *transfer functions*. The transfer function builds on the theory of linearity. If a structure is subjected to a sinusoidal force the structure will respond with a sinusoidal displacement at the same frequency. Where the system's linear response is proportional to an increase in amplitude of the forcing function. The transfer function is defined as response per input load at each frequency. It is therefore possible to predict the system's response by multiplying the transfer function with the amplitude of the load. The response can be in any form as long as the relationships are linear; displacement, acceleration, stress, strain etc.

In order to get the transfer function in correct units for a PSD analysis, the response parameter must be squared. The relationship between the transfer function, input PSD and response PSD is shown in equation (3.7) with regard of the stress response used for fatigue analysis.

$$\underbrace{\left[\frac{MPa}{G}\right]^2}_{\text{Transfer Function}} \times \underbrace{\frac{G^2}{Hz}}_{\text{Input PSD}} = \underbrace{\frac{MPa^2}{Hz}}_{\text{Response PSD}} \tag{3.7}$$

3.3.2 The PSD Moments

When performing fatigue analysis for a structural system in the frequency domain it is necessary to extract the spectral moments of the stress response PSD. This is often referred to as the *nth* moments of the PSD function. Equation (3.8) is used for calculating the relevant spectral moments from a one sided PSD.

$$m_n = \int_0^\infty f^n G(f) df = \sum {f_k}^n G_k(f) \delta f \tag{3.8}$$

Where *G(f)* is the one sided PSD in units of Hertz and f the given frequency.

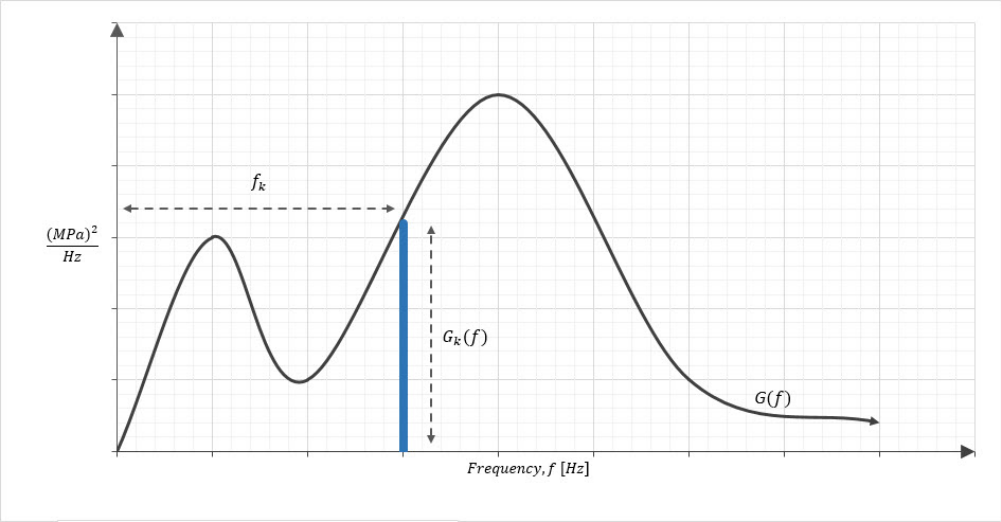

Figure 3.8: Calculating moments from response PSD

In theory an infinite number of moments can be calculated, but for fatigue analysis it is representative to only calculate the zeroth, first, second and fourth moment (m_0, m_1, m_2, m_4). SO Rice [12] developed in 1954 the important relation between the number of upward zero crossings per second, E[0], and number of peaks per second, E[P], for a random signal expressed by the spectral moments from a one sided PSD. The relation is shown in equations (3.9) and (3.10).

$$E[0] = \sqrt{\frac{m_2}{m_0}}; \quad E[P] = \sqrt{\frac{m_4}{m_2}} \tag{3.9}$$

$$\gamma = \frac{E[0]}{E[P]} = \sqrt{\frac{{m_2}^2}{m_0 m_4}} \tag{3.10}$$

γ is the irregularity factor which have a value between 0 and 1, depending on E[0] and E[P]. As γ converges towards 1, the process is considered narrow band. A pure narrow band response is easily identified by its characteristic single peaked PSD function.

The RMS value indicates how much "energy" the PSD function contains. The RMS is calculated by the square root of the zeroth moment, which basically is the integral of the single sided PSD, G(f).

$$rms = \sqrt{m_0} = \sqrt{\int_0^\infty G(f)df} \tag{3.11}$$

3.3.3 Probability Density Function

A *probability density function* (pdf) is used for storing response histogram information. For fatigue analysis the pdf of stress ranges is most used since stress response is of highest interest. The pdf of stress ranges has the annotation $p(S)$, and the random vibration fatigue calculation methods presented in this thesis are based on calculating pdf's of stress ranges.

3.3.4 Expected Fatigue Damage

Expected fatigue damage, *E[D]*, is calculated through equation (3.12), and is based on the calculation of the pdf of stress ranges.

$$E[D] = \frac{E[P] \cdot T}{k} \int_0^\infty S^m p(S) dS \tag{3.12}$$

By calculating the number of stress cycles, *N(S)*, the total fatigue life in seconds, T, can be estimated through equation (3.14).

$$N(S) = E[P] \cdot T \cdot p(S) \tag{3.13}$$

$$T = \frac{N(S)}{E[P] \cdot p(S)} \tag{3.14}$$

Where k and m are material fatigue parameters obtained from a S-N diagram.

3.3.5 Narrow-Band Method

The narrow band method was developed by Bendat in 1964 [13]. It was the first frequency domain method for predicting fatigue damage directly from a response PSD. A limitation of the method is that it is only suitable for a narrow band response, hence the name. The solution assumes that the pdf of stress amplitudes is equal to the pdf of peaks. When utilizing this method on a wide band response, the solution will be very conservative. The reason for this is that a wide band process is characterized by its positive troughs and negative peaks. The narrow band method ignores the positive troughs and negative peaks by matching all positive peaks with corresponding troughs even though they don't actually form stress cycles. In short terms, the narrow band method converts a wide band response to a narrow-band response.

$$p(S)_{NB} = \frac{S}{4m_0} e^{\frac{-S^2}{8m_0}} \tag{3.15}$$

$$E[D] = \frac{E[P] \cdot T}{k} \int S^m \cdot \left[\frac{S}{4m_0} e^{\frac{-S^2}{8m_0}} \right] dS \tag{3.16}$$

$$N(S) = E[P] \cdot T \cdot \left[\frac{S}{4m_0} e^{\frac{-S^2}{8m_0}} \right] \tag{3.17}$$

N is the expected number of cycles of stress range S over the period of T seconds. m_0 is the zeroth moment of the response PSD, *E[P]* is the expected number of peaks and the term inside the brackets is the *Rayleigh probability distribution.*

3.3.6 Steinberg Solution

Steinberg based the solution on the assumption that all stress cycles occur with no greater range than 6 RMS. The distribution of stress ranges follows a Gaussian or normal distribution (see table 3.2). The pdf of stress ranges is found through equation (3.18).

$$p(S)_S = 0.683 \cdot 2RMS + 0.271 \cdot 4RMS + 0.043 \cdot 6RMS \tag{3.18}$$

$$N(S) = E[P] \cdot T \cdot \begin{vmatrix} 0.683 \cdot 2RMS \\ +0.271 \cdot 4RMS \\ +0.043 \cdot 6RMS \end{vmatrix} \tag{3.19}$$

3.3.7 The Dirlik Method

The Dirlik method was developed by Dirlik in 1985 [14]. It is an empirical closed form expression for the pdf of rainflow ranges which was obtained using computer simulations to model the signals using the Monte Carlo technique. It is shown to be the most accurate method of calculating fatigue damage caused by vibrations for any process. The method is predicting fatigue life directly from a PSD based on its *nth* moments, m_n, and was theoretically verified by Bishop in 1988 [15].

The Dirlik formula for the pdf of stress ranges is given in equation (3.20).

$$p(S)_D = \frac{\frac{D_1}{Q}e^{\frac{-Z}{Q}} + \frac{D_2 Z}{R^2}e^{\frac{-Z^2}{2R^2}} + D_3 Z e^{\frac{-Z^2}{2}}}{2\sqrt{m_0}} \tag{3.20}$$

$$Z = \frac{S}{2\sqrt{m_0}}; \quad R = \frac{\gamma - x_m - D^2}{1 - \gamma - D_1 + {D_1}^2} \tag{3.21}$$

$$Q = \frac{5(\gamma - D_3 - (D_2 R))}{4D_1}; \quad x_m = \frac{m_1}{m_0}\sqrt{\frac{m_2}{m_4}} \tag{3.22}$$

$$D_1 = \frac{2(x_m - \gamma^2)}{1 + \gamma^2}; \quad D_2 = \frac{1 - \gamma - D_1 + {D_1}^2}{1 - R}; \quad D_3 = 1 - D_1 - D_2 \tag{3.23}$$

$$E[D] = \sum^{i} \frac{n_i}{N_i} = \sum^{i} \frac{E[P] \cdot T \cdot p(S_i)\ dS}{k \cdot {S_i}^{-b}} = \frac{T \cdot E[P]}{k} \int_0^\infty S^m \cdot p(S)\ dS \tag{3.24}$$

$$N(S_i) = E[P] \cdot T \cdot p(S_i)\ dS \tag{3.25}$$

3.4 Accelerated Vibration Testing

The methods of converting a random vibration event from the time domain to the frequency domain is discussed earlier. The signal represent a certain load condition depending on the environmental conditions during the physical measurements. When performing vibration fatigue analysis or testing on a component using this random signal as input load, the test engineer or analyst must decide for how long the component should withstand this type of load. If the original random signal represent a moderate vibration event, the test time required might be unreasonably long. In order to make the test more efficient and reduce operation cost the test can be accelerated by increasing the input acceleration PSD. It is very important that this accelerated test ensures that the same damage is being applied as if the component is in service. The methods presented are therefore only valid and acceptable within the specified limits.

3.4.1 Miner-Palmgren Hypothesis

The most common method of accelerating a input PSD in order to achieve a reduction in test duration is the Miner-Palmgren hypothesis [16] by using a fatigue-based power law relationship to relate exposure time and amplitude.

$$\frac{t_2}{t_1} = \Bigg[\underbrace{\frac{S_1}{S_2}}_{\text{exaggeration factor}} \Bigg]^m \tag{3.26}$$

t_1 = equivalent test time
t_2 = in-service time for specified condition
S_1 = RMS at test condition
S_2 = RMS at in-service condition
m = slope coefficient from S-N diagram

Alternatively equation (3.26) can be written in terms of the PSD function amplitudes at the certain frequency, f. This can often be more convenient since most random vibration events are already expressed on this form. The derived equation is shown in (3.27) below.

$$\frac{t_2}{t_1} = \Bigg[\underbrace{\frac{W(f)_1}{W(f)_2}}_{\text{exaggeration factor}} \Bigg]^{m/2} \tag{3.27}$$

$W(f)_1$ = PSD amplitude at test condition, g^2/Hz
$W(f)_2$ = PSD amplitude at in-service condition, g^2/Hz

By recommendations, the exaggeration factors should be within a certain value that is consistent with the constraints of in-service time and desired test time. In general should $S_1/S_2 \leq 1.4$ and $W(f)_1/W(f)_2 \leq 2.0$ in order to meet this requirement.

An alternative method is Halfpenny's method on synthesized PSDs for accelerated vibration testing [17]. This method builds on the theory of Biot's *shock response spectrum* (SRS), Miles' *extreme response spectrum* (ERS) and Lalanne's *fatigue damage spectrum* (FDS). This is a more extensive method that requires several calculation operations, but is proven to be more accurate than the Miner-Palmgren hypothesis.

3.4.2 Biot's Shock Response Spectrum

Biot [18] researched in 1932 the effect of earthquakes by assuming the response of a single degree of freedom (SDOF) system. The response is narrow band, and dominated by a single peak at the natural frequency of the system. The system behaves quasi-static at frequencies below the natural frequency, while the response is attenuated at frequencies

above the natural frequency. At the natural frequency the system responds dynamically and is amplified with a maximum response limited by damping in the system.

Although Biot did not know the actual natural frequency of the system in advance, he reasoned that he could create a response spectrum by sweeping the natural frequency and plotting maximum response over a range of natural frequencies. Biot [19] published in 1933 a paper on earthquake analysis, and used the term *Shock Spectrum* for the first time. This is now often referred to as the *Shock Response Spectrum* (SRS) and can be expressed as acceleration or displacement response. In context of fatigue analysis, it is the displacement response that is of highest interest because fatigue crack initiation and growth is a result of cyclic release of strain energy. The displacement response has a proportional connection with the energy that leads to fatigue failure, although in most cases it is the acceleration that is providing the input load to the system.

The SRS is given by equation (3.28) for an undamped system, and (3.29) for a damped system.

$$S_A = \left|\omega \int_0^t \ddot{u}_b(\tau) sin\omega(t-\tau) d\tau\right|_{max} \quad \text{undamped system} \tag{3.28}$$

$$S_A = \left|\omega \int_0^t \ddot{u}_b(\tau) e^{-\xi\omega(t-\tau)} sin\omega(t-\tau) d\tau\right|_{max} \quad \text{damped system} \tag{3.29}$$

3.4.3 Miles' Extreme Response Spectrum

Miles [20] presented in 1953 an equation where he derived a spectrum of the RMS acceleration response to a random input PSD applied to a SDOF system with the natural frequency, f_n. The formula is given in equation (3.30). Halfpenny [8] showed a modification of this formula which gives the corresponding displacement spectrum shown in equation (3.31).

$$G_{\ddot{X}RMS}(f_n) = \sqrt{\frac{\pi}{2} \cdot f_n \cdot Q \cdot G_{\ddot{Z}}(f_n)} \tag{3.30}$$

$$G_{XRMS}(f_n) = \frac{G_{\ddot{X}RMS}(f_n)}{(2\pi \cdot f_n)^2} \tag{3.31}$$

Where $G_{\ddot{Z}}(f_n)$ is the acceleration input PSD amplitude at frequency f_n and Q is the dynamic amplification factor.

Miles suggested using the Gaussian approximation to the amplitude distribution in order to estimate the extreme response. And by multiplying the spectrum with for instance the factor 3, the statistical 99.97% highest local amplitude acceleration or displacement response can be estimated.

Bendat [13] found in 1964 that the amplitude distribution for a narrow band response is not Gaussian, but Rayleigh distributed. Lalanne [21] came in 1978 up with a refinement to Miles equation by substituting the Rayleigh probability function. Lalannes equation (3.32) is known as the *maximax response spectrum* (MRS) or the *extreme response spectrum* (ERS), and gives the most likely extreme response amplitude of a SDOF system excited by a random input PSD for a time span of T seconds. Halfpenny [8] showed the modified expression in terms of displacement, equation (3.33).

$$ERS_{acc}(f_n) = \sqrt{\pi \cdot f_n \cdot Q \cdot G_{\ddot{Z}}(f_n) \cdot ln(f_n \cdot T)} \tag{3.32}$$

$$ERS_{disp}(f_n) = \frac{ERS_{acc}(f_n)}{(2\pi \cdot f_n)^2} \tag{3.33}$$

The ERS is similar to the time domain SRS. Even though both spectra in essence is providing the same information, SRS is most used for determining the maximum response to a transient shock of high damage to the system, where ERS is used for estimating the expected response to a long lasting vibration loading.

3.4.4 Lalanne's Fatigue Damage Spectrum

Lalanne [22] proposed in 2002 the *fatigue damage spectrum* (FDS) whilst working on the ERS hypothesis. This was a continuation of initial work of Bendat and Rice with purpose of determining fatigue damage from a response PSD of stress directly. Lalanne came up with a closed form calculation for the FDS directly from the acceleration PSD, given in equation (3.34).

$$FDS(f_n) = f_n \cdot T \cdot \frac{K^b}{C} \cdot \left[\frac{Q \cdot G_{\ddot{Z}}(f_n)}{2(2\pi \cdot f_n)^3}\right]^{\frac{b}{2}} \cdot \Gamma\Big(1 + \frac{b}{2}\Big) \tag{3.34}$$

$$\Gamma(g) = \int_0^\infty x^{(g-1)} \cdot e^{-x} dx \tag{3.35}$$

Where K is the stiffness of the system, $\Gamma()$ is the Gamma function defined by equation (3.35), b and C are fatigue parameters describing the Wöhler line from a S-N diagram.

The total lifetime fatigue damage is found by summing all FDS over the life of the component.

3.4.5 Halfpenny's Synthesized PSD

The method for accelerated frequency domain testing based on the FDS and SRS for creating a synthesized PSD was presented by Halfpenny in 2006 [8] [17]. Halfpenny have used this method in a number of projects with considerable success, and can be further studied in *Mission Profiling and Test Synthesis Based on Fatigue Damage Spectrum* [23]. He found the relationship between the FDS, SRS and ERS in context of accelerating an input PSD for testing.

By inverting equation (3.34) the synthesized test PSD is obtained, shown in equation (3.36).

$$G_{synth}(f_n) = \frac{2(2\pi \cdot f_n)^3}{Q} \cdot \left[\frac{k \cdot \Sigma FDS(f_n) \cdot C}{K^b \cdot f_n \cdot T_{eq} \cdot \Gamma(1 + {}^b/_2)} \right]^{2/b} \tag{3.36}$$

Where $\Sigma FDS(f_n)$ is the lifetime FDS, T_{eq} is the required test duration and k is the combined factor of safety. k is the product of the safety factor obtained from equations below depending on whether a Gaussian-normal or Log-normal distribution is assumed.

Gaussian-normal probability:

$$k = \frac{1 + \sqrt{1 - (1 - a'^2 \cdot {V_R}^2) \cdot (1 - a'^2 \cdot {V_E}^2)}}{(1 - a'^2 \cdot {V_R}^2)} \tag{3.37}$$

$$k_{test} = 1 + \frac{a'}{\sqrt{n} \cdot V_R} \tag{3.38}$$

Log-normal probability:

$$k = exp\left\{ a'^2 \cdot \sqrt{ln[(1 + {V_E}^2)(1 + {V_R}^2)]} - ln\left[\sqrt{\frac{1 + {V_E}^2}{1 + {V_R}^2}} \right] \right\} \tag{3.39}$$

$$k_{test} = exp\left\{ \frac{a'}{\sqrt{n}} \cdot \sqrt{ln(1 + {V_R}^2)} \right\} \tag{3.40}$$

Where *a'* is the probability of success (1 - probability if failure), σ_R is the standard deviation of strength, and σ_E is the standard deviation of loading environment damage.

$$\text{Variability of strength} \quad V_R = \frac{\sigma_R}{\bar{R}} \tag{3.41}$$

$$\text{Variability of loading environment damage} \quad V_E = \frac{\sigma_E}{\bar{E}} \tag{3.42}$$

These statistical factors of safety are necessary in order to account for applied load variations and variations in fatigue strength of the component.

The synthesized test PSD can be verified and investigated by comparing test FDS with the lifetime FDS. As well as test ERS should be compared with the ERS and SRS measured over the lifetime of the component. In order to ensure that all likely maximum values are covered in the test, the test ERS should ideally be greater than the lifetime ERS. But at the same time be less than the lifetime SRS in order to reduce the risk of failure due to unlikely high loading conditions during the test.

4. Vibration Testing

4.1 Vibration Testing Procedure

Common procedure for physical vibration testing is to first perform a sine-sweep test. The load is represented by a sinusoidal with constant 1G amplitude over a frequency range. By measuring acceleration and displacement the response amplification is found. If there are no extreme amplifications in the system, a random vibration test is then performed with a certain input PSD load curve. Where the input PSD is either derived from physical measurements, customer spec or design standard. Following function testing of the component are necessary to check whether it could withstand the random vibration load or not.

By performing random vibration tests with strain gauges makes it possible to obtain a strain response PSD from the test. A stress response PSD can then be achieved and it is possible to perform fatigue calculations of the component. The expected damage calculated is then the damage occurred within the specified test duration.

4.1.1 Fixture Requirements

The dynamic behaviour of a vibration test fixture is critical for the outcome of the test. The ideal test fixture will transmit the vibration motion from the shaker table to the test object with zero distortion at all frequencies within the test range. It is important that the fixture itself does not amplify or reduce the dynamic response of the test object. General rule of thumb is to have a fixture design which first eigenfrequency is twice the maximum test frequency.

Center of gravity should always be as low as possible and located as close to the center axis of the shaker table as possible in order to reduce risk of inducing bending loads. This is specially important for a single-axis operating shaker table as illustrated in figure 4.1.

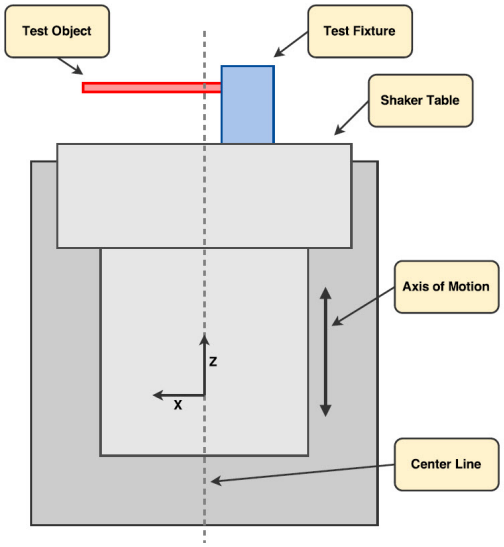

Figure 4.1: Illustration of single-axis shaker table

Important factors when designing a fixture for vibration testing

- **Mass** - Low weight and low center of gravity.
- **Stiffness** - First eigenfrequency should be twice max test frequency.
- **Positioning** - Center of gravity at the center axis of shaker table.
- **Dynamic behaviour** - Investigate mode shapes and response amplification within the scheduled test frequency range.

4.1.2 Placement of Sensors

Typical sensors used for vibration testing are accelerometers of either single-axis or multi-axis type, depending on the desired output measurement data. For vibration fatigue testing additional use of strain gauges are required in order to measure strain during the test period.

Depending on the type of vibration testing to be executed, an eigenfrequency analysis of the component and visualizing the mode shapes gives an approximate indication of where to place sensors.

This can be sufficient enough for a SSD sine-sweep type of vibration test where the load amplitude is constant over the entire frequency range.

For a random vibration test where the input load amplitude is varying at different frequencies. The dynamic response can be very much different compared with the response during a sine-sweep test.

It will in this case be necessary to perform either a random response or SSD analysis and obtaining the response PSDs of acceleration and displacement. Resonance frequencies are identified by distinctive peaks in the response plot. Each resonance frequency have a corresponding mode shape. Response peaks located at non-resonance frequencies will not have a related mode shape.

By knowing the excited mode shapes, it is also possible to accurately place sensors in regions of interest. Critical stress regions will be identified through a RMS stress plot. These regions are then labeled and mounted strain gauges to monitor strain during the test.

5. Designing The Problem

A test design for performing both physical vibration testing and linear dynamic analyses were created. The model design is intended to be very simple in order to easily identify critical regions and dynamic behaviour. The model were designed based on the following criteria:

- **Manufacturability** - Both fixture and test object(s) should be easy and cheap to manufacture.
- **Tuneability** - It should be possible to test different test objects of various geometry.
- **Weight** - The overall weight of the complete assembly should be low in order to reduce risk of overloading the shaker table.
- **Stiffness** - The fixture must be stiff enough in order to isolate the test object(s).
- **Complexity** - The test object(s) should have distinct stress concentration regions and have various dynamic behaviour.

5.1 Test Object Design

Four test object designs were decided, all manufactured in the same material but with different geometry. The specifications are given in table 5.1. The purpose of different test objects is to investigate the dynamic response and behaviour for different geometries. Mechanical drawings are presented in appendix C.

Test object specifications

Name	Thickness	Material	Description
TP04	4mm	6082-T6	Straight plate with no cutouts
TP04C	4mm	6082-T6	Circular cutouts at center of length
TP06	6mm	6082-T6	Straight plate with no cutouts
TP06C	6mm	6082-T6	Circular cutouts at center of length

Table 5.1: Test object specifications

Variable	Value
ρ	2.7E-09 Mg/mm^3
E	69000 MPa
ν	0.35
K	361.86 MPa
m	0.14183

Table 5.2: Material properties of 6082-T6

5.2 Fixture Design

The fixture consists of two parts. A base which is bolted onto the shaker table, and a top which secures the test plates by clamping them together. To reduce test time the fixture can hold two test objects at the time, provided equal thickness. Mechanical drawings are presented in appendix C.

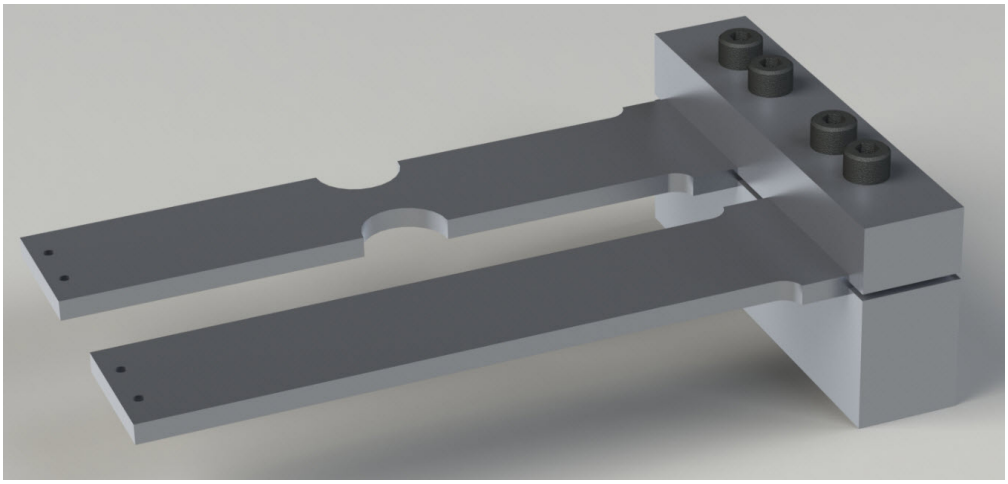

Figure 5.1: CAD rendering of test design

For the analysis performed in this thesis, where the frequency range is 0 to 2000 Hz, the first eigenfrequncy of the fixture should, according to previous statement, be at 4000 Hz or higher. A frequency analysis were performed on the fixture design to check the eigenfrequencies. Result is shown in table 5.3 below.

Mode	Frequency [Hz]
1	5264.1
2	6607.5
3	8658.5
4	10756
5	12084

Table 5.3: Fixture eigenfrequencies

The results shows that the first eigenfrequency are above the stated lower limit.

A second analysis of the fixture were performed. Now with added rigid body point mass representing the mass of two test objects.

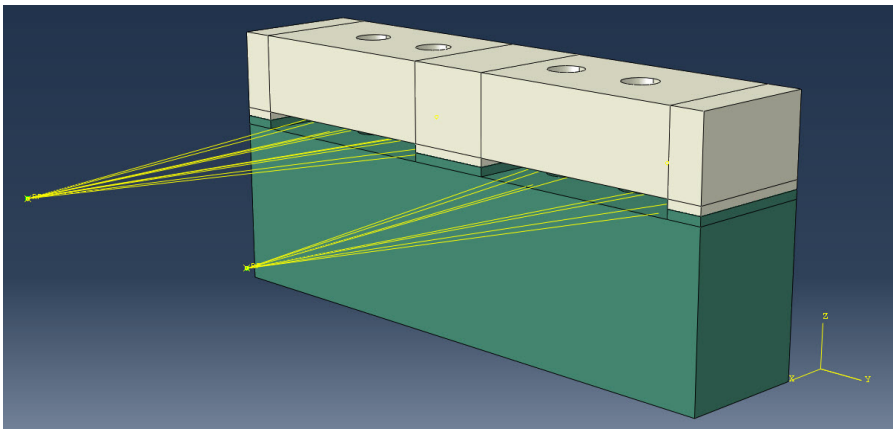

Figure 5.2: Analysis including two point masses

Mode	Frequency [Hz]
1	2132.6
2	2616.0
3	3295.1
4	3945.3
5	7499.2

Table 5.4: Fixture eigenfrequencies with two point masses

The first eigenfrequency are almost within the test frequency range when including two point masses presenting the heaviest test objects, TP06. This will most certainly affect the dynamic response and result in unpredictable results.

A third eigenfrequency analysis were performed by including only one test object. The eigenfrequencies are listed in table 5.5.

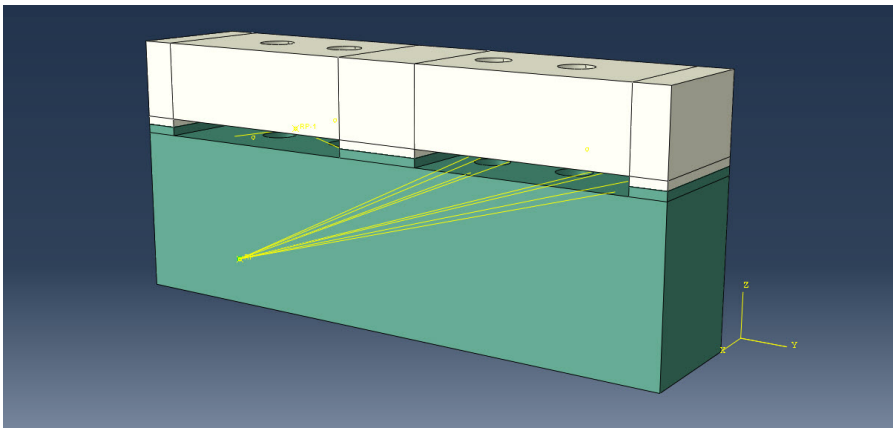

Figure 5.3: Analysis including single point mass

Mode	Frequency [Hz]
1	2423.7
2	3265.4
3	7273.0
4	9265.8
5	11451.0

Table 5.5: Fixture eigenfrequencies with single point mass

The eigenfrequencies are still drastically reduced compared with the first eigenfrequency analysis. The first eigenfrequency is located above the test frequency range, but can affect the dynamic response of the system. This will be investigated when outputting analysis results.

6. Linear Dynamic FE Analysis

The most common procedures for random vibration analysis in the FEA environment are steady-state dynamics and random response types of analysis. Both analysis procedures will in essence achieve the same results depending on the input variables, requested outputs and post-processing methods.

This chapter describes how the system was defined and how to perform linear dynamic analyses in Abaqus/CAE using Abaqus/Standard with input loads in form of random vibrations. The object is to compare results obtained from SSD and random response.

6.1 Pre-Processing Input Data

6.1.1 Units

Abaqus/CAE is a "unitless" system, where it is up to the user to define the units. It is important to keep this in mind and always be consistent when specifying inputs and variables in order to get correct output units. Table 6.1 below shows the unit system used.

Quantity	**Unit (SI)**
Length	mm
Force	N
Mass	$10^6 g$ (Mg)
Density	Mg/mm^3
Stress	MPa
Time	sec
Energy	$10^{-3} J$ (mJ)

Table 6.1: Units used in analysis

6.1.2 Mesh

In order to find a suitable mesh type and density for the model, a mesh convergence test was performed. The mesh convergence test is here used to check which mesh that gives best results with regard of bending. The object is to measure tip displacement for a cantilever beam subjected to a vertical static load at the freely moving end. By comparing the measured tip displacement with the theoretical maximum static tip displacement gives an indication of mesh quality. All measured values and total CPU time are given in table A.1 in appendix A.1. The table gives a good overview of which element definitions that will result in both accurate and efficient analysis.

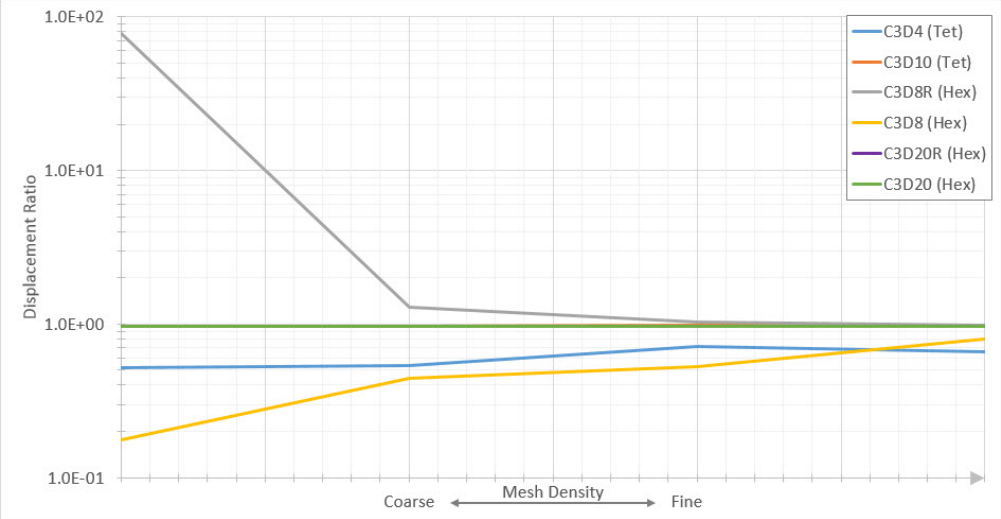

Figure 6.1: Mesh convergence plot

The test shows that the 4-node linear tethrahedron elements (C3D4) are not suitable because it is to stiff, even for high mesh density and small elements. 10-node quadratic tethrahedron elements (C3D10) gives good results for coarse mesh density, but is significantly slower and less effective than most of the hex element types with same density.

The 8-node hex element with reduced integration (C3D8R) gives good results if the mesh density is relatively fine, and have at least 4 elements through the thickness. The 20-node hex element with reduced integration (C3D20R) is not as vulnerable for number of elements through the thickness, and gives good results even with a more coarse mesh density. The table below shows the two best element definitions where both displacement deviation and total CPU time are considered as important factors.

Element Definition	Deviation	Tot CPU Time [sec]
C3D8R (50x10x4)	3.4 %	2.1
C3D20R (40x8x2)	2.8 %	4.3

Table 6.2: Mesh types suitable for analysis

Most linear dynamic analysis procedures are mode-based. It is therefore important to use high enough mesh density to give an accurate representation of the mode shapes associated to the structure's natural frequencies. Figure 6.2 shows the difference between a coarse and fine mesh, where it is obvious that the fine mesh gives a better visualisation of the mode shape and will result in a better representation of the system's response.

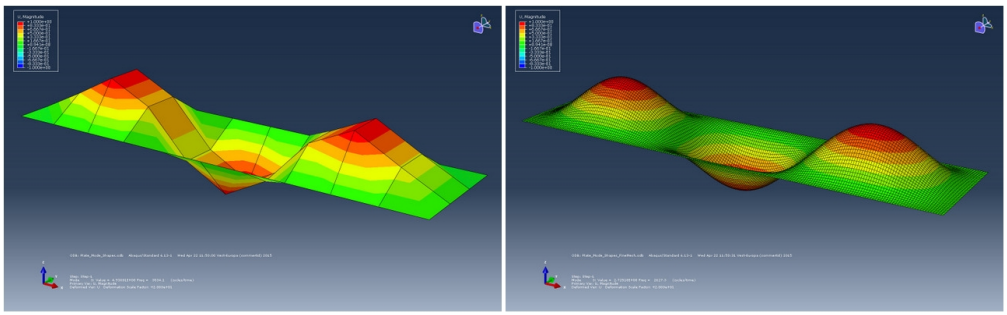

Figure 6.2: Mesh density and mode shape

6.1.3 Boundary Conditions

The shaker table is assumed to be infinitely stiff compared to the fixture. A fixed boundary condition is applied at the surface where the fixture is in contact with shaker table. The definition of the boundary condition is given in equation (6.1) and applied to the surface shown in figure 6.3.

$$U1 = U2 = U3 = UR1 = UR2 = UR3 = 0 \tag{6.1}$$

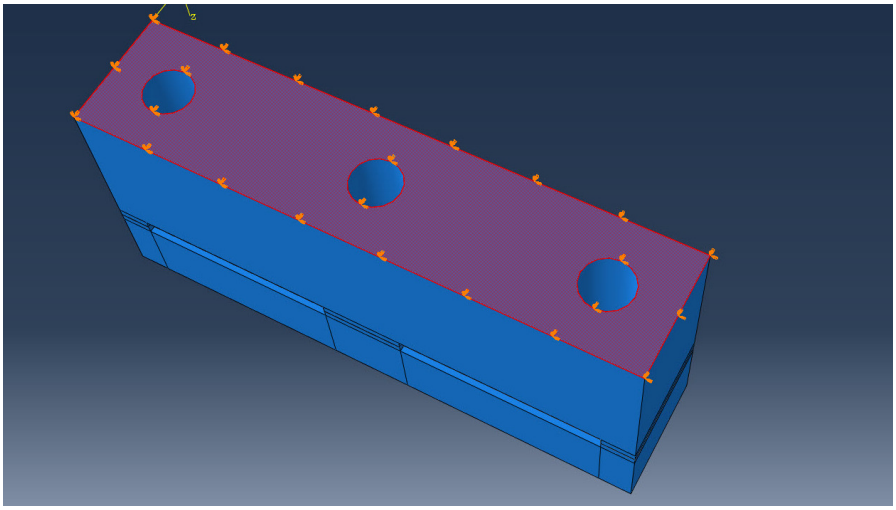

Figure 6.3: Fixed boundary condition region

This means that all nodes at the surface will have zero relative displacement. Which in reality is not perfectly representable, but assumed sufficiently accurate for the purpose of the analysis.

6.1.4 Constraints

The parts interact by a surface-to-surface mesh tie constraint. Active degrees of freedom and translational and rotational motion is equal for the surface pairs. Surface pairs are composed by a slave and master surface, where nodes are tied only when inside the position tolerances defined in the tie constraint properties.

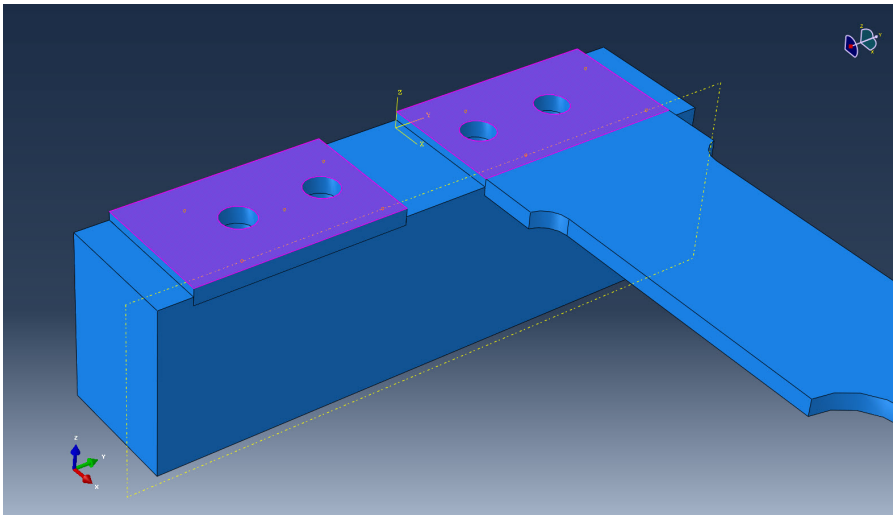

Figure 6.4: Slave surfaces

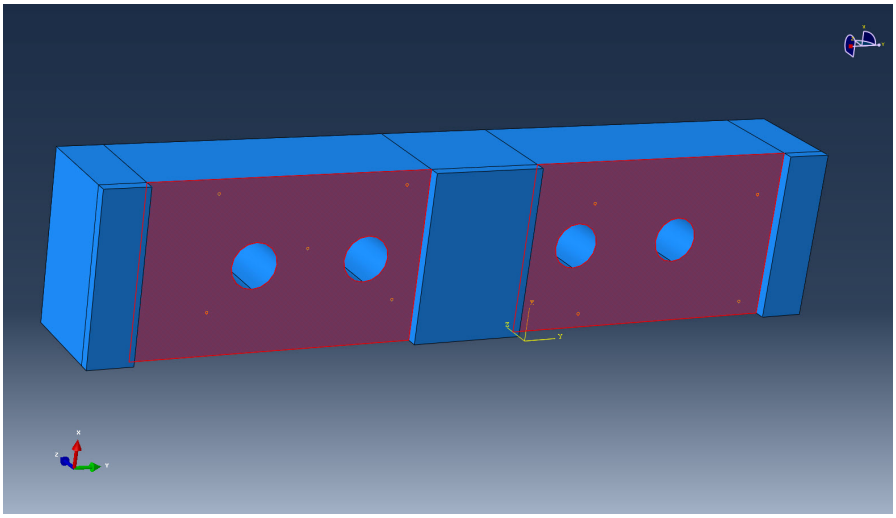

Figure 6.5: Master surfaces

6.1.5 Load Case

The stationary random vibration load is defined according to the input PSD in table 6.3 and figure 6.6. The PSD data origins from the transformed random signal in previous section 3.2.2.

Real [G^2/Hz]	**Imaginary**	**Frequency [Hz]**
0	0	50
0.02	0	50
0.03	0	500
0.03	0	2000

Table 6.3: Input PSD definition

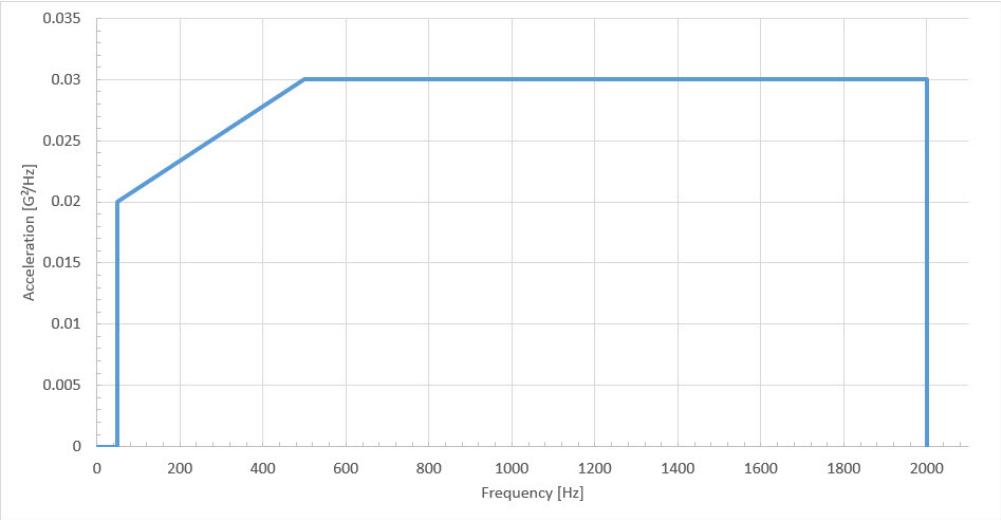

Figure 6.6: Input PSD plot

6.2 Performing Modal Analysis in Abaqus/CAE

This section gives a detailed step-by-step description of how to perform both a random response and SSD analysis in Abaqus/CAE. Although the user interface will be different depending on the analysis software being used, but as mentioned before, the methods of performing these analyses are often very similar.

6.2.1 Eigenvalue Extraction

As mentioned in section 2.2 earlier, all linear perturbation steps requires an initial frequency or eigenvalue extraction step. In the step editor window the eigensolver and frequency range are user specified parameters. The eigensolver type must be chosen according to the problem size. For this specific problem size, solver type Lanczos is used.

It is critical that the specified frequency range is defined according to the SSD or random response step frequency ranges. Frequencies to be extracted can either be defined by number of requested eigenmodes, or by a start and end frequency. This is up to the user to choose, but it can be beneficial to define the frequency range by a start and end frequency to ensure that all natural frequencies are covered for the following step.

6.2.2 Steady-State Dynamics

A mode-based SSD step is created by choosing *linear perturbation* and *steady-state dynamics, modal* in the create step dialog box. Frequency range, number of points, bias and damping is specified in the step editor.

Figure 6.7 shows the main steps for performing a SSD fatigue analysis in Abaqus/CAE.

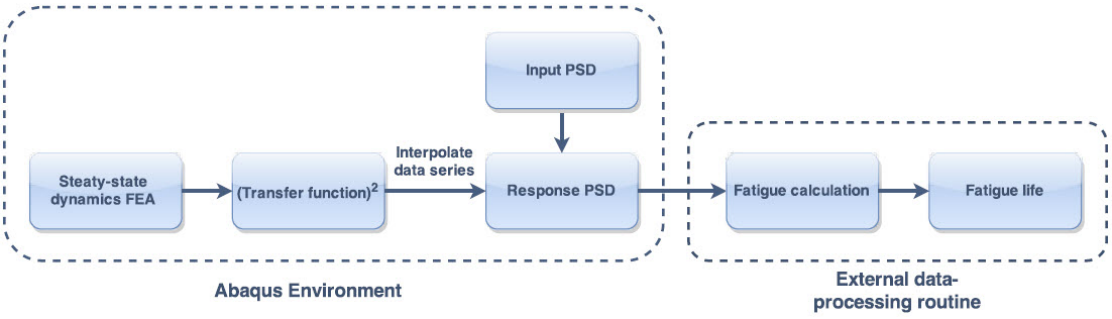

Figure 6.7: Steady-state dynamics procedure

The step editor

The frequency range is simply set by a start and stop frequency value. Note that the range can not exceed the frequency range specified in the previous eigenvalue extraction step. This because the mode-based SSD is entirely dependant on the system's eigenfrequencies and modes in order to calculate the response.

The number of points defines the output resolution. Higher value gives more calculation points and denser output response curves. By default this is set to 20, which means that the interval between mode n and mode $n+1$ is divided into 20 calculation points.

The bias parameter alter the spacing between the points, where a bias of 1 gives equal spacing in the entire interval and bias above 1 gives closer spacing towards the eigenfrequencies. Typical values are 20 to 50 number of points and bias value of 3 to 5.

Damping can either be defined as direct modal, composite modal, Rayleigh or structural specified over a range of modes or frequencies. For this analysis direct modal damping is chosen for a range of frequencies. The damping is set to be equal over the entire range by setting the critical damping fraction, ξ, for the system.

Variable	**Value**
f_1	1 Hz
f_2	2000 Hz
N o P	50
Bias	3
ξ	0.04
Load	9810 mm/s^2 (sine-sweep)

Table 6.4: Input variables for SSD analysis

Specifying the input load

The load is specified by a acceleration base motion and a tabular input where the frequency spectrum is defined. The range of the sine-sweep and amplitude is respectively set to 0-2000 Hz and 9810 (mm/s^2).

Base motions are applied as a boundary condition. The degree-of-freedom decides in which direction the base motion will act. Abaqus automatically finds the previous defined fixed boundary condition and use this as the base where the motion is to be applied. The amplitude can be scaled by a factor, and is here set to default value of 1.

Defining output requests

In mode-based SSD analysis the output variables are complex values with real and imaginary components. It is therefore important to choose *magnitude* for numeric form in the result options in order to plot the absolute valued response curve used for post-processing and fatigue life calculation. Either max principal or Von-Mises stress at an integration point can be outputted. Acceleration and displacement response is plotted to visualize the dynamic behaviour of the system.

The direct output from a SSD analysis is on transfer function form, and must be squared and then multiplied with the input PSD to obtain the response PSD. The stress response PSD is exported to an external data processing routine in order to perform fatigue life calculation.

6.2.3 Random Response

The random response analysis setup procedures are very similar to SSD. The step is created by choosing *linear perturbation* and *random response* in the create step dialog box.

Figure 6.8 shows the main steps for performing a random response fatigue analysis in Abaqus/CAE.

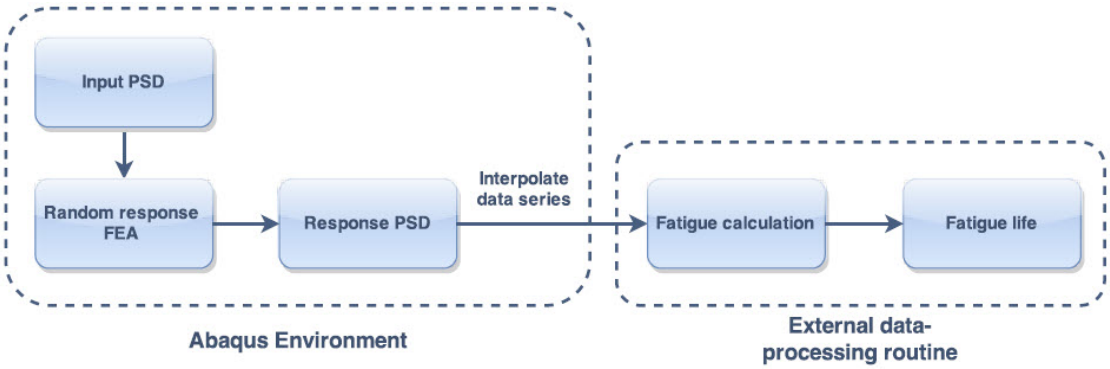

Figure 6.8: Random response procedure

The step editor

The frequency range, number of points, bias and damping is specified similar to the SSD step.

Variable	Value
f_1	1 Hz
f_2	2000 Hz
N o P	50
Bias	3
ξ	0.04
Input Load	PSD-definition

Table 6.5: Input variables for random response analysis

Specifying the input load

As opposed to the input load for a SSD analysis (sine-sweep), the input load is now defined directly by the input PSD function. The input PSD is created as a *PSD definition* type amplitude. Specification units is set to *gravity (base motion)* with reference gravity of 9810 (mm/s^2). Both real and imaginary values at each frequency can be used. In most cases only real values are defined, and the imaginary column is left with zeros.

The base motion is applied in the same way as for the SSD analysis. But for a random response analysis the cross-correlation between applied nodal loads or base motions can be specified as *correlated* or *uncorrelated*, as well as scaling factor of real and imaginary values. The correlation type is not of importance for this case since there is only one acting load on the system.

Defining output requests

Random response analysis calculates the PSDs and corresponding RMS values of response variables directly. These variables are displacement, acceleration, strain, stress etc. A disadvantage with random response compared with SSD is that it is not possible to output max principal stress, only in-plane stress presented in the global coordinate system. But at the same time it is possible to create a RMS color plot of stress showing critical regions in the model where fatigue most likely will occur.

Good practice is to first run a random response analysis and create a RMS stress color plot, then taking notice of critical elements and run a SSD analysis with max principal stress response output from critical regions.

6.3 Post-Processing Output Data

Many FEA applications does not have an embedded fatigue analysis module. Output data must then be post-processed in an external data processing routine. This section will address the steps from modifying and exporting data from Abaqus/CAE and creating response PSD curves of displacement, acceleration and stress.

6.3.1 Eigenvalue Extraction

The *.dat* file which is automatically generated when submitting an analysis contains data from the solved eigenvalue problem. Eigenvalues, modal participation factors and effective modal mass for the modes within the specified range are presented here.

6.3.2 Steady-State Dynamics

When executing a SSD analysis the input is sinusoidal with amplitude of 1G. The output from a SSD analysis is the transfer function, described in section 3.3.1, on response-per-input form.

In order to calculate the response PSD for the system, the transfer function is squared and multiplied with the input PSD. It is important that *df* is constant for all data series, which in most cases requires interpolation of the data. This can be done directly in Abaqus visualization module by choosing *create XY data* and *operate on XY data*.

6.3.3 Random Response

A random response type analysis gives outputs on PSD form directly. Stress output available is in-plane stress variables, which for fatigue analysis is not directly applicable. The main advantage of the random response analysis is the possibility to output the RMS values of available response variables.

7. FEA Results

From performing eigenvalue analysis on the fixture, all analyses are performed with only one test object. This results in four analysis cases, where both random response and SSD procedures was performed.

The results presented are from analysis of model TP04C, where results for the other models are presented in appendix B, *Linear Dynamic FEA Results*.

Figure 7.1 shows the CAD model submitted for analysis.

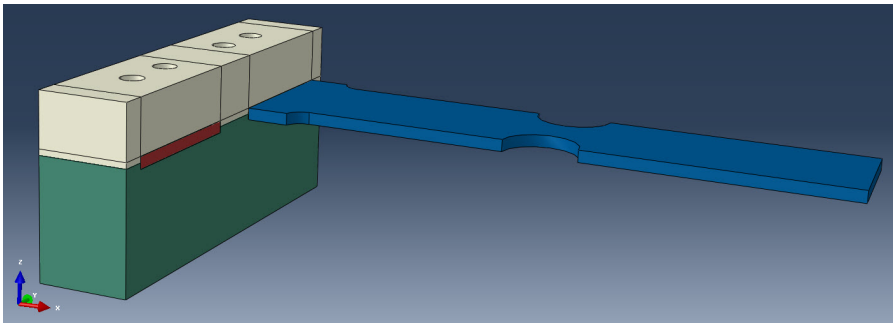

Figure 7.1: CAD model showing fixture and TP04C

7.1 Eigenvalue Extraction Data

Tables 7.1 to 7.3 shows the eigenvalue output for model TP04C. For this model there are five eigenmodes within the specified frequency range. The modal participation factors and effective modal mass are presented with regard of the global coordinate system.

Eigenvalue Output (TP04C)

Mode	Eigenvalue	Frequency [Hz]	Generalized Mass
1	2.43783E+05	78.582	1.98971E-05
2	8.83401E+06	473.04	2.35153E-05
3	1.40013E+07	595.53	1.77448E-05
4	2.01852E+07	715.05	1.18218E-05
5	7.39362E+07	1368.5	2.27777E-05

Table 7.1: Eigenvalue output

Modal Participation Factors (TP04C)

Mode	X-Comp	Y-Comp	Z-Comp	X-Rot	Y-Rot	Z-Rot
1	-5.63941E-03	3.80836E-04	1.5393	38.481	-276.63	8.52601E-02
2	4.32105E-02	-6.23223E-03	-0.83481	-20.862	64.767	-1.3140
3	1.19689E-03	1.5398	-3.10521E-03	-3.0494	0.34381	289.26
4	-5.18287E-04	-8.82132E-03	-3.40665E-04	24.924	2.49889E-02	-1.3395
5	-0.20145	-6.86862E-04	0.51760	12.925	-30.031	0.38450

Table 7.2: Modal participation factors

Effective Modal Mass (TP04C)

Mode	X-Comp	Y-Comp	Z-Comp	X-Rot	Y-Rot	Z-Rot
1	6.32786E-10	2.88580E-12	4.71437E-05	2.94631E-02	1.5226	1.44638E-07
2	4.39067E-08	9.13350E-10	1.63880E-05	1.02342E-02	9.86406E-02	4.05991E-05
3	2.54203E-11	4.20711E-05	1.71101E-10	1.65009E-04	2.09757E-06	1.4848
4	3.17560E-12	9.19923E-10	1.37196E-12	7.34397E-03	7.38207E-09	2.12108E-05
5	9.24344E-07	1.07461E-11	6.10237E-06	3.80497E-03	2.05422E-02	3.36750E-06
TOTAL	9.68912E-07	4.20729E-05	6.96342E-05	5.10112E-02	1.6418	1.4849

Table 7.3: Effective modal mass (Mg)

Because the random vibration is a vertically applied excitation, the effective modal mass in z-direction will obviously be of great importance. Table 7.3 shows the first two modes are dominated by vertical motion, which is the most critical because of strain build-up due to the geometry of the model. But also motion in y-direction can have significant effect if present. This is seen at the third mode, where a large part of the relative mass is present. By plotting acceleration and displacement for each direction at a specific node the actual motion behaviour of the model can be studied in detail. This is presented in the next section.

7.2 Modal Analysis Results

7.2.1 RMS Plots

RMS of response variables are obtained from a random response analysis. Critical stress concentration regions are detected plotting RMS of stress for the entire model. RS11, RMS of stress in the longitudinal direction (x-direction), is most critical. Figure 7.2 shows RS11, where red color is indicating high stress values. RMS of in-plane stress at critical point for the corresponding directions is shown in figure 7.3.

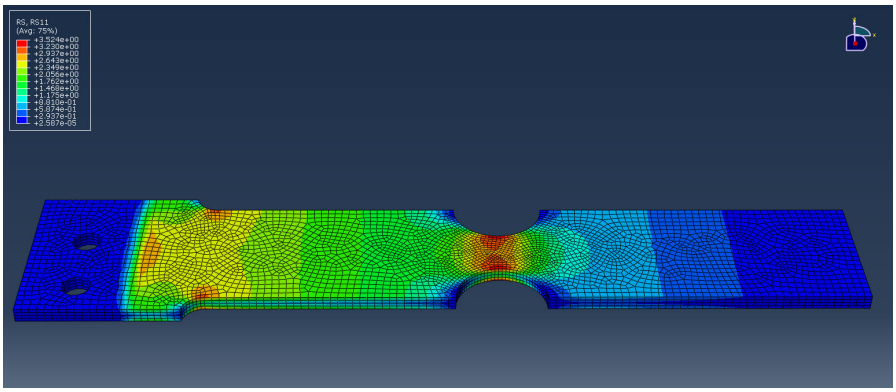

Figure 7.2: RS11 color plot

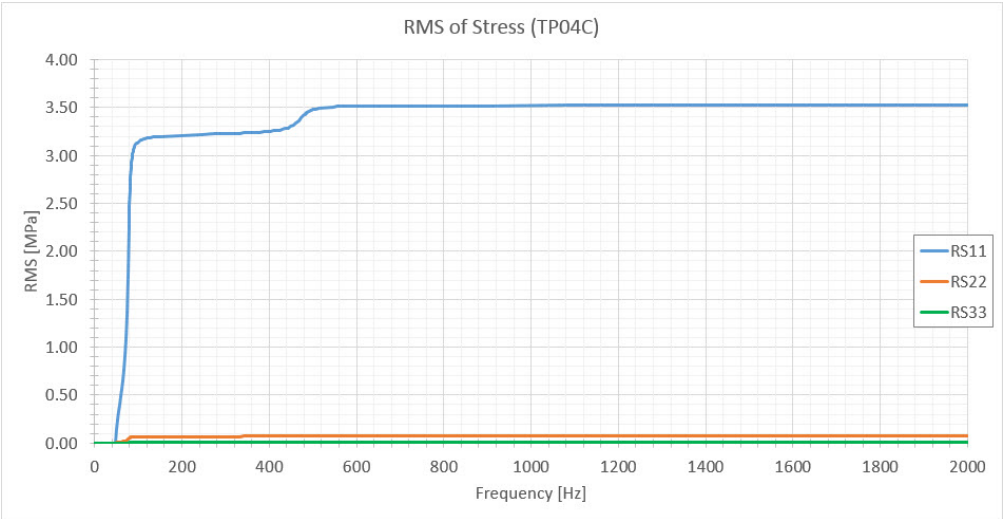

Figure 7.3: RMS of stress at critical integration point

7.2.2 Transfer Functions

Resonance frequencies are shown as distinctive peaks in the response plots. From studying the eigenvalue output and effective modal mass the peaks are expected to appear, where the first eigenfrequency is resulting in highest acceleration response amplitude.

The acceleration transfer function obtained from the SSD analysis shows acceleration output per input load. Since the input load is defined with units of mm/s^2, the output is also presented in units of mm/s^2. Dividing output on gravitational constant (g = 9810 mm/s^2) over the entire frequency range, shows acceleration in units of G per input G, figure 7.4.

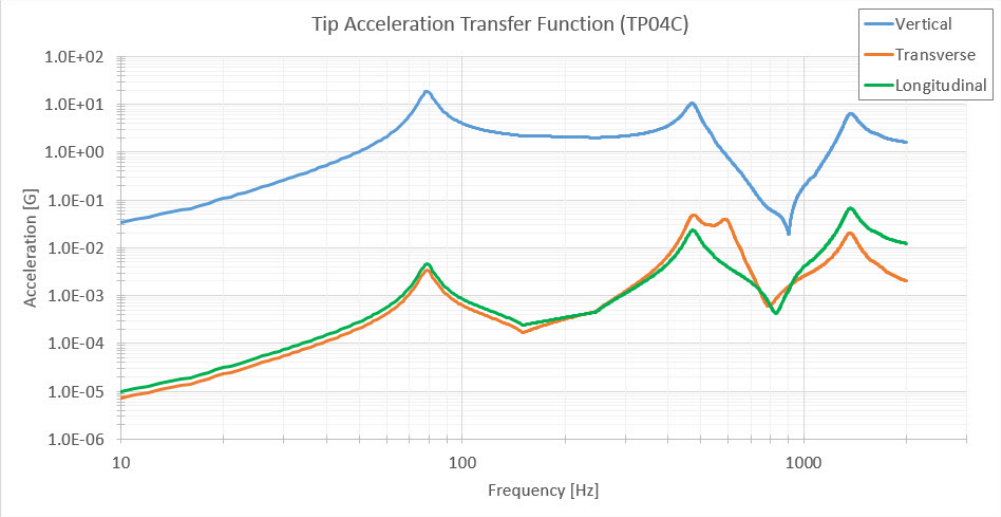

Figure 7.4: Acceleration transfer function (G/G) (log-log)

Since the input load is 1G, the acceleration amplification is shown by dividing the response by 1, figure 7.5. The valleys located in the interval of 900 to 950 Hz shows anti-resonance in the system.

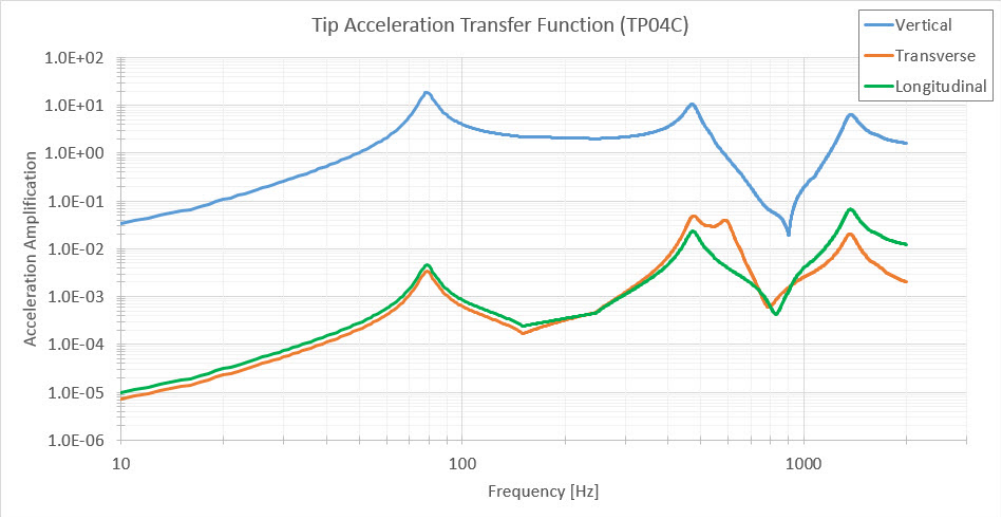

Figure 7.5: Tip acceleration amplification (log-log)

Since the specimen has a circular cut-out in the middle region, both vertical and transverse motion will result in stress contributions. As expected, the vertical acceleration amplification is the most significant and have a peak amplitude at the first resonance frequency of almost 20 G at the tip.

The displacement transfer function is shown in figure 7.6 and shows displacement response in all three directions at the tip of the specimen. The tip displacement plot is following the same trend as the acceleration plot, with a predominant peak at the first eigenfrequency.

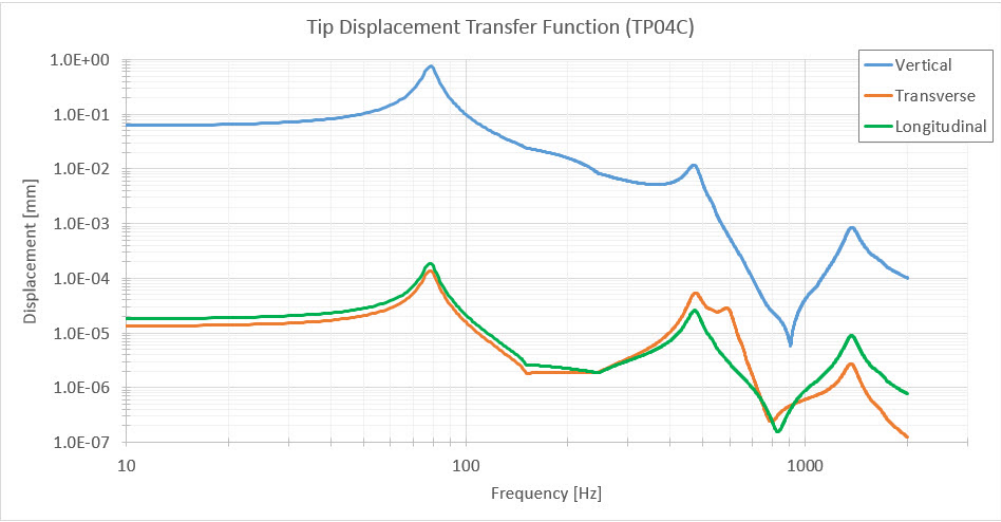

Figure 7.6: Displacement transfer function (mm/G) (log-log)

The resulting max principal stress transfer function is plotted in figure 7.7 below and shows the resulting stress at the most critical point of the specimen subjected to the 1G input load. The critical point is located from the RMS color plot (figure 7.2).

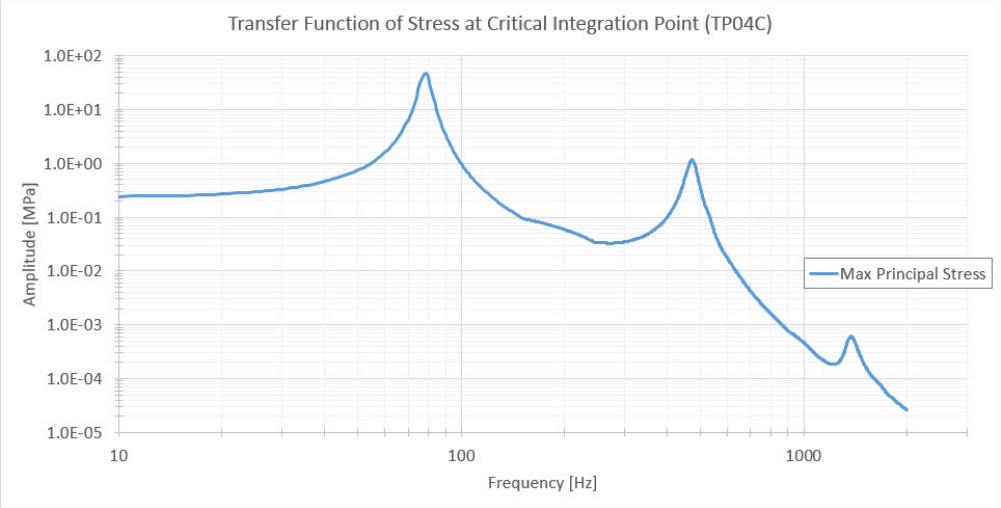

Figure 7.7: Max principal stress (MPa/G) (log-log)

The plot shows that the greatest stress contribution in the specimen occurs at the first resonance frequency, which is expected from studying the acceleration and displacement response.

7.2.3 Response PSDs

All following response PSDs are plotted for both random response and SSD analysis procedures. The red dotted line corresponding to random response values, and blue solid line corresponding to SSD values.

Both curves match for most frequencies inside the range, but some deviations are present at certain frequencies. This is a common phenomenon related to the individual interpolation of the discrete data series. The deviations are here denoted as insignificant, and accepted for further processing.

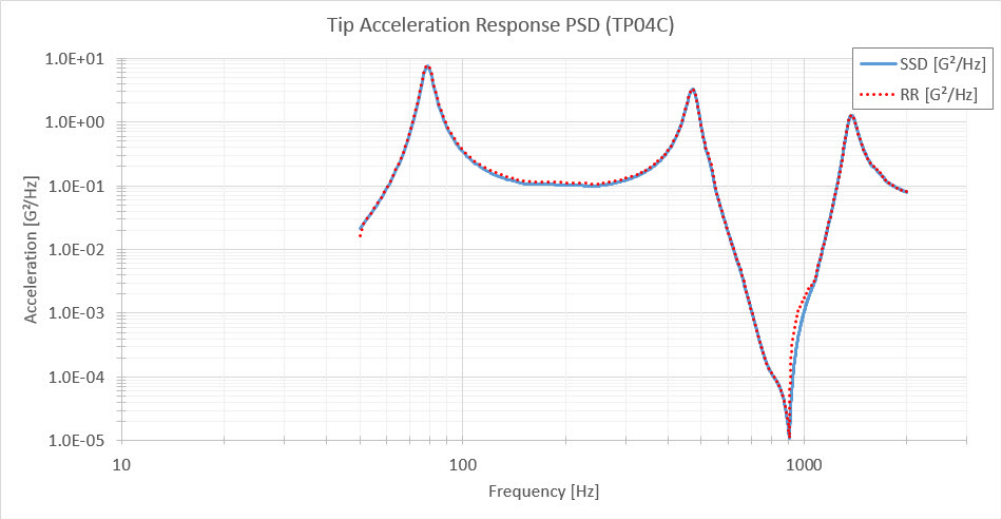

Figure 7.8: Vertical tip acceleration response, RR vs SSD (log-log)

Seen from both acceleration and displacement response PSDs, the anti-resonance frequency at 950 Hz results in a valley with amplitude drastically lower than the peak amplitudes.

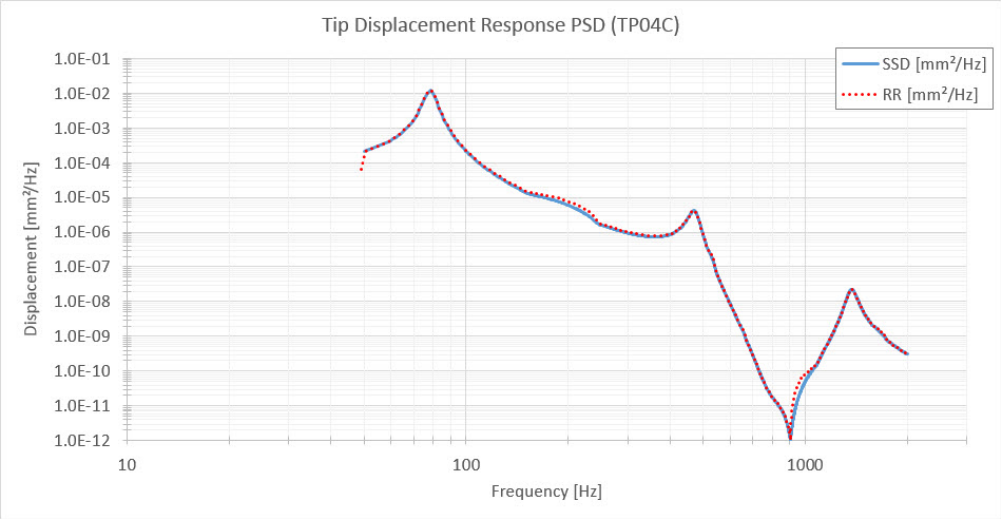

Figure 7.9: Vertical tip displacement response, RR vs SSD (log-log)

It is in essence only necessary to obtain the stress response PSD in order to perform fatigue life calculations. But both acceleration and displacement response PSDs are valuable in order to understand and visualize the dynamic behaviour of the system when subjected to the specified random excitation load.

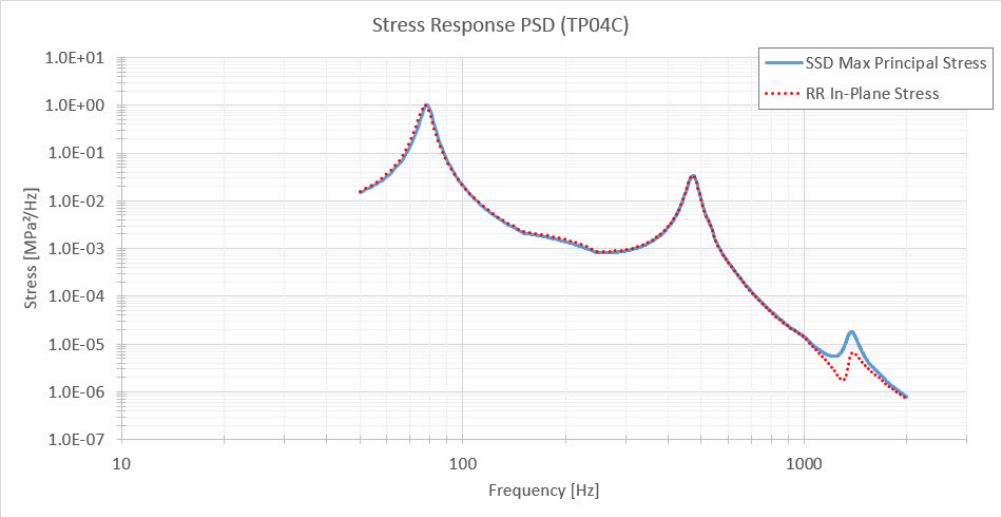

Figure 7.10: Maximum stress response RR vs SSD (log-log)

Evident deviations at the end of the frequency range is shown in the stress response PSDs. The amplitude variations in this area are considered very low compared with the peak amplitudes, and is therefore considered to not influence the fatigue calculation results.

7.3 Fatigue Life Calculation

The moments m_0 to m_4 from the stress response PSD (figure 7.10) are calculated and shown in table 7.4 below. The RMS of stress from both random response and SSD analysis shows good conformity.

	PSD Moments	Value	
Random Response	m_0	1.24E+01	MPa^2
	m_1	1.77E+03	MPa^2
	m_2	5.17E+05	MPa^2
	m_4	1.18E+11	MPa^2
	RMS	3.519	MPa
Steady-State Dynamics	m_0	1.19E+01	MPa^2
	m_1	1.73E+03	MPa^2
	m_2	5.18E+05	MPa^2
	m_4	1.26E+11	MPa^2
	RMS	3.444	MPa

Table 7.4: PSD moments and RMS values

7.3.1 Hand Calculation in Frequency Domain

A simple hand calculation approach can in many situations be a good starting point in order to get an idea of expected fatigue life and whether the analysed component are in the ballpark of the requirements or not.

Simplified PSD Approach

The stress response PSD shown in figure 7.10 have three distinctive peaks. The first at 78.6 Hz with amplitude 9.92E-01 MPa^2/Hz, the second at 473.0 Hz with amplitude 3.41E-02 MPa^2/Hz and third at 1375.8 Hz with amplitude 1.82E-05 MPa^2/Hz.

Peak Nr	Stress Amplitude	Frequency
1	9.92E-01 MPa^2/Hz	78.6 Hz
2	3.41E-02 MPa^2/Hz	473.0 Hz
3	1.82E-05 MPa^2/Hz	1375.8 Hz

Table 7.5: Stress amplitudes from stress response PSD

By creating a simplified stress response PSD where the peaks are represented as columns of a certain amplitude and width, df, the original signal can be assumed composed of a number of sine waves. Where each column represents one sine wave of certain amplitude and frequency.

The stress response PSD is therefore simplified into the bar chart shown in figure 7.11. Where the df is calculated through equation (7.1).

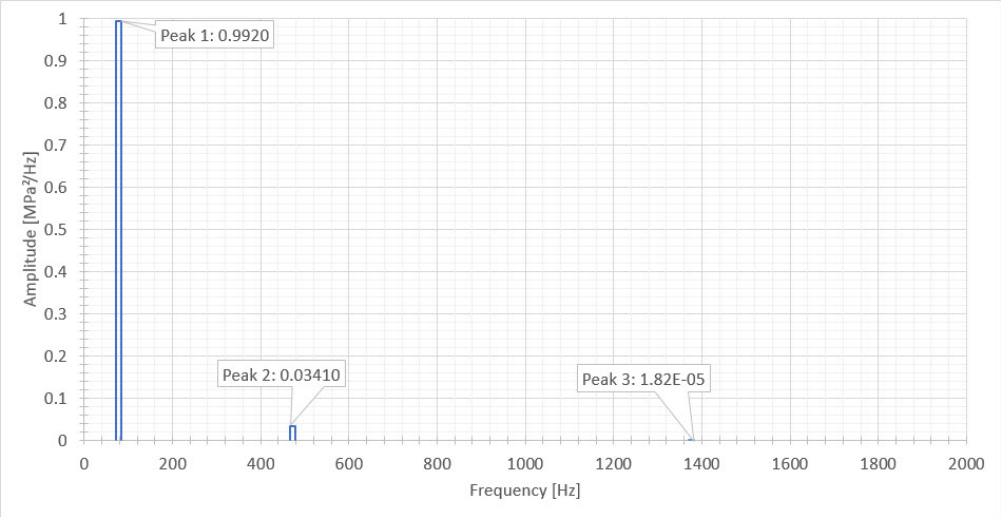

Figure 7.11: Simplified stress response PSD

$$\sqrt{(\Sigma Peak_{n+1}) \cdot df} = RMS \ for \ n = [0, \infty > \tag{7.1}$$

Solving for df gives $df = 11.56$ Hz. The stress ranges are then calculated through equation (7.2).

$$\sqrt{Peak_n \cdot df} \cdot \sqrt{2} \cdot 2 = \text{Magnitude of sine wave } n \tag{7.2}$$

$$\begin{aligned}
&\sqrt{(9.92E-01) \cdot 11.56} \cdot \sqrt{2} \cdot 2 = 9.5791 \text{ MPa} && \text{(first sine wave)} \\
&\sqrt{(3.41E-02) \cdot 11.56} \cdot \sqrt{2} \cdot 2 = 1.7758 \text{ MPa} && \text{(second sine wave)} \\
&\sqrt{(1.82E-05) \cdot 11.56} \cdot \sqrt{2} \cdot 2 = 0.0410 \text{ MPa} && \text{(third sine wave)}
\end{aligned}$$

This gives that at 78.58 cycles per second the stress range is 9.579 MPa, at 473.04 cycles per second the stress range is 11.355 MPa, and at 1375.8 cycles per second the stress range is 11.396 MPa.

Cycles per Second	**Stress Range**
78.58	9.579 MPa
473.04	11.355 MPa
1375.8	11.396 MPa

Table 7.6: Sine wave stress ranges (magnitudes)

The S-N data for 6082-T6 aluminium alloy is on the form $N(S) = \frac{S}{K}^{(\frac{1}{-m})}$. Where *N(S)* is the number of cycles to failure at the stress level, *S*. K and m are material constants shown in material properties table 5.2.

Stress Range	Cycles to Failure
9.579 MPa	1.31E+11
11.355 MPa	3.94E+10
11.396 MPa	3.84E+10

Table 7.7: Cycles to failure for corresponding stress ranges

$$E[D] = \frac{\text{Cycles per Second}}{\text{Cycles to Failure}} \tag{7.3}$$

$$E[D] = \frac{78.58}{1.31E+11} + \frac{473.04}{3.94E+10} + \frac{1375.8}{3.84E+10} = 4.84E-08$$

$$T = \frac{1}{E[D]} \tag{7.4}$$

This yields a fatigue life of 2.06E+07 seconds.

Direct RMS Approach

The same sinusoidal approach can be assumed for estimating fatigue life in the frequency domain by calculating the equivalent sine wave magnitude from the RMS value. The sine wave magnitude is equal to the stress range.

$$RMS \cdot \sqrt{2} \cdot 2 = \text{Stress Range} \tag{7.5}$$

$$3.444 \cdot \sqrt{2} \cdot 2 = 9.741 \text{ MPa}$$

Stress Range	Cycles to Failure
9.741 MPa	1.17E+11

Table 7.8: Cycles to failure for corresponding stress range

$$E[D] = \frac{1375.8}{1.17E + 11} = 1.17E - 08$$

This yields a fatigue life of 8.50E+07 seconds.

7.3.2 Computer Based Calculations

The fatigue life results presented are based on the fatigue calculation methods described in section 3.3.

The table below summarizes the obtained fatigue life in seconds for the different methods.

Method		**Fatigue Life [sec]**
Narrow Band	RR	1.15E+07
	SSD	1.29E+07
Steinberg	RR	2.22E+07
	SSD	2.49E+07
Dirlik	RR	9.35E+07
	SSD	1.06E+08

Table 7.9: Fatigue life obtained from computer based methods

All methods of fatigue life estimation shows good correlation. Narrow band method yields the lowest fatigue life, which is expected since it is proven to be very conservative for wide band response PSDs. Although the stress response PSD obtained from max principal stress in the SSD analysis is very close to narrow band, because of its predominant peak at the first resonance frequency. This will result in less deviations between narrow band and Dirlik.

7.3.3 High Amplitude Cycle Hypothesis

As calculated in section 3.1, the standard deviation of the random vibration time history is 4.11σ.

The fatigue life calculations performed in the previous section needs to be scaled accordingly in order to account for the possibility of high amplitude cycles. As mentioned, the typical assumption is that random vibrations has a peak value of 3σ for common design purposes.

The following values are retrieved from the max principal stress PSD. And the relationship

between σ and RMS is shown in table 7.10 because the original random vibration signal have a zero mean.

RMS	=	3.44 MPa
2σ	=	$2 \cdot$ RMS
3σ	=	$3 \cdot$ RMS

Table 7.10: RMS and σ relationship

The RMS of a response PSD is known through (7.6).

$$RMS = \sqrt{m_0} \tag{7.6}$$

This means that the following applies

$$n \cdot RMS = n \cdot \sqrt{m_0} = \sqrt{n^2 \cdot m_0} \tag{7.7}$$

In order to obtain the stress response PSD for ranges inside $\pm[1\sigma$ to $2\sigma]$ and $\pm[2\sigma$ to $3\sigma]$, the entire PSD must be multiplied by 2^2 and 3^2 respectively. Which basically is the same as multiplying the PSD moments with the same factors.

The resulting moments for the corresponding σ-limits are listed below.

Limit	$\mathbf{m_0}$	$\mathbf{m_1}$	$\mathbf{m_2}$	$\mathbf{m_4}$	**RMS**
Inside $\pm1\sigma$	1.19E+01	1.73E+03	5.18E+05	1.26E+11	3.44
Inside $\pm[1\sigma$ to $2\sigma]$	4.75E+01	6.94E+03	2.07E+06	5.05E+11	6.89
Inside $\pm[2\sigma$ to $3\sigma]$	1.07E+02	1.56E+04	4.66E+06	1.14E+12	10.33

Table 7.11: Max principal stress response PSD moments

By utilizing the Dirlik method yields three values of estimated fatigue damage, E[D], represented for the different σ-limits.

Limit	**E[D]**
Inside $\pm1\sigma$	1.39E-08
Inside $\pm[1\sigma$ to $2\sigma]$	1.84E-06
Inside $\pm[2\sigma$ to $3\sigma]$	3.21E-05

Table 7.12: Estimated damage using Dirlik method

The statistical probabilities for a Gaussian or normal distribution with zero mean applies.

Limit	E[D]
Inside $\pm 1\sigma$	(1.39E-08 · 0.6827)
Inside $\pm 2\sigma$	(1.39E-08 · 0.6827) + (1.84E-06 · 0.2718)
Inside $\pm 3\sigma$	(1.39E-08 · 0.6827) + (1.84E-06 · 0.2718) + (3.21E-05 · 0.0428)

Table 7.13: Total estimated damage from statistical probabilities

This yields the estimated fatigue life of the component inside the corresponding limits shown in table 7.14.

Limit	E[D]	Fatigue Life [sec]
Inside $\pm 1\sigma$	9.47E-09	1.06E+08
Inside $\pm 2\sigma$	5.10E-07	1.96E+06
Inside $\pm 3\sigma$	1.88E-06	5.31E+05

Table 7.14: Total fatigue life for corresponding limits

From the table above an evident reduction in fatigue life is shown when taking the probability of high amplitude cycles into account.

7.4 Summary of Fatigue Life Results

This section presents a summary of fatigue life calculations using each method with regard of max principal stress response PSDs for all test objects.

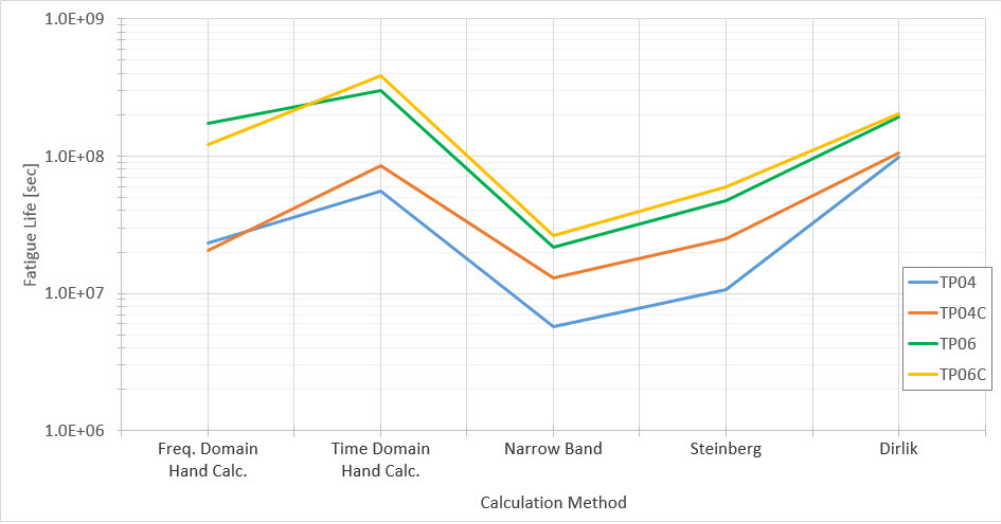

Figure 7.12: Fatigue life for different calculation methods

Total fatigue life time is generally higher for the plates with cut-outs. This is because the cut-out section creates a different bending shape, and will have lower stress values at critical regions. A different geometry which would induce higher stress values could be beneficial in order to cause greater variation of fatigue life.

Figure 7.12 shows how conservative the narrow band method are for all test objects compared with the Dirlik method.

By plotting the fatigue life of each component for σ-limits up to $\pm 3\sigma$ shows the most critical reduction of fatigue life are when including $\pm 2\sigma$.

Fatigue Life in Seconds

Limit	TP04	TP04C	TP06	TP06C
Inside $\pm 1\sigma$	9.73E+07	1.06E+08	1.93E+08	2.03E+08
Inside $\pm 2\sigma$	1.81E+06	1.96E+06	3.59E+06	3.78E+06
Inside $\pm 3\sigma$	4.90E+05	5.31E+05	9.73E+05	1.02E+06

Table 7.15: Total fatigue life for corresponding limits

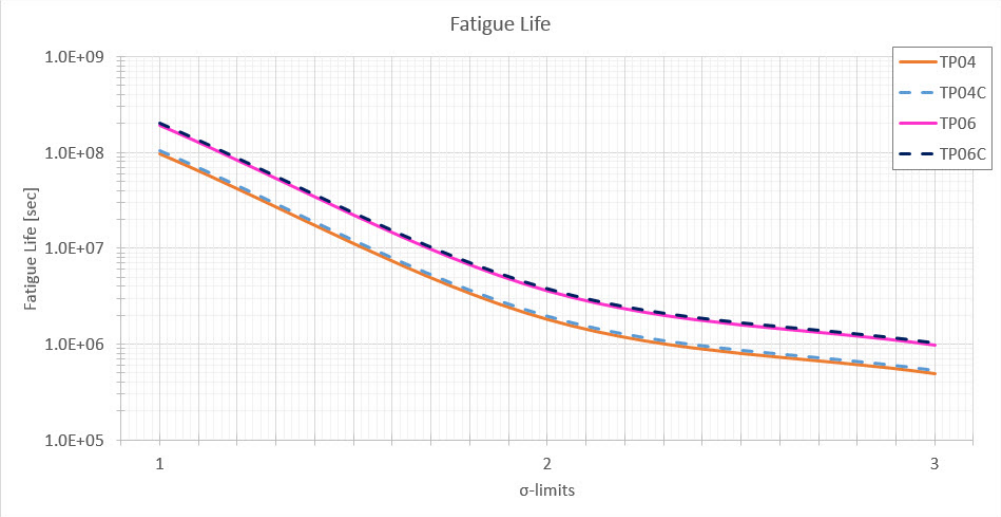

Figure 7.13: Fatigue life for $\pm 1\sigma$ to $\pm 3\sigma$ limits

8. Discussion

8.1 Boundary Conditions and Interactions

The fixed boundary condition is applied to the entire surface where fixture is in contact with shaker table. This is assumed reasonable for the analyses performed. But it can result in an unnatural increase of stiffness for the system. Bolts to be used are 12.9 grade alloy steel bolts, which compared to 6082-T6 aluminium are significantly stiffer. A model where bolt interaction are modelled could be performed in order to investigate the effect of variation in system response. This would have been carried out if great deviations between obtained response through FEA and physical vibration testing were present. As mentioned, physical testing was unfortunately not performed, and it is therefore difficult to correlate and verify the FEA model.

8.2 Response and Fatigue Life

Both random response and steady-state dynamics analyses was performed in the frequency domain using same input variable values to obtain comparable results. The response curves shows deviation at certain frequencies, specially in the stress response PSD plots. This is mainly because stress response output from random response is in-plane stress, while SSD outputs max principal stress. Because of the geometry and input load this is a reasonable comparison because the resulting stress are of highest value in the longitudinal direction. This is again shown in the fatigue life calculations, where the results are very close to each other.

Since the output data are discrete, not continuous, deviations will be present because of interpolation. In order to reduce this source of error, the analysis resolution can be increased by increasing number of calculation points. Several analyses with different output resolution was performed. The presented results shows the best compromise of resolution, conformity and CPU time.

Five fatigue life calculation methods are performed simultaneously for each test specimen,

where all methods gives relatively equal results. Although the vulnerability of the narrow band method is evident, where the stress response PSDs are of narrow band character, the narrow band method still yields the most conservative fatigue life results. Hand calculations by creating a simplified stress response PSD is shown to give good approximate results.

A different geometry of the test objects could been carried out in order to induce greater stress and fatigue life variance.

8.3 Fixture Design

The concern about fixture stiffness were investigated through the four analyses. Longitudinal acceleration response at the top of the fixture indicates movement which will influence the results. Figure 8.1 shows fixture response for each analysis.

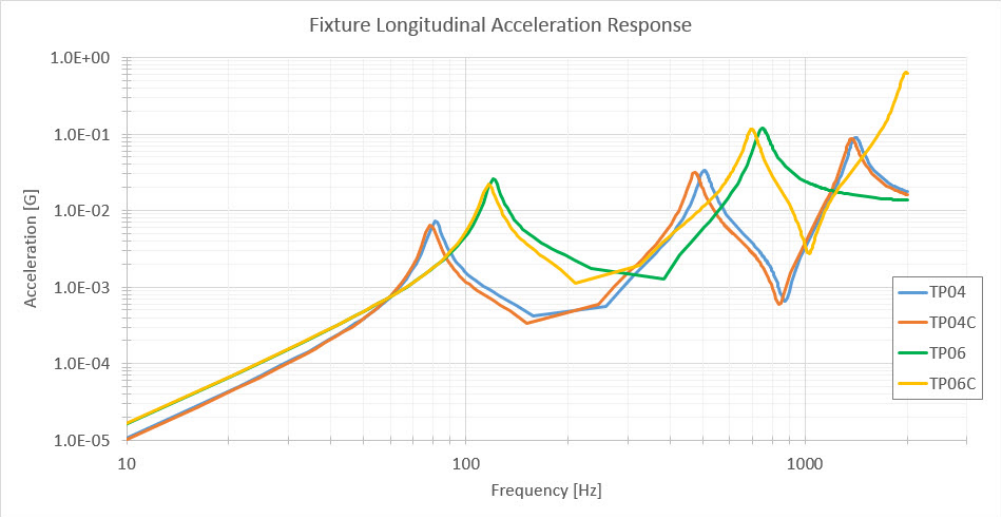

Figure 8.1: Fixture acceleration response in longitudinal x-axis (log-log)

Maximum peak response for the 4mm plates are less than 0.1G, and can be considered insignificant for the analysis results.

For the 6mm plates the maximum response are above 0.1G, and for TP06C maximum peak response are almost 6G. This will affect the results greatly, and a different fixture design should be used for this specific analysis/test.

The calculated fatigue life are therefore considered reliable for TP04C and TP04, debatable for TP06, and non-reliable for TP06C. Expected fatigue life for TP06C will be higher

than the obtained results because of fixture deformation. A stiffer and more rigid fixture will give accurate and reliable results for all test objects.

9. Conclusion

This thesis have investigated methods of estimating fatigue life of a component subjected to a random vibration load. From converting a measured signal from the time to frequency domain and characterization of a random signal, to using a random dynamic event as load case for a random vibration analysis. Important factors when designing vibration test fixtures, placement of sensors and linear dynamic analysis in Abaqus/CAE are clarified.

Fatigue life estimations are considered reliable for analyses performed on models TP04 and TP04C, while considered debatable for TP06 and non-reliable for TP06C. This based on the fixture design and measured fixture response for each analysis.

Unfortunately, because of unforeseen events, the shaker testing at Kongsberg Automotive could not be performed according to the plan. This results in that fatigue life estimations needs verification by performing physical vibration testing and correlation with the FE analyses. Expected possible error sources are boundary conditions, constraints and mesh.

10. Further Work

In the course of working with this thesis, there have been identified issues that needs further work.

Fixture design does not satisfy the criteria stated, and is shown to give inaccurate results for two of the test objects. A better fixture design should be used in order to reduce response amplification during testing and analysis of the specified test objects.

Physical vibration testing on shaker table should be performed in order to correlate both the FE model and analysis input variables. Both sine-sweep and random vibration tests should be performed and compared with output response curves obtained from the FE analyses. This will verify the results presented in this thesis, and reveal necessary modifications of FE analysis setup to adjust the output response accordingly.

Bibliography

[1] Dassault Systèmes Simulia Corp., *Linear dynamics with Abaqus*. Dassault Systèmes Simulia Corp., 2013.

[2] Dassault Systèmes Simulia Corp., *Abaqus/CAE 6.13 User's Guide*. Dassault Systèmes Simulia Corp., 2013. `http://ivt-abaqusdoc.ivt.ntnu.no:2080/v6.13/books/usi/default.htm`.

[3] Dassault Systèmes Simulia Corp., *Abaqus Theory Guide*. Dassault Systèmes Simulia Corp., 2013. `http://ivt-abaqusdoc.ivt.ntnu.no:2080/v6.13/books/stm/default.htm`.

[4] T. Irvine, "Integration of the power spectral density function, revision b," March 18th 2000. `http://www.vibrationdata.com/tutorials/psdinteg.pdf`.

[5] T. Irvine, "An introduction to random vibration, revision b," October 26th 2000. `http://www.vibrationdata.com/tutorials2/random.pdf`.

[6] M.A. Miner, "Cumulative damage in fatigue," *J Appl Mech, Vol. 12*, 1945.

[7] "Astm e 1049-85 (2005) rainflow counting method," May 2015. .

[8] A. Halfpenny, "A frequency domain approach for fatigue life estimation from finite element analysis," 1999. `http://www.ncode.com/fileadmin/mediapool/nCode/downloads/Whitepaper_nCode_frequency_domain_fatigue-Halfpenny.pdf`.

[9] N. Bishop, "Vibration fatigue analysis in the finite element environment," April 1999. `http://www.academia.edu/8156228/Vibration_Fatigue_Analysis_in_the_finite_Element_Environment`.

[10] M.T Heidemann, D.H Johnson and C.S. Burrus, "Gauss and the history of the fast fourier transform," *IEEE ASSP Magazine*, October 1984.

[11] T. Irvine, "Power spectral density units: $[g^2/hz]$, revision b," March 15th 2007. `http://www.vibrationdata.com/tutorials/psdinteg.pdf`.

[12] S.O. Rice, "Mathematical analysis of random noise," *Selected Papers on Noise and Stochastic Processes, Dover, New York, USA*, 1954.

[13] J.S. Bendat, "Probability functions for random responses: Prediction of peaks, fatigue damage and catastrophic failures.," *NASA report on contract NAS-5-4590, USA*, 1964.

[14] T. Dirlik, "Application of computers in fatigue analysis," January 1985.

[15] N. Bishop, "The use of frequency domain parameters to predict structural fatigue," December 1988. `http://go.warwick.ac.uk/wrap/34794`.

[16] "MIL-STD-810G, Department of Defense Test Method Standard for Environmental Engineering Considerations and Laboratory Tests. United States Department of Defense.," 31 October 2008.

[17] A. Halfpenny, "Methods for accelerating dynamic durability tests," *9th International Conference on Recent Advances in Structural Dynamic, Southampton, UK*, 2006.

[18] M.A. Biot, "Transient oscillations in elastic systems," *Thesis No. 259, Aeronautics Dept., California Institute of Technology, Pasadena*, 1932.

[19] M.A. Biot, "Theory of elastic systems vibrating under transient impulse, with an application to earthquake-proof buildings," *Proceedings of the National Academy of Science, 19 No2, pp. 262-268*, 1933.

[20] J.W. Miles, "On structural fatigue under random loading," *Journal of the Aeronautical Sciences, pp. 753*, 1954.

[21] C. Lalanne, "Les vibrations aleatoires," *Cours ADERA*, 1978.

[22] C. Lalanne, "Mechanical vibration & shock, volume V," *Hermes Penton Ltd. London*, 2002.

[23] A. Halfpenny, "Mission profiling and test synthesis based on fatigue damage spectrum. ref. ft342," *9th Int. Fatigue Cong. Atlanta, USA. Elsevier, Oxford, UK*, 2006.

A. Figures and Tables

A.1 Linear Dynamic FE Analysis

Element Type	Mesh Density	Tip Displacement [mm]	Displacement Ratio	Deviation (%)	Total CPU Time [sec]
C3D4 (Tet)	75x15x1	0.421	0.516	48.4 %	6.60
	75x15x3	0.437	0.536	46.4 %	6.90
	150x30x3	0.581	0.713	28.7 %	39.60
	150x30x6	0.542	0.664	33.6 %	37.30
C3D10 (Tet)	75x15x1	0.794	0.974	2.6 %	23.80
	75x15x3	0.794	0.974	2.6 %	26.40
	150x30x3	0.795	0.975	2.5 %	206.30
	150x30x6	0.795	0.975	2.5 %	190.70
C3D8R (Hex)	20x4x1	63.475	77.862	7686.2 %	0.7
	40x8x2	1.051	1.289	28.9 %	0.9
	50x10x4	0.843	1.034	3.4 %	2.1
	100x20x8	0.806	0.988	1.2 %	28
C3D8 (Hex)	20x4x1	0.143	0.176	82.4 %	0.3
	40x8x2	0.360	0.442	55.8 %	1.5
	10x50x4	0.433	0.532	46.8 %	4.1
	20x100x8	0.654	0.802	19.8 %	43.8
C3D20R (Hex)	20x4x1	0.785	0.963	3.7 %	0.5
	40x8x2	0.793	0.972	2.8 %	4.3
	50x10x4	0.794	0.974	2.6 %	14.6
	100x20x8	0.794	0.974	2.6 %	292.9
C3D20 (Hex)	20x4x1	0.783	0.960	4.0 %	1.1
	40x8x2	0.791	0.971	2.9 %	7.4
	50x10x4	0.793	0.972	2.8 %	23.9
	100x20x8	0.794	0.974	2.6 %	386

Table A.1: Mesh convergence table

B. Linear Dynamic FEA Results

B.1 Model TP04

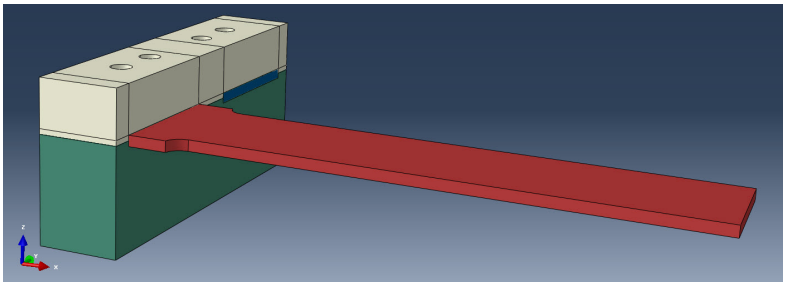

Figure B.1: CAD model showing fixture and TP04

B.1.1 Eigenvalue Extraction Data

Eigenvalue Output (TP04)

Mode	Eigenvalue	Frequency [Hz]	Generalized Mass
1	2.59910E+05	81.139	2.13857E-05
2	1.00337E+07	504.14	2.15290E-05
3	2.31576E+07	765.89	1.36402E-05
4	2.41478E+07	782.09	2.23452E-05
5	7.78043E+07	1403.9	2.14790E-05

Table B.1: Eigenvalue output

Modal Participation Factors (TP04)

Mode	X-Comp	Y-Comp	Z-Comp	X-Rot	Y-Rot	Z-Rot
1	-6.04744E-03	-4.21797E-04	1.5679	-70.555	-275.51	-0.21579
2	4.87676E-02	4.97429E-03	-0.87757	39.485	64.238	2.0627
3	-7.33677E-04	-0.13819	-3.41821E-04	-25.465	3.50628E-02	-24.976
4	-1.08602E-04	1.5631	3.71395E-04	-4.5286	-0.17101	277.65
5	-0.22321	5.21998E-03	0.53117	-23.895	-30.623	-4.2727

Table B.2: Modal participation factors

Effective Modal Mass (TP04)

Mode	X-Comp	Y-Comp	Z-Comp	X-Rot	Y-Rot	Z-Rot
1	7.82110E-10	3.80480E-12	5.25748E-05	0.10646	1.6233	9.95871E-07
2	5.12019E-08	5.32704E-10	1.65799E-05	3.35650E-02	8.88401E-02	9.16020E-05
3	7.34227E-12	2.60484E-07	1.59374E-12	8.84532E-03	1.67692E-08	8.50853E-03
4	2.63549E-13	5.45975E-05	3.08217E-12	4.58268E-04	6.53503E-07	1.7225
5	1.07014E-06	5.85263E-10	6.06011E-06	1.22642E-02	2.01421E-02	3.92126E-04
TOTAL	1.12213E-06	5.48591E-05	7.52148E-05	0.16159	1.7323	1.7315

Table B.3: Effective modal mass (Mg)

B.1.2 Modal Analysis Results

RMS Plots

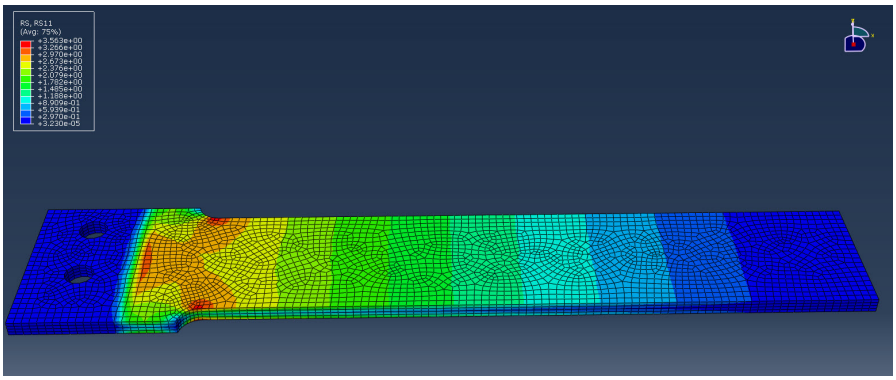

Figure B.2: RS11 color plot

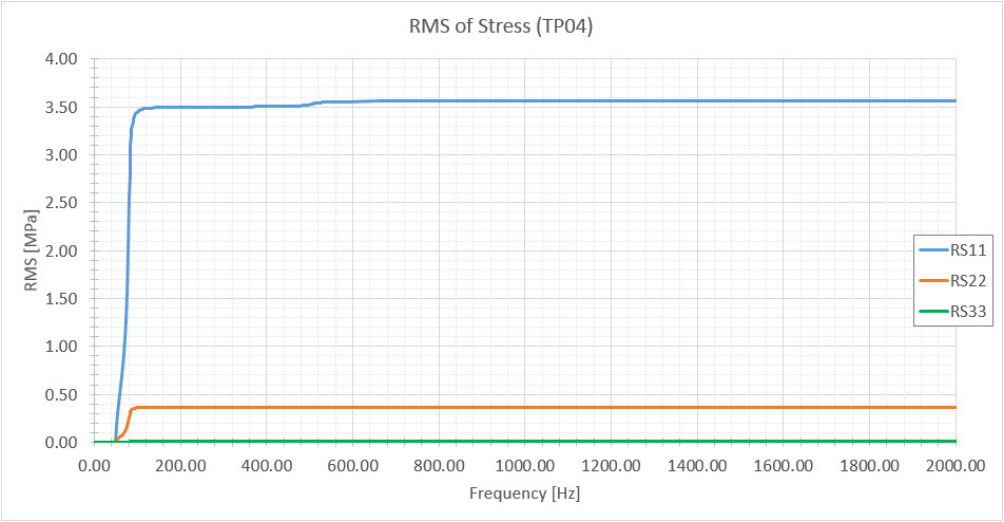

Figure B.3: RMS of stress at critical integration point

Transfer Functions

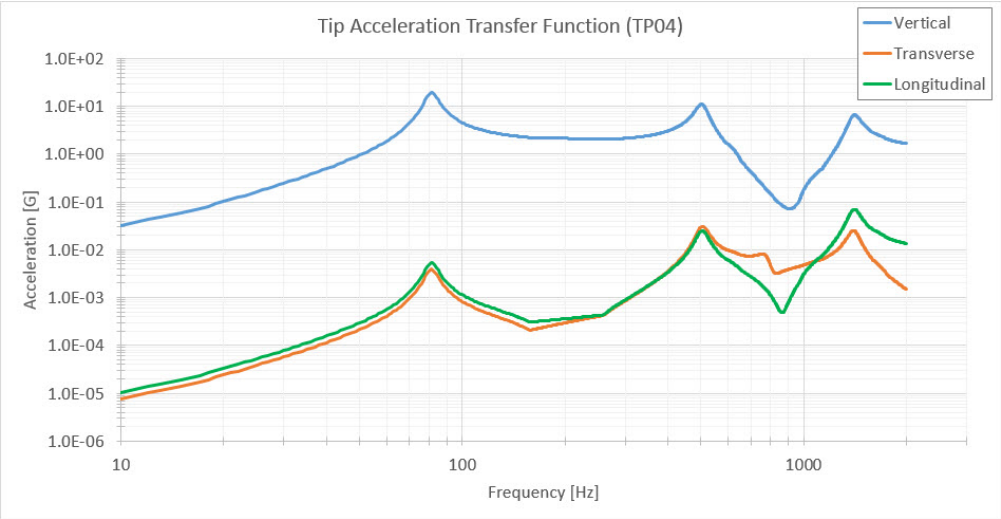

Figure B.4: Acceleration transfer function (G/G) (log-log)

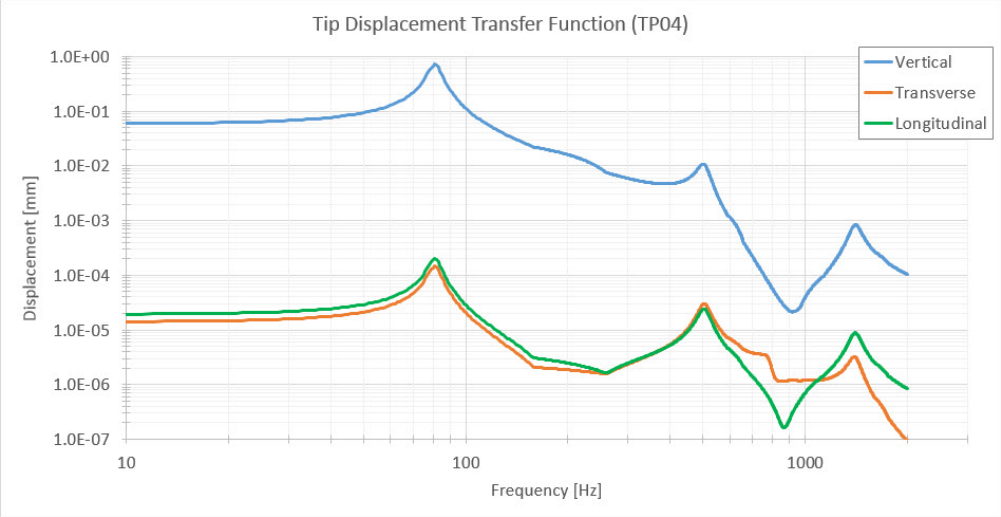

Figure B.5: Displacement transfer function (mm/G) (log-log)

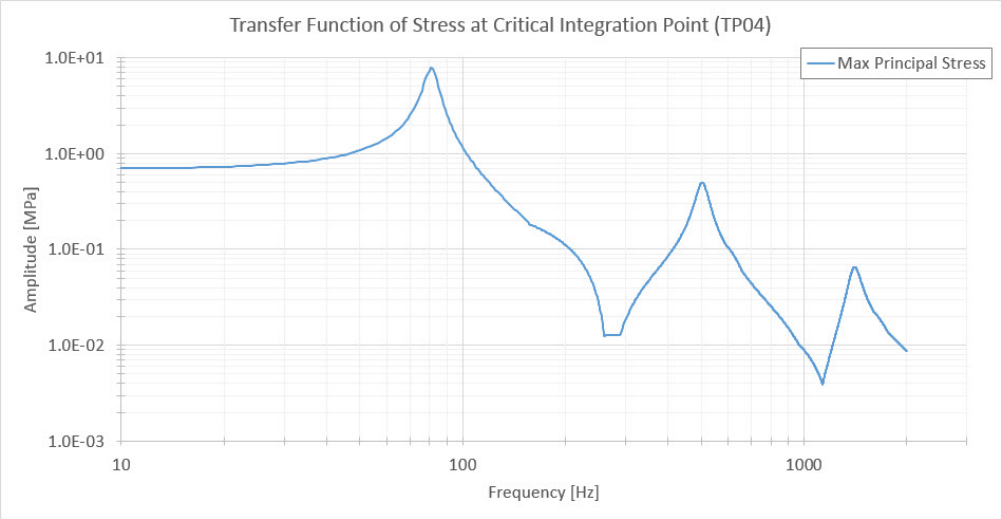

Figure B.6: Max principal stress (MPa/G) (log-log)

Response PSDs

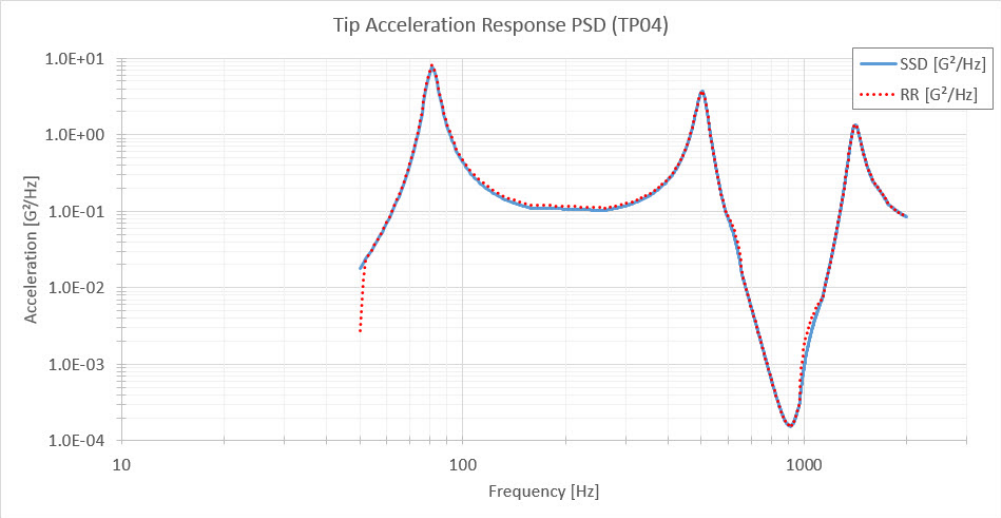

Figure B.7: Vertical tip acceleration response, RR vs SSD (log-log)

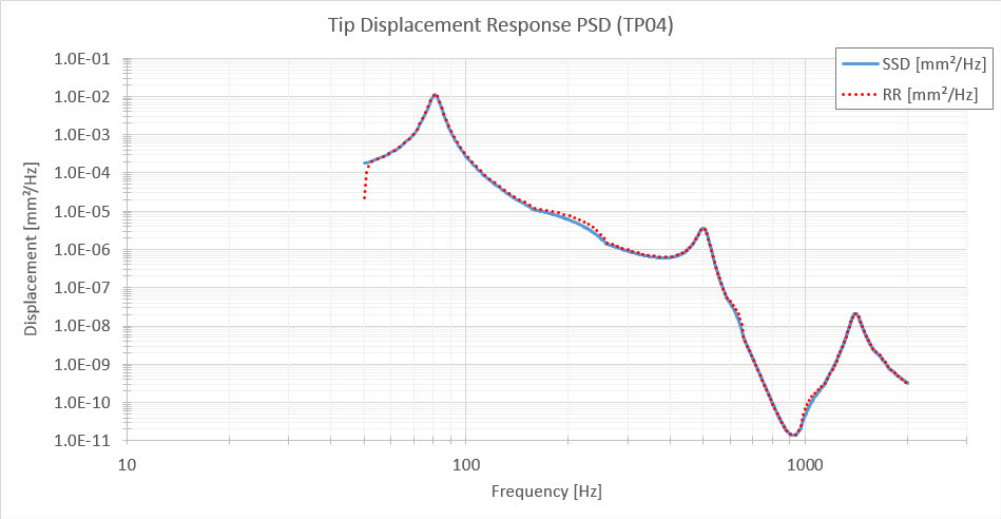

Figure B.8: Vertical tip displacement response, RR vs SSD (log-log)

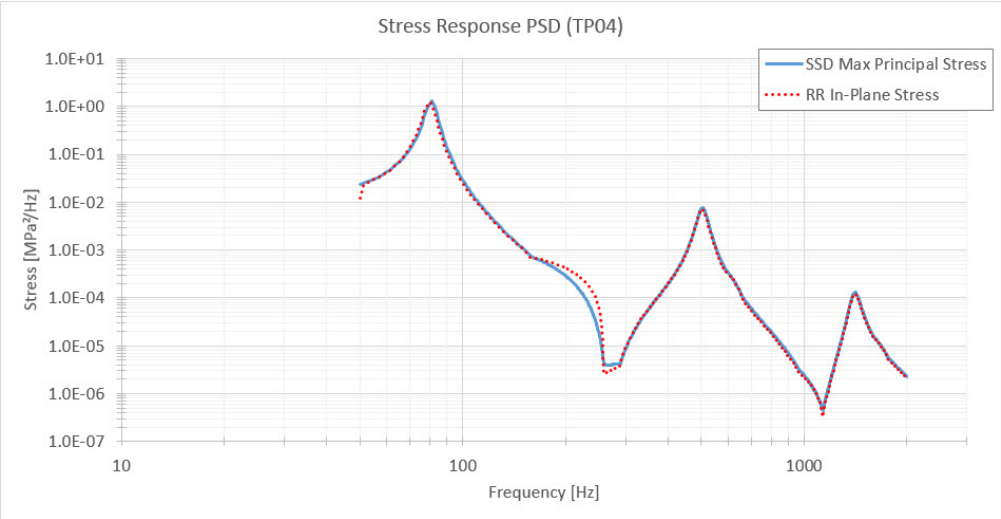

Figure B.9: Maximum stress response RR vs SSD (log-log)

B.1.3 Fatigue Life Calculation

	PSD Moments	Value	
Random Response	m_0	1.27E+01	MPa^2
	m_1	1.22E+03	MPa^2
	m_2	2.28E+05	MPa^2
	m_4	1.22E+11	MPa^2
	RMS	3.563	MPa
Steady-State Dynamics	m_0	1.33E+01	MPa^2
	m_1	1.29E+03	MPa^2
	m_2	2.45E+05	MPa^2
	m_4	1.32E+11	MPa^2
	RMS	3.651	MPa

Table B.4: PSD moments and RMS values

Hand Calculation in Frequency Domain - Simplified PSD Approach

Peak Nr	Stress Amplitude	Frequency
1	1.30E+00 MPa^2	81.1 Hz
2	7.51E-03 MPa^2	504.1 Hz
3	1.29E-04 MPa^2	1407.3 Hz

Table B.5: Stress amplitudes from stress response PSD

Stress Range	Cycles to Failure
10.296 MPa	7.93E+10
11.078 MPa	4.74E+10
11.180 MPa	4.44E+10

Table B.6: Cycles to failure for corresponding stress ranges

This gives a fatigue life of 2.31E+07 seconds.

Hand Calculation in Frequency Domain - Direct RMS Approach

Stress Range	Cycles to Failure
10.328 MPa	7.76E+10

Table B.7: Cycles to failure for corresponding stress range

This gives a fatigue life of 5.51E+07 seconds.

Computer Based Calculations

Method		Fatigue Life [sec]
Narrow Band	RR	6.83E+06
	SSD	5.71E+06
Steinberg	RR	1.31E+07
	SSD	1.07E+07
Dirlik	RR	1.17E+08
	SSD	9.73E+07

Table B.8: Fatigue life obtained from computer based methods

B.1.4 High Amplitude Cycle Hypothesis

Limit	E[D]	Fatigue Life [sec]
Inside $\pm 1\sigma$	1.03E-08	9.73E+07
Inside $\pm 2\sigma$	5.53E-07	1.81E+06
Inside $\pm 3\sigma$	2.04E-06	4.90E+05

Table B.9: Total fatigue life for corresponding limits

B.2 Model TP06

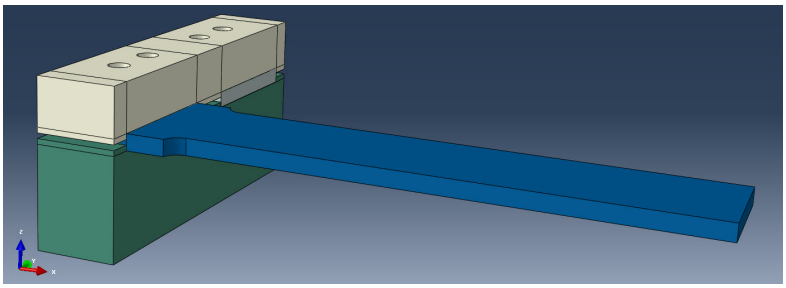

Figure B.10: CAD model showing fixture and TP06

B.2.1 Eigenvalue Extraction Data

Eigenvalue Output (TP06)

Mode	Eigenvalue	Frequency [Hz]	Generalized Mass
1	5.72289E+05	120.40	3.22638E-05
2	2.18789E+07	744.45	3.35349E-05
3	2.27643E+07	759.36	3.53268E-05
4	4.90898E+07	1115.1	2.07203E-05

Table B.10: Eigenvalue output

Modal Participation Factors (TP06)

Mode	X-Comp	Y-Comp	Z-Comp	X-Rot	Y-Rot	Z-Rot
1	-1.53336E-02	-1.41890E-03	1.5678	-70.548	-275.09	-0.62694
2	0.12700	0.25259	-0.85622	37.812	62.290	47.833
3	-1.15591E-02	1.5189	0.13335	-10.410	-9.9362	268.15
4	-2.60153E-03	1.60189E-02	-7.72158E-04	-26.012	6.07200E-02	1.8739

Table B.11: Modal participation factors

Effective Modal Mass (TP06)

Mode	X-Comp	Y-Comp	Z-Comp	X-Rot	Y-Rot	Z-Rot
1	7.58580E-09	6.49563E-11	7.93032E-05	0.16058	2.4415	1.26814E-05
2	5.40926E-07	2.13965E-06	2.45847E-05	4.79475E-02	0.13012	7.67264E-02
3	4.72012E-09	8.15034E-05	6.28182E-07	3.82825E-03	3.48776E-03	2.5402
4	1.40234E-10	5.31692E-09	1.23540E-11	1.40203E-02	7.63939E-08	7.27577E-05
TOTAL	5.53372E-07	8.36484E-05	1.04516E-04	0.22637	2.5751	2.6170

Table B.12: Effective modal mass

B.2.2 Modal Analysis Results

RMS Plots

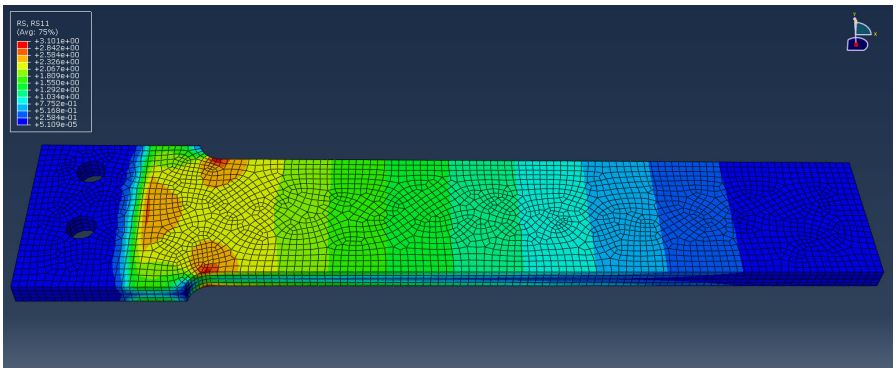

Figure B.11: RS11 color plot

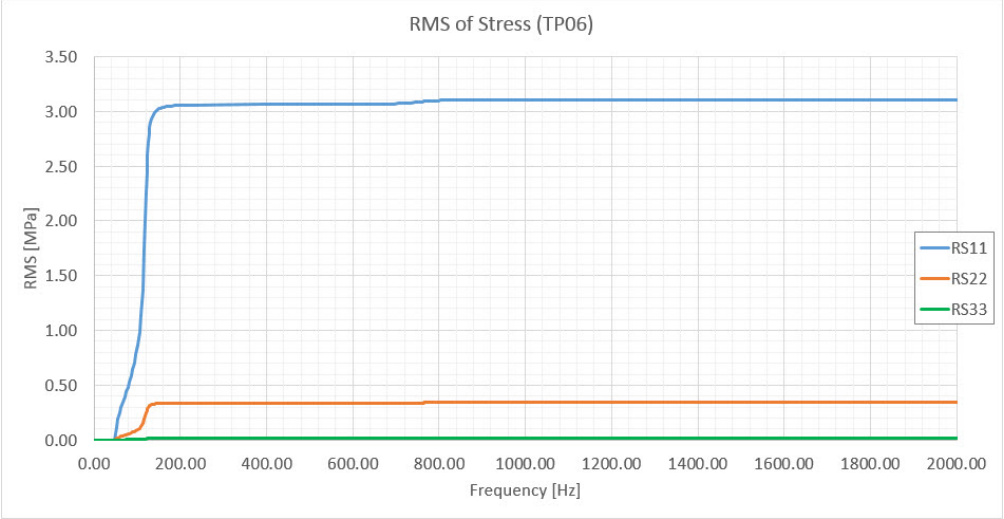

Figure B.12: RMS of stress at critical integration point

Transfer Functions

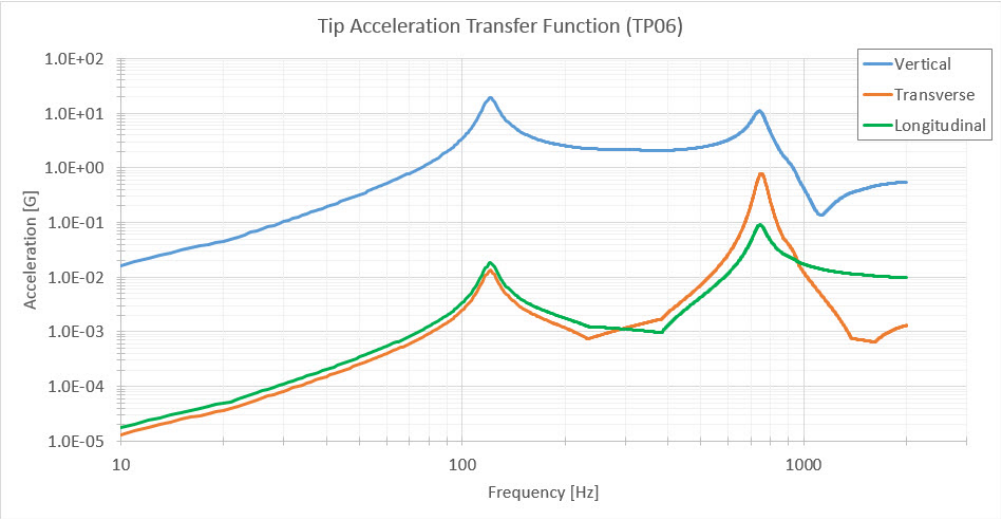

Figure B.13: Acceleration transfer function (G/G) (log-log)

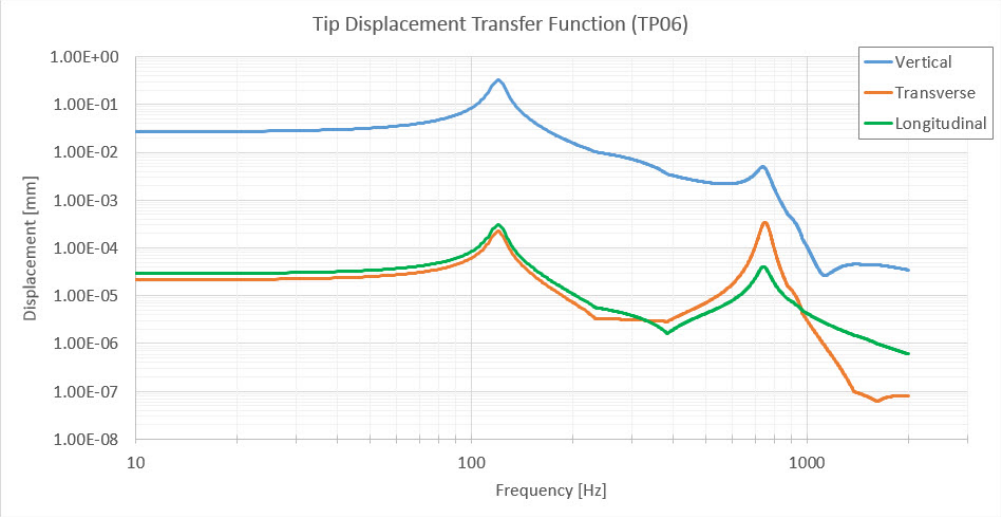

Figure B.14: Displacement transfer function (mm/G) (log-log)

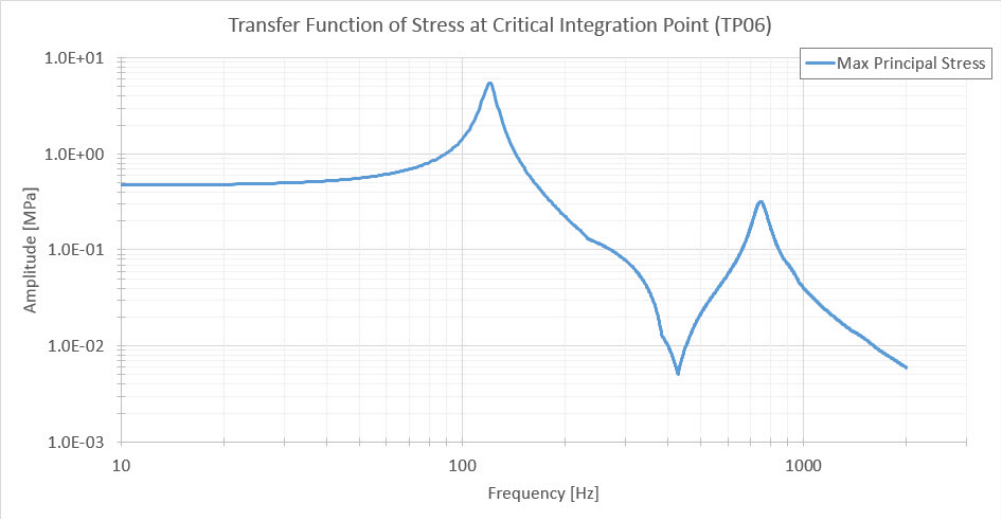

Figure B.15: Max principal stress (MPa/G) (log-log)

Response PSDs

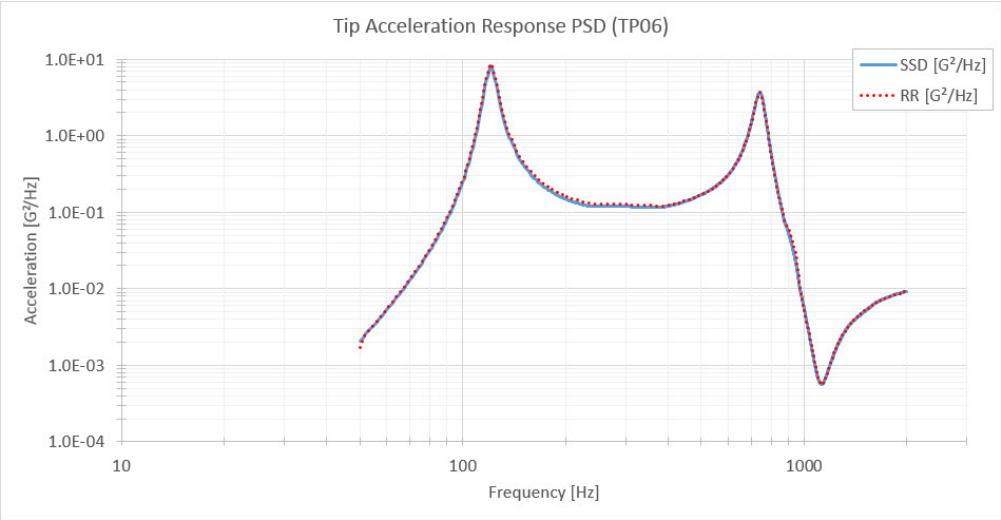

Figure B.16: Vertical tip acceleration response, RR vs SSD (log-log)

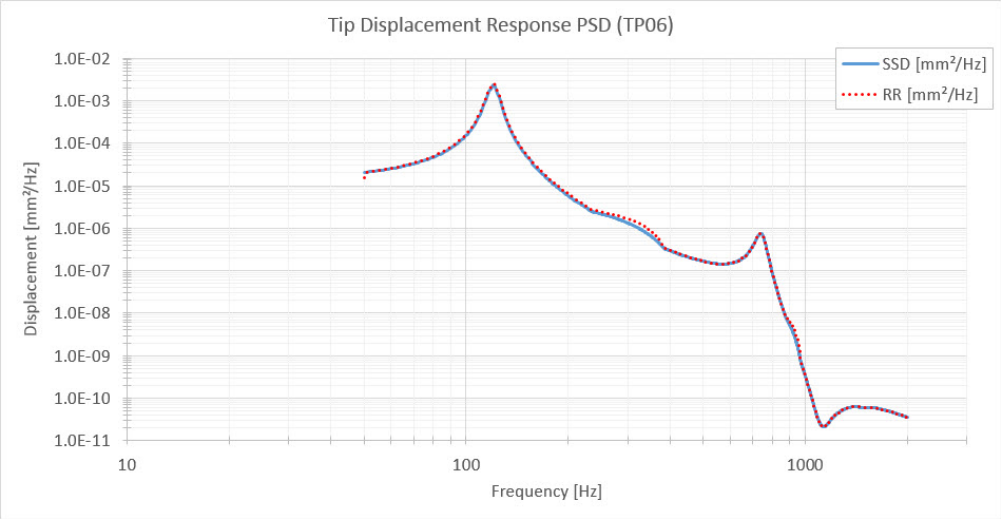

Figure B.17: Vertical tip displacement response, RR vs SSD (log-log)

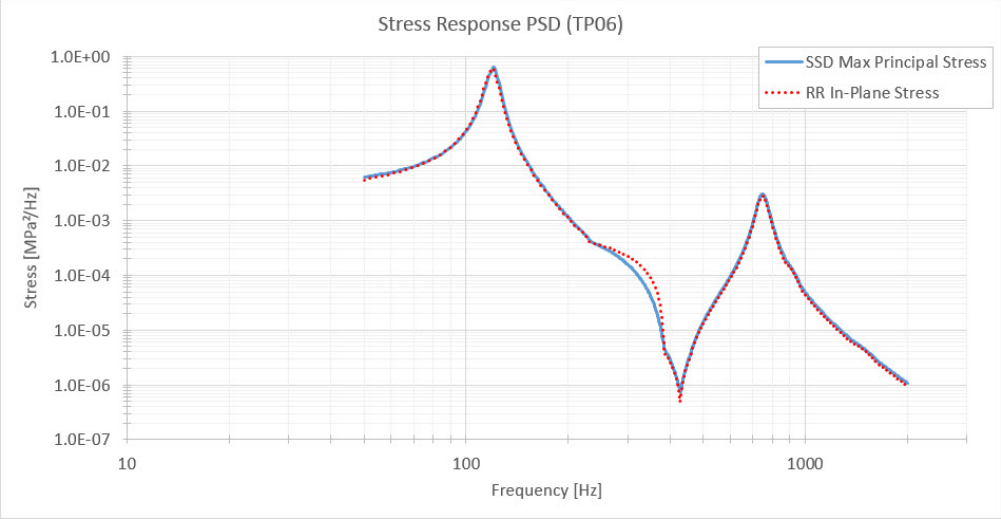

Figure B.18: Maximum stress response RR vs SSD (log-log)

B.2.3 Fatigue Life Calculation

	PSD Moments	Value	
Random Response	m_0	9.65E+00	MPa^2
	m_1	1.31E+03	MPa^2
	m_2	2.92E+05	MPa^2
	m_4	1.10E+11	MPa^2
	RMS	3.107	MPa
Steady-State Dynamics	m_0	9.88E+00	MPa^2
	m_1	1.36E+03	MPa^2
	m_2	3.13E+05	MPa^2
	m_4	1.21E+11	MPa^2
	RMS	3.144	MPa

Table B.13: PSD moments and RMS values

Hand Calculation in Frequency Domain - Simplified PSD Approach

Peak Nr	Stress Amplitude	Frequency
1	6.29E-01 MPa^2	120.4 Hz
2	3.06E-03 MPa^2	747.6 Hz

Table B.14: Stress amplitudes from stress response PSD

Stress Range	Cycles to Failure
8.863 MPa	2.28E+11
9.481 MPa	1.42E+11

Table B.15: Cycles to failure for corresponding stress ranges

This gives a fatigue life of 1.73E+08 seconds.

Hand Calculation in Frequency Domain - Direct RMS Approach

Stress Range	Cycles to Failure
8.892 MPa	2.23E+11

Table B.16: Cycles to failure for corresponding stress range

This gives a fatigue life of 2.99E+08 seconds.

Computer Based Calculations

Method		Fatigue Life [sec]
Narrow Band	RR	2.18E+07
	SSD	1.98E+07
Steinberg	RR	4.70E+07
	SSD	4.22E+07
Dirlik	RR	2.13E+08
	SSD	1.93E+08

Table B.17: Fatigue life obtained from computer based methods

B.2.4 High Amplitude Cycle Hypothesis

Limit	E[D]	Fatigue Life [sec]
Inside $\pm 1\sigma$	5.17E-09	1.93E+08
Inside $\pm 2\sigma$	2.78E-07	3.59E+06
Inside $\pm 3\sigma$	1.03E-06	9.73E+05

Table B.18: Total fatigue life for corresponding limits

B.3 Model TP06C

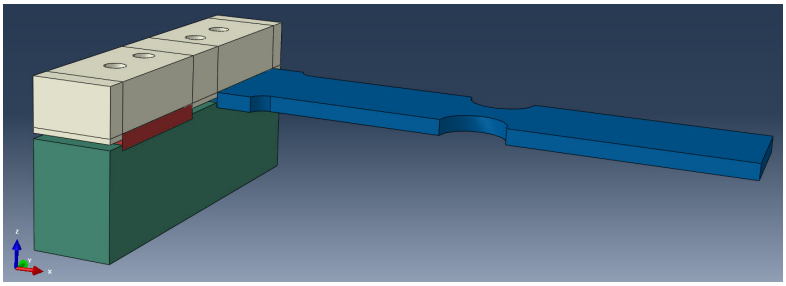

Figure B.19: CAD model showing fixture and TP06C

B.3.1 Eigenvalue Extraction Data

Eigenvalue Output (TP06C)

Mode	Eigenvalue	Frequency [Hz]	Generalized Mass
1	5.36469E+05	116.57	2.99797E-05
2	1.35705E+07	586.30	2.69457E-05
3	1.91692E+07	696.82	3.57137E-05
4	4.23941E+07	1036.3	1.80262E-05
5	1.55115E+08	1982.2	3.84651E-05

Table B.19: Eigenvalue output

Modal Participation Factors (TP06C)

Mode	X-Comp	Y-Comp	Z-Comp	X-Rot	Y-Rot	Z-Rot
1	-1.42728E-02	1.28248E-03	1.5397	38.489	-276.35	0.28942
2	-5.58447E-03	1.5448	1.33578E-02	-4.2281	-0.83642	288.88
3	0.11264	1.63924E-02	-0.83574	-20.952	64.562	2.6065
4	-1.87867E-03	-4.81846E-03	-7.79969E-04	24.998	6.80783E-02	-0.25739
5	-1.0676	1.24108E-02	0.48851	12.132	-32.099	3.6486

Table B.20: Modal participation factors

Effective Modal Mass (TP06C)

Mode	X-Comp	Y-Comp	Z-Comp	X-Rot	Y-Rot	Z-Rot
1	6.10726E-09	4.93096E-11	7.10727E-05	4.44127E-02	2.2895	2.51115E-06
2	8.40335E-10	6.43041E-05	4.80794E-09	4.81702E-04	1.88510E-05	2.2486
3	4.53167E-07	9.59669E-09	2.49444E-05	1.56774E-02	0.14887	2.42628E-04
4	6.36218E-11	4.18525E-10	1.09663E-11	1.12644E-02	8.35452E-08	1.19422E-06
5	4.38405E-05	5.92473E-09	9.17927E-06	5.66178E-03	3.96334E-02	5.12061E-04
TOTAL	4.43007E-05	6.43201E-05	1.05201E-04	7.74979E-02	2.4780	2.2494

Table B.21: Effective modal mass (Mg)

B.3.2 Modal Analysis Results

RMS Plots

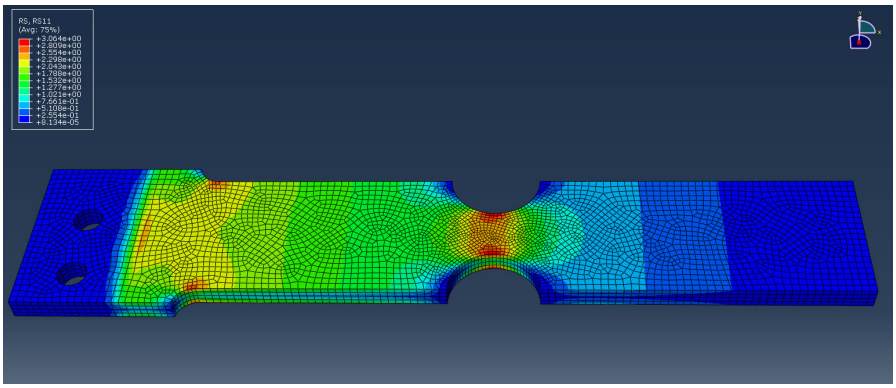

Figure B.20: RS11 color plot

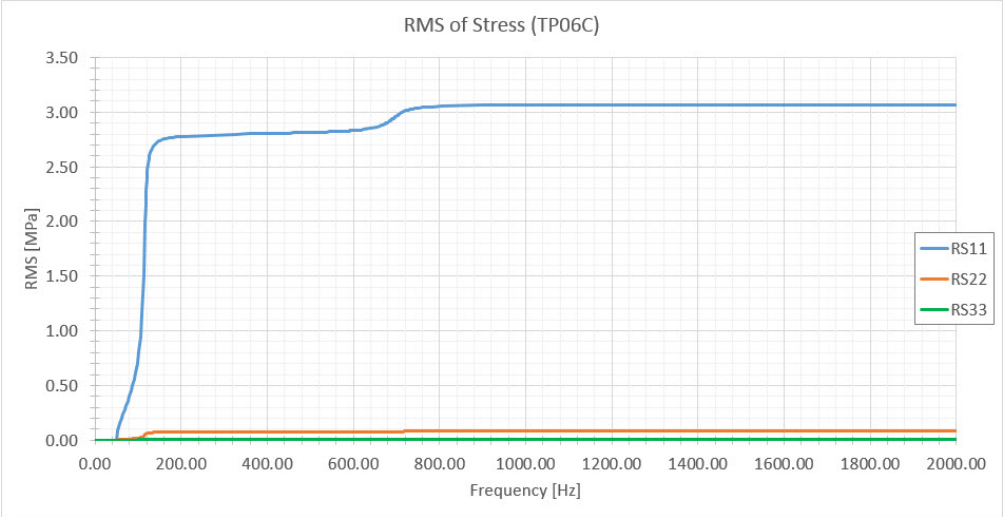

Figure B.21: RMS of stress at critical integration point

Transfer Functions

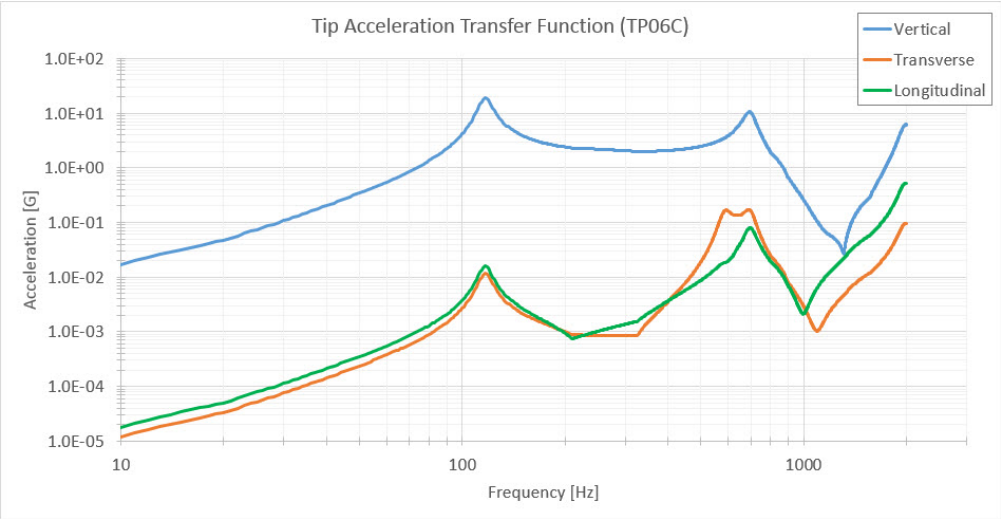

Figure B.22: Acceleration transfer function (G/G) (log-log)

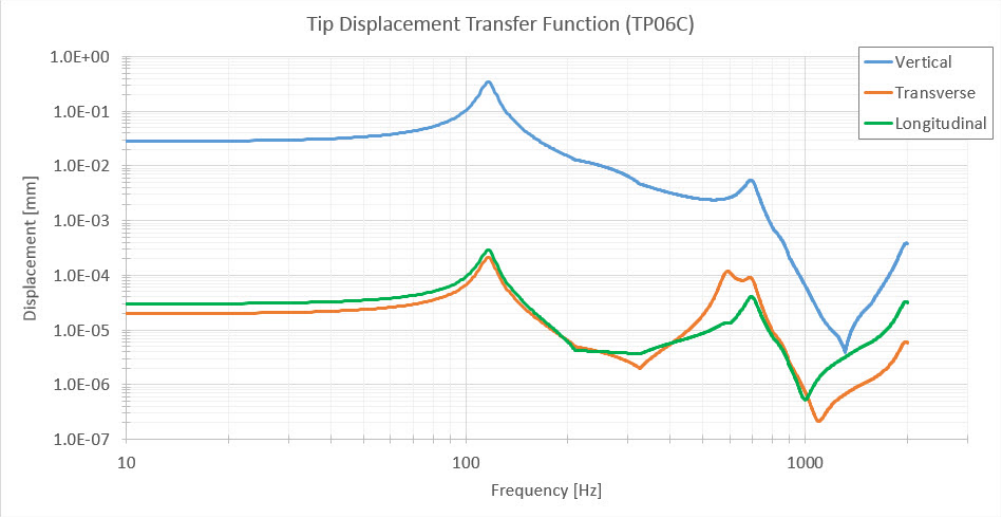

Figure B.23: Displacement transfer function (mm/G) (log-log)

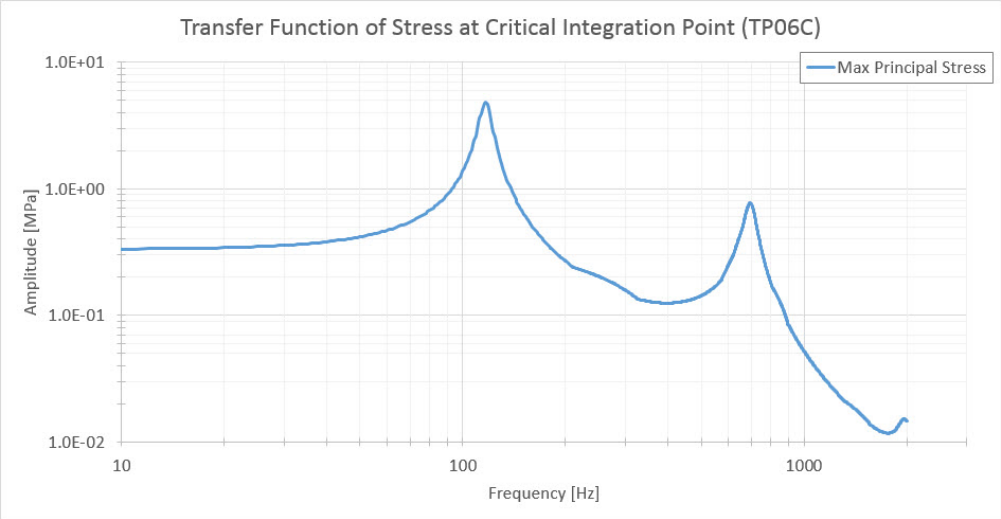

Figure B.24: Max principal stress (MPa/G) (log-log)

Response PSDs

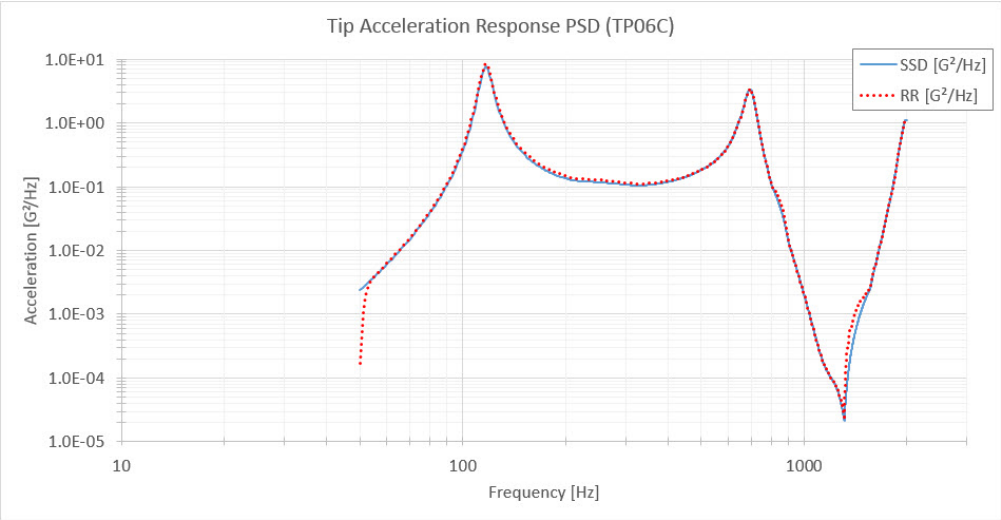

Figure B.25: Vertical tip acceleration response, RR vs SSD (log-log)

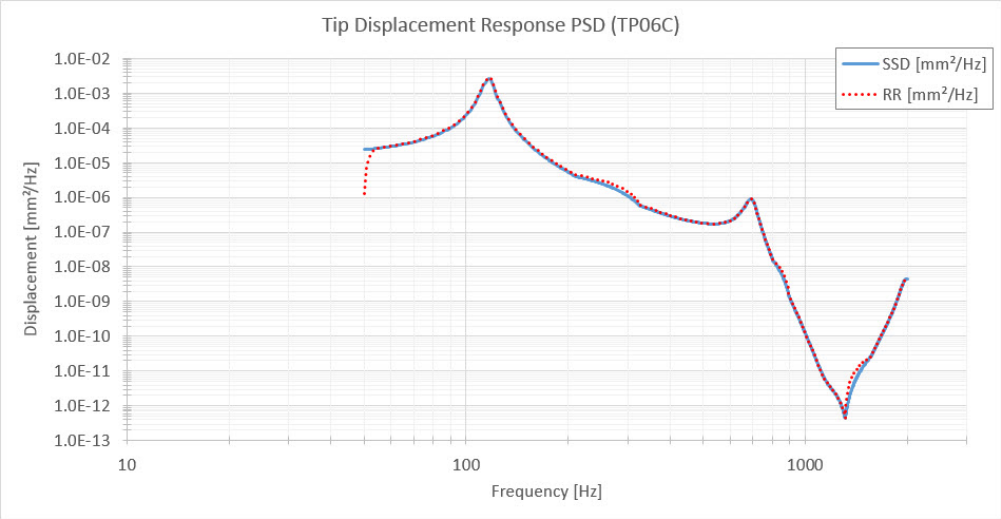

Figure B.26: Vertical tip displacement response, RR vs SSD (log-log)

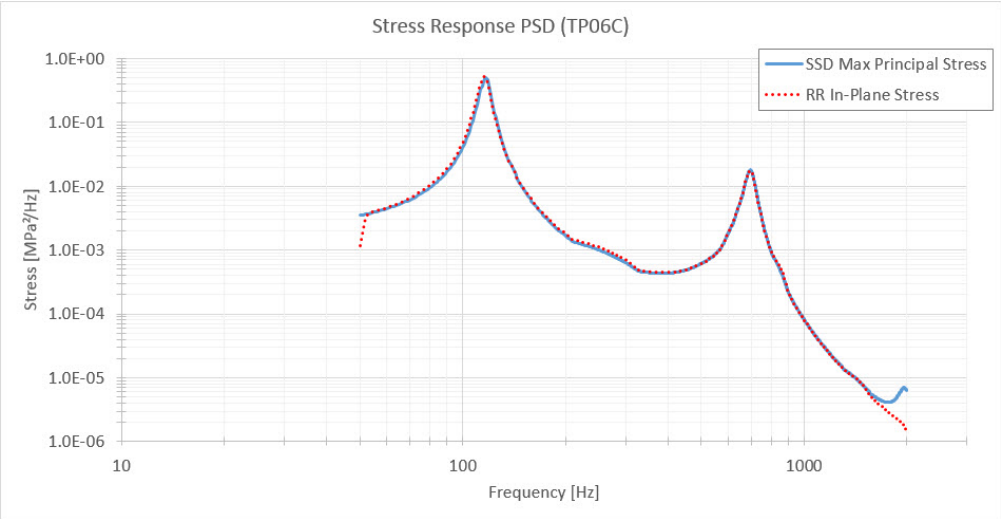

Figure B.27: Maximum stress response RR vs SSD (log-log)

B.3.3 Fatigue Life Calculation

	PSD Moments	Value	
Random Response	m_0	9.40E+00	MPa^2
	m_1	1.99E+03	MPa^2
	m_2	8.55E+05	MPa^2
	m_4	3.93E+11	MPa^2
	RMS	3.066	MPa
Steady-State Dynamics	m_0	8.85E+00	MPa^2
	m_1	1.94E+03	MPa^2
	m_2	8.56E+05	MPa^2
	m_4	4.08E+11	MPa^2
	RMS	2.975	MPa

Table B.22: PSD moments and RMS values

Hand Calculation in Frequency Domain - Simplified PSD Approach

Peak Nr	Stress Amplitude	Frequency
1	4.95E-01 MPa^2	116.6 Hz
2	1.79E-02 MPa^2	694.3 Hz

Table B.23: Stress amplitudes from stress response PSD

Stress Range	Cycles to Failure
8.520 MPa	3.02E+11
10.141 MPa	8.83E+10

Table B.24: Cycles to failure for corresponding stress ranges

This gives a fatigue life of 1.21E+08 seconds.

Hand Calculation in Frequency Domain - Direct RMS Approach

Stress Range	Cycles to Failure
8.672 MPa	2.66E+11

Table B.25: Cycles to failure for corresponding stress range

This gives a fatigue life of 3.83E+08 seconds.

Computer Based Calculations

Method		Fatigue Life [sec]
Narrow Band	RR	2.17E+07
	SSD	2.65E+07
Steinberg	RR	4.72E+07
	SSD	5.92E+07
Dirlik	RR	1.69E+08
	SSD	2.03E+08

Table B.26: Fatigue life obtained from computer based methods

B.3.4 High Amplitude Cycle Hypothesis

Limit	E[D]	Fatigue Life [sec]
Inside $\pm 1\sigma$	4.92E-09	2.03E+08
Inside $\pm 2\sigma$	2.65E-07	3.78E+06
Inside $\pm 3\sigma$	9.78E-07	1.02E+06

Table B.27: Total fatigue life for corresponding limits

C. Mechanical Drawings

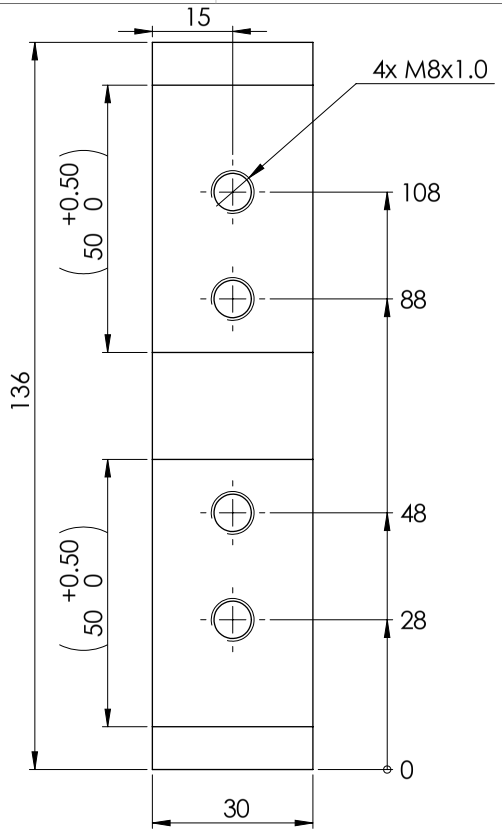

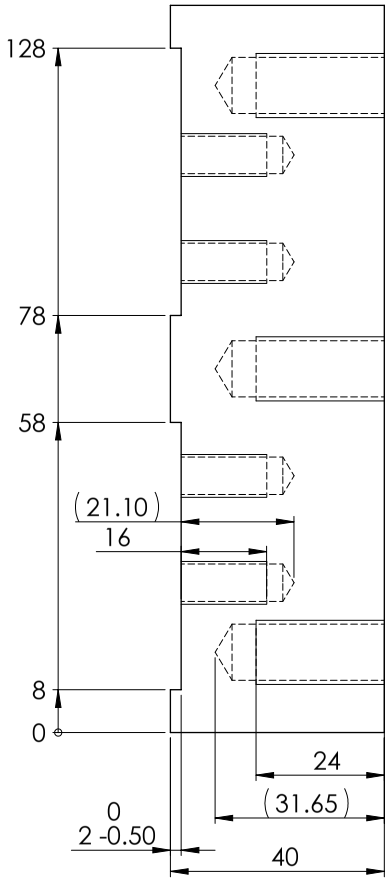

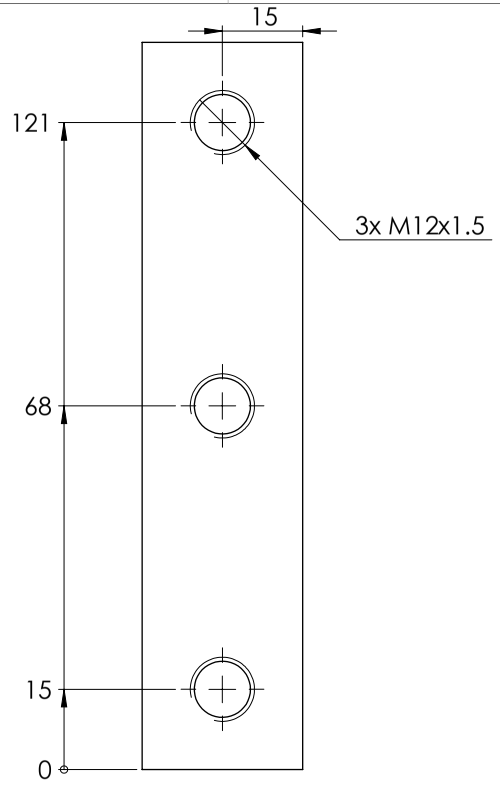

For this drawing the following standards apply

Surface
All dimensions on the drawing includes surface treatment unless otherwise specified

Requirement class
Marked with [ ] according to SS2222 / NS1450 unless otherwise specified

Material type: 6082-T6

Material standard

Basic dim / colour

View

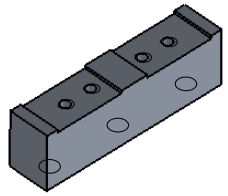

CAD system : Solidworks
3D data: / / /
Status 3D data: Valid

Customer material number

Calculated mass: Type in mass value followed by unit here (g, kg)

Replaces

Calculated volume: Type in desired volume value followed by unit (mm³, cm³)

KONGSBERG AUTOMOTIVE

Designed by	Changed by	Document description
A.Daving		FB02W Fixture Base Part
Checked by	Released by	
Released for	Released date	

ECN number	No	Document part	Document number	Phase	Version

Projection	Scale	Format	Sheet (of)
ISO 128	1:1	A3	1(1)

SolidWorks Student Edition.
For Academic Use Only.

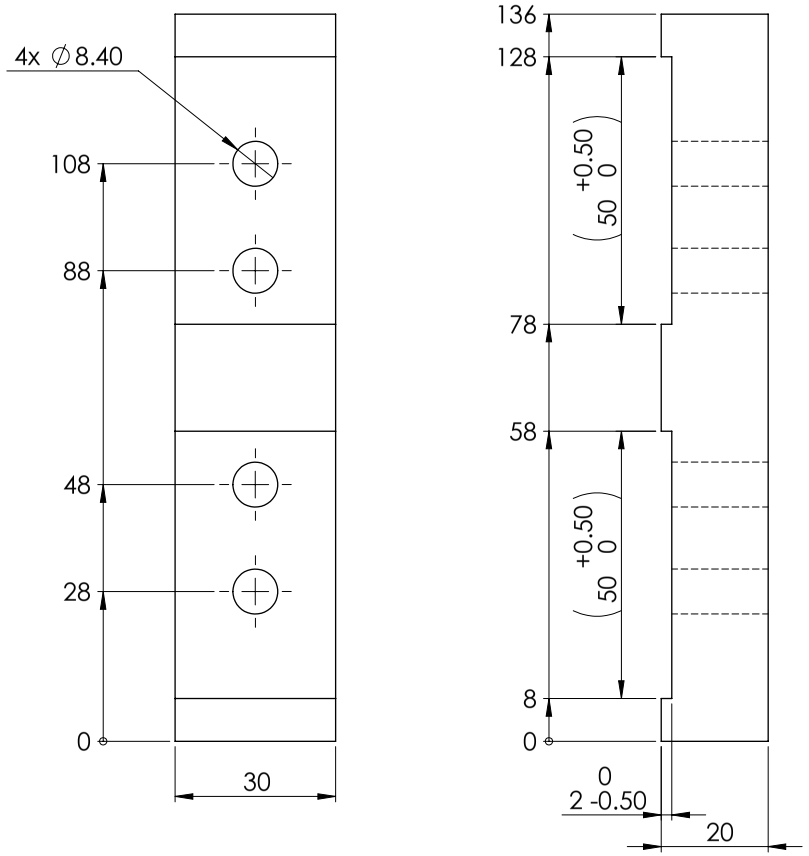

SolidWorks Student Edition.
For Academic Use Only.

For this drawing the following standards apply				View	
Surface: All dimensions on the drawing includes surface treatment unless otherwise specified	Requirement class: Marked with [ ] according to SS2222 / NS1450 unless otherwise specified				
Material type: 6082-T6					
Material standard				CAD system : Solidworks	
Basic dim / colour				3D data: / / /	
				Status 3D data: Valid	
Customer material number: Type in mass value followed by unit here (g, kg)		Calculated mass		KONGSBERG AUTOMOTIVE	
Replaces: Type in desired volume value followed by unit (mm³, cm³)		Calculated volume			
Designed by: A.Daving	Changed by	Document description: FT02W Fixture Top Part			
Checked by	Released by				
Released for	Released date				
ECN number	No	Document part	Document number	Phase	Version

Projection	Scale	Format	Sheet (of)
ISO 128	1:1	A3	1(1)

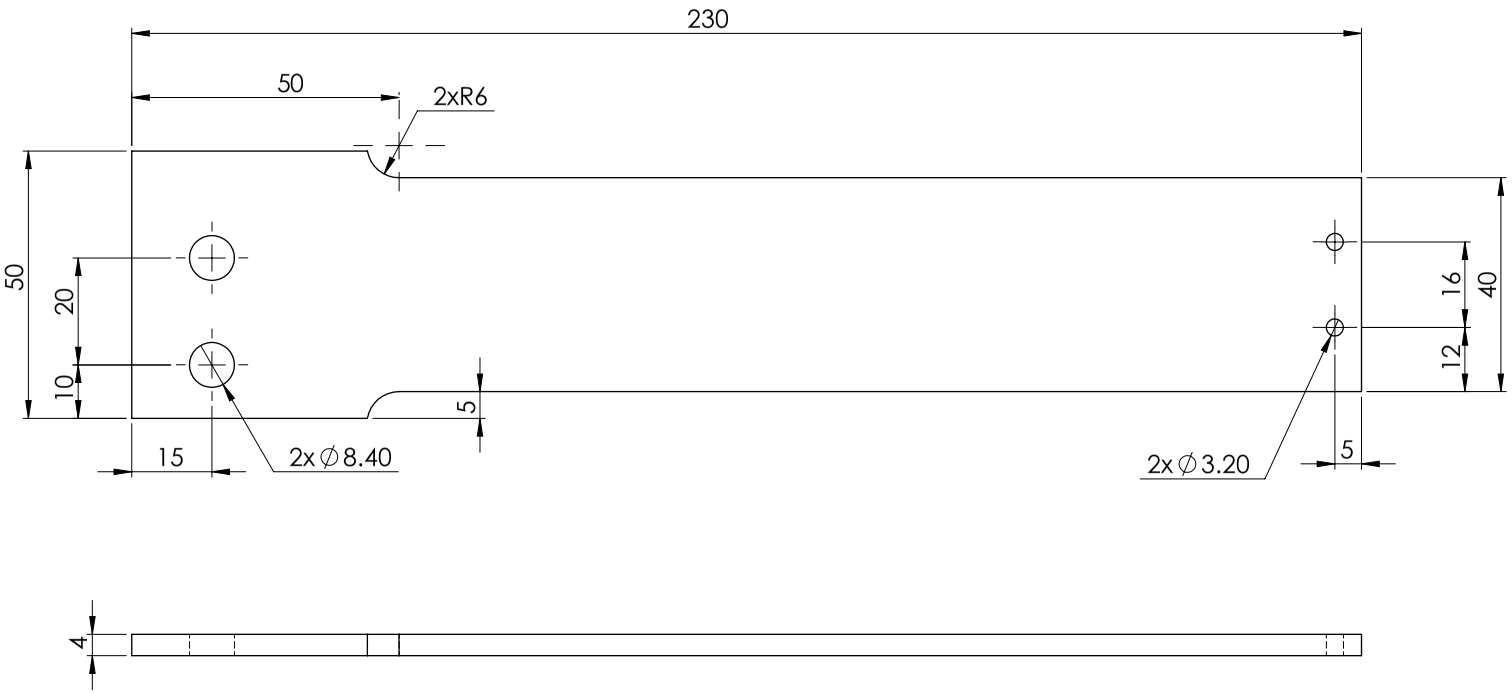

For this drawing the following standards apply		View
Surface All dimensions on the drawing includes surface treatment unless otherwise specified	Requirement class Marked with [ ] according to SS2222 / NS1450 unless otherwise specified	
Material type Material standard Basic dim / colour		CAD system : Solidworks 3D data: / / / Status 3D data: Valid
Customer material number Type in mass value followed by unit here (g, kg)	Calculated mass	KONGSBERG AUTOMOTIVE
Replaces Type in desired volume value followed by unit (mm³, cm³)	Calculated volume	
Designed by A.Daving	Changed by	Document description TP04
Checked by	Released by	
Released for	Released date	

ECN number	No	Document part	Document number	Phase	Version

Projection	Scale	Format	Sheet (of)
ISO 128	1:1	A3	1(1)

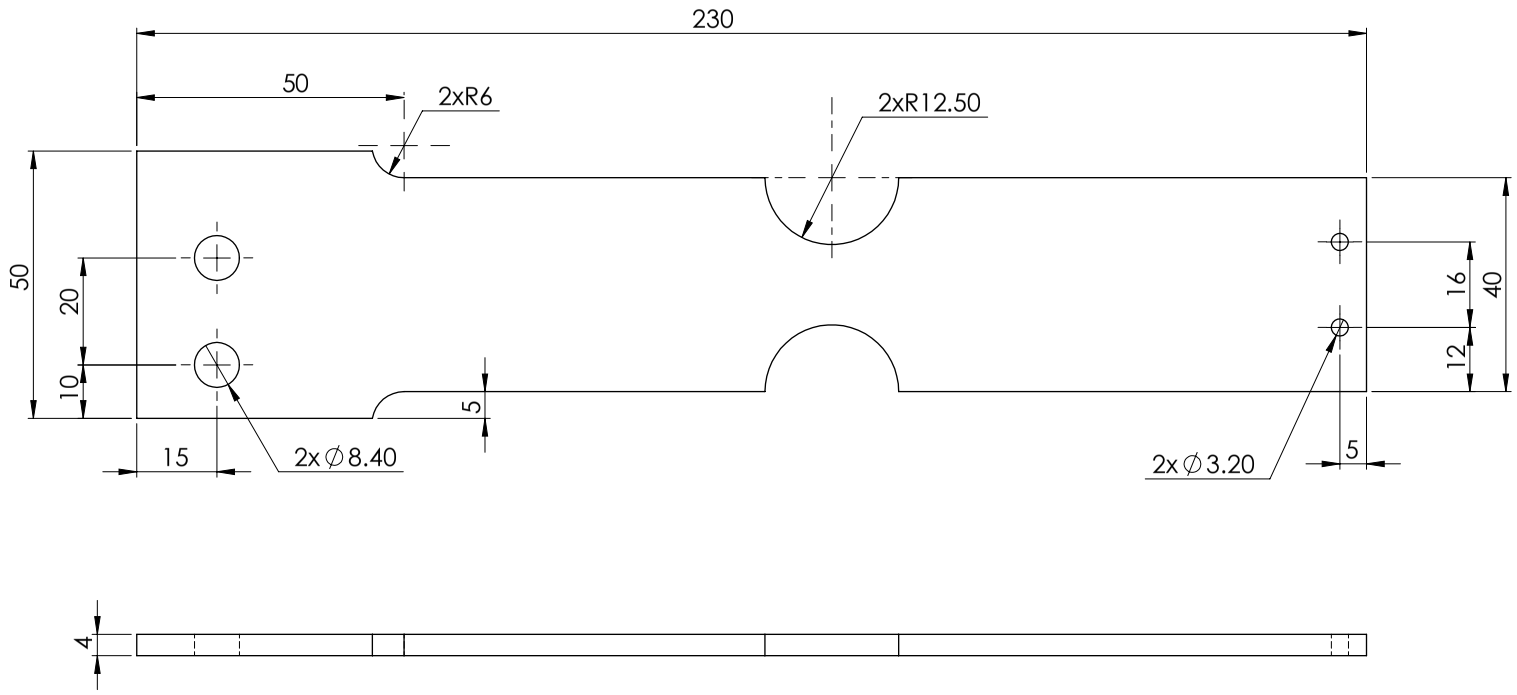

For this drawing the following standards apply			View
Surface All dimensions on the drawing includes surface treatment unless otherwise specified	Requirement class Marked with [ ] according to SS2222 / NS1450 unless otherwise specified		
Material type Material standard Basic dim / colour			CAD system : Solidworks 3D data: / / / Status 3D data: Valid
Customer material number Type in mass value followed by unit here (g, kg)		Calculated mass	KONGSBERG AUTOMOTIVE
Replaces Type in desired volume value followed by unit (mm³, cm³)		Calculated volume	
Designed by A.Daving	Changed by	Document description TP04C	
Checked by	Released by		
Released for	Released date		

ECN number	No	Document part	Document number	Phase	Version

Projection	Scale	Format	Sheet (of)
ISO 128	1:1	A3	1(1)

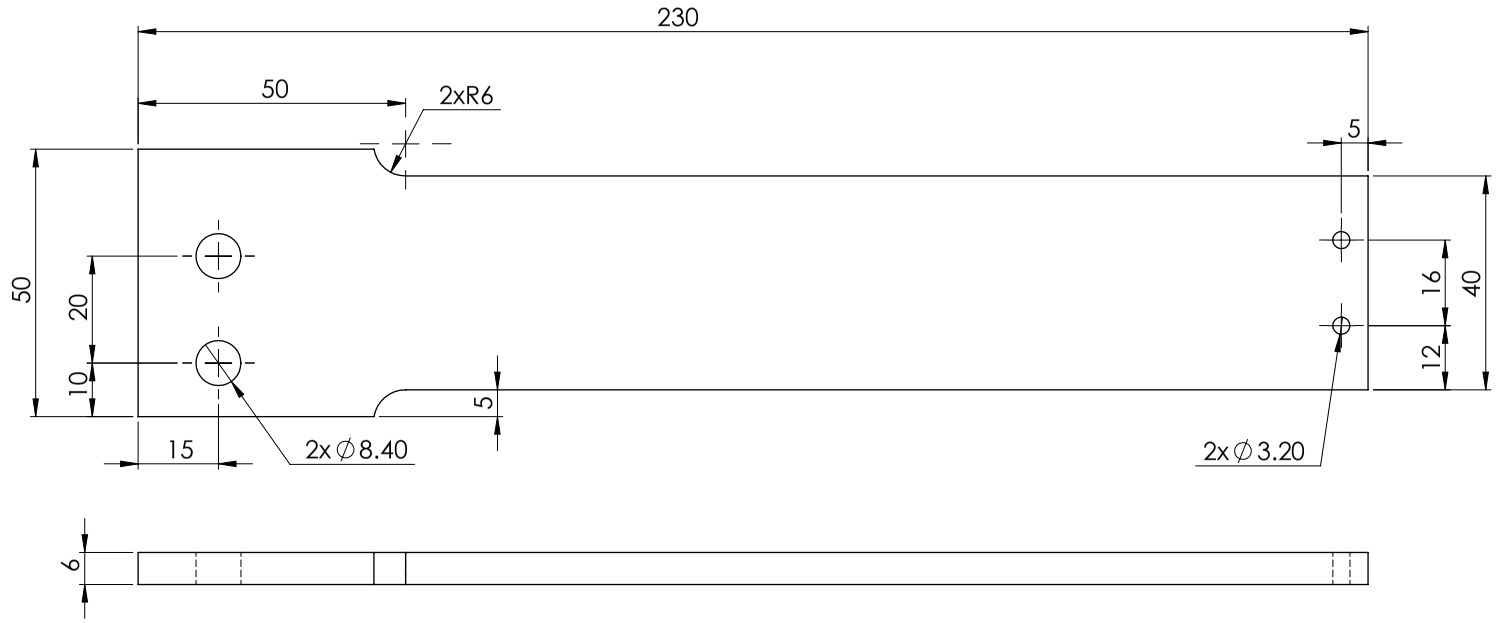

For this drawing the following standards apply		View
Surface All dimensions on the drawing includes surface treatment unless otherwise specified	Requirement class Marked with [ ] according to SS2222 / NS1450 unless otherwise specified	
Material type 6182-T6		
Material standard		CAD system : Solidworks
Basic dim / colour		3D data: / / /
		Status 3D data: Valid
Customer material number	Calculated mass Type in mass value followed by unit here (g, kg)	KONGSBERG AUTOMOTIVE
Replaces	Calculated volume Type in desired volume value followed by unit (mm³, cm³)	
Designed by A.Daving	Changed by	Document description TP06
Checked by	Released by	
Released for	Released date	

ECN number	No	Document part	Document number	Phase	Version

Projection	Scale	Format	Sheet (of)
ISO 128	1:1	A3	1(1)

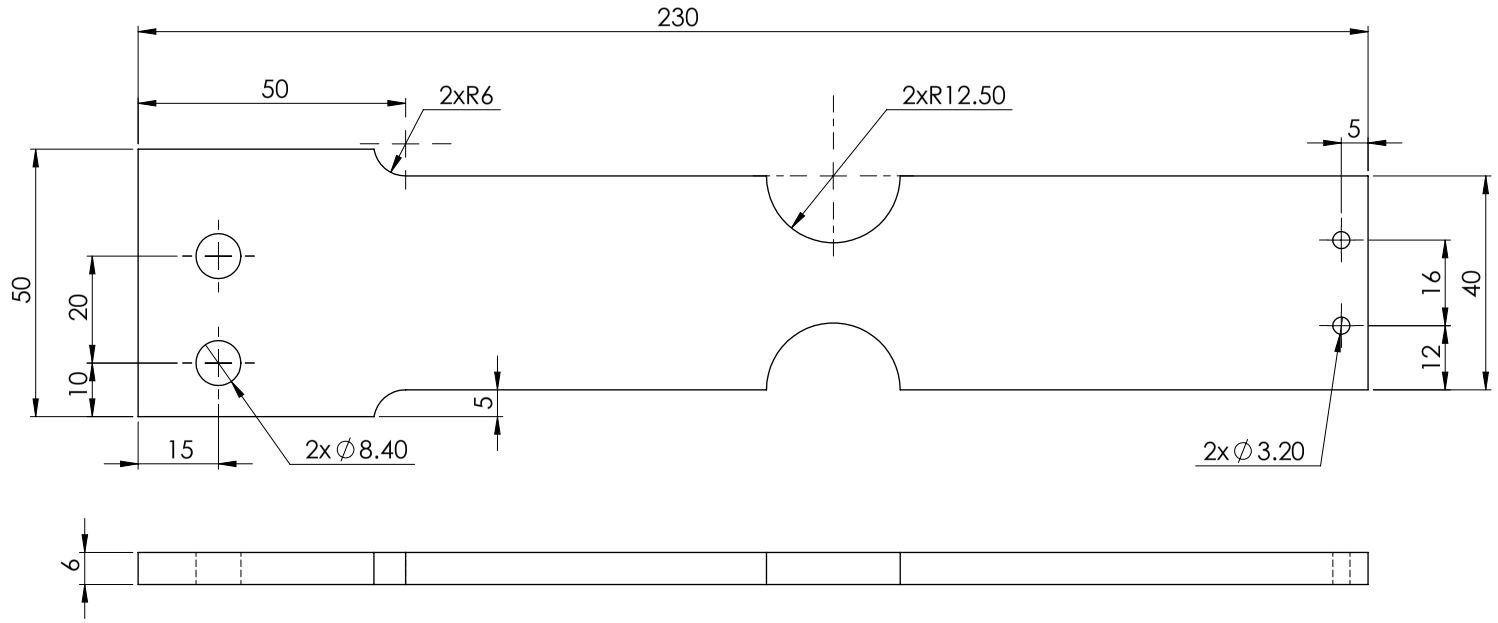

For this drawing the following standards apply		View
Surface All dimensions on the drawing includes surface treatment unless otherwise specified	Requirement class Marked with [ ] according to SS2222 / NS1450 unless otherwise specified	
Material type 6182-T6		
Material standard		CAD system : Solidworks
Basic dim / colour		3D data: / / /
		Status 3D data: Valid
Customer material number	Calculated mass Type in mass value followed by unit here (g, kg)	KONGSBERG AUTOMOTIVE
Replaces	Calculated volume Type in desired volume value followed by unit (mm³, cm³)	
Designed by A.Daving	Changed by	Document description TP06C
Checked by	Released by	
Released for	Released date	

ECN number	No	Document part	Document number	Phase	Version

Projection	Scale	Format	Sheet (of)
ISO 128	1:1	A3	1(1)

D. Assignment Description

NORGES TEKNISK-
NATURVITENSKAPELIGE UNIVERSITET
INSTITUTT FOR PRODUKTUTVIKLING
OG MATERIALER

MASTEROPPGAVE VÅR 2015

FOR

STUD.TECHN. ANDREAS DAVING

Verifikasjon og korrelering av utmattingsberegninger ved bruk av testkonstruksjon og ristebord

Verification and correlation of fatigue calculations for a test structure and shaker table

Kongsberg Automotive ønsker å etablere metodikk for fysisk testing ved bruk av ristebord. Konstruksjonene ønskes å ha relativt kort levetid, omtrent en time.

Resultatene fra de fysiske testene skal korreleres med forskjellige analysemetoder basert på elementmetoden. Aktuelle metoder er dynamiske beregninger i tidsplanet og frekvensplanet.

Arbeidet kan legges opp etter følgende plan:

1. Bygg en fysisk variant av konstruksjonen som ble brukt i forprosjektet som testes tilsvarende på KA's shaker. Både Steady State Dynamics og Random Vibration bør kjøres. Korrelér med beregningsresultatet fra prosjektoppgaven og ny kjøring med lavere last for å få en lengre utmattingskjøring på shaker. Herunder må en testfikstur konstrueres, analyseres og verifiseres, slik at det gir troverdige resultater på shaker.

2. Bruk lærdommen fra prosjektoppgaven og punkt 1. til å utarbeide en metodikk på hvordan man bør gå frem for å kunne korrelere en fysisk test med beregningsmodellen på best mulig måte. Dette kan innebære å lage en sjekkliste på hva man må gjennom av analyser, hva som er viktig å huske å få med, krav til fikstur, hvordan avgjøre hvilke sensorer som skal brukes i test og hvor de skal plasseres.
   Herunder skal også metodikken evalueres i forhold til korrelasjon og presisjon på resultatene i prosjektoppgaven og punkt 1.

3. Anvend metodikken på en komponent fra KA, dvs. FE-modellering og beregninger, finne estimert levetid, finn fornuftig nivå som shakeren bør gå på, plassering av sensorer osv. Målet er å gjøre all jobben man ville gjort før man sender det til test slik at testansvarlig kan vite hva han/hun skal gjøre.

4. Dersom tiden tillater det: Konstruer og lag fikstur for KA-del. Kjør test på KA-del, ut fra spesifikasjonen som kommer fra Oppgave 3. Evaluer korrelasjon/presisjon og metodikken.

Det er viktig arbeidet fokuserer på metoden, og ikke på selve produktet.

Formelle krav:

Senest 3 uker etter oppgavestart skal et A3 ark som illustrerer arbeidet leveres inn. En mal for dette arket finnes på instituttets hjemmeside under menyen masteroppgave (http://www.ntnu.no/ipm/masteroppgave). Arket skal også oppdateres en uke før innlevering av masteroppgaven.

Risikovurdering av forsøksvirksomhet skal alltid gjennomføres. Eksperimentelt arbeid definert i problemstilling skal planlegges og risikovurderes innen 3 uker etter utlevering av oppgavetekst. Konkrete forsøksvirksomhet som ikke omfattes av generell risikovurdering skal spesielt vurderes før eksperimentelt arbeid utføres. Risikovurderinger skal signeres av veileder og kopier skal inngå som vedlegg til oppgaven.

Besvarelsen skal ha med signert oppgavetekst, og redigeres mest mulig som en forskningsrapport med et sammendrag på norsk og engelsk, konklusjon, litteraturliste, innholdsfortegnelse, etc. Ved utarbeidelse av teksten skal kandidaten legge vekt på å gjøre teksten oversiktlig og velskrevet. Med henblikk på lesning av besvarelsen er det viktig at de nødvendige henvisninger for korresponderende steder i tekst, tabeller og figurer anføres på begge steder. Ved bedømmelse legges det stor vekt på at resultater er grundig bearbeidet, at de oppstilles tabellarisk og/eller grafisk på en oversiktlig måte og diskuteres utførlig.

Besvarelsen skal leveres i elektronisk format via DAIM, NTNUs system for Digital arkivering og innlevering av masteroppgaver.

Kontaktperson: Ketil Pettersen, Kongsberg Automotive

for Torgeir Welo
Instituttleder

Bjørn Haugen
Faglærer

NTNU
Norges teknisk-naturvitenskapelige universitet
Institutt for produktutvikling og materialer